Configuration spaces of thick particles on graphs

Kenneth Deeley

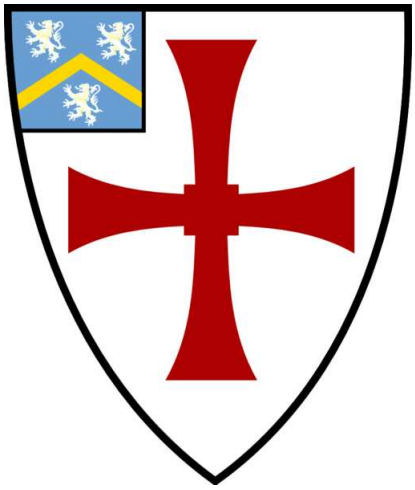

A thesis presented for the degree of
Doctor of Philosophy

Pure Mathematics
Department of Mathematical Sciences
Durham University

2011

Abstract

Configuration spaces of thick particles on graphs

Kenneth Deeley

In this thesis, we study the topology of configuration spaces of particles of variable radius $r > 0$ moving on a metric graph. Our main tool is a piecewise linear (PL) Morse–Bott theory for affine polytope complexes, which extends the Morse theory for such complexes introduced by M. Bestvina and N. Brady in paper [8].

As the size parameter r increases, the topological properties of the corresponding configuration spaces vary. We show that there are finitely many critical values where the homotopy type of these spaces changes, and describe these critical values in terms of metric properties of the graph. This provides an upper bound on the number of critical values in terms of the metric data. Moreover, we apply PL Morse–Bott theory to analyse the change in homotopy type of configuration spaces of thick particles when the radius transits a critical value.

Provided that r is sufficiently small, we show that the thick particle configuration space is homotopy equivalent to the familiar configuration space of zero-size points on the graph. We also investigate discrete models for configuration spaces of two thick particles. Moreover, given a metric graph and the size parameter r, we provide an algorithm for computing the number of path-components of the configuration space of two thick particles.

Declaration

The work in this thesis is based on research carried out in the Pure Mathematics Group at the Department of Mathematical Sciences, Durham University. No part of this thesis has been submitted elsewhere for any other degree or qualification and it is all my own work unless referenced to the contrary in the text.

Acknowledgements

Firstly, I would like to thank my PhD supervisor Professor Michael Farber for his advice, patience, kindness and support throughout my postgraduate studies at Durham University. His enthusiasm for topological robotics and copious encouragement have inspired and subsequently guided the results contained in this thesis. I also thank Dr. Robert Ghrist and Dr. Elizabeth Hanbury for fruitful discussions and valuable feedback. I thank Professors John Toland and Hartmut Logemann for their inspirational teaching during my undergraduate degree and for encouraging me to apply for postgraduate study. Going back even further, I thank my school teachers Eric McCallum, John Campbell, Iain Holton and Tam Strachan for their excellent mathematics and physics training.

Many thanks are due to Durham University for providing their Doctoral Fellowship scheme. Similarly, I thank Dr. Gillian Boughton for administering the Willmore Award and encouraging me to apply to Durham and St Mary's College. I am grateful to the C. K. Marr Educational Trust for their generous support over eight years of university education. I would also like to thank the members of the Department of Mathematical Sciences for their assistance and support. Special thanks are due to Andy Hayden for his invaluable help and enthusiasm, especially with the computer programming in Appendix B of this thesis. I also thank Ben Lambert for always listening to ideas and suggesting improvements.

Finally, I thank my parents, my sister Hazel, and Dr. Betti Pusceddu for their consistent encouragement, support and love throughout my time in Durham. I especially thank my mother Dr. Susan Deeley and my father Norman Deeley for inspiring me to pursue a PhD and for their appreciation of science, mathematics, language, music and literature.

Contents

Chapter 0

Introduction

0.1 Background and motivation

0.1.1 Topological robotics

In this thesis we investigate topological properties of configuration spaces of thick particles moving on a metric graph. This work is motivated by various problems arising in the area of *topological robotics*. Topological robotics is "a new mathematical discipline studying topological problems inspired by robotics and engineering as well as problems of practical robotics requiring topological tools" [20, Preface]. An excellent introduction is provided by M. Farber's book [20]. Interesting topics of topological robotics analysed in [20] include configuration spaces of mechanical linkages, knot theory of robotic arms, and the motion planning problem (namely, the control problem of safely scheduling a trajectory between an initial configuration of robots and a desired configuration). As an example of the latter, consider the problem of permuting the positions of the three groups of robots in a workplace containing obstacles as shown in Figure 1. There are clearly many different solutions to this problem.

Moreover, many mathematical and engineering problems involving mechanical devices have important historical significance. For example, Archimedes' screw (see Figure 2)[1] enabled agricultural expansion in early civilisations, and is still in use

[1]Image: Wikimedia Commons, public domain, from Chambers' Encyclopedia (1875).

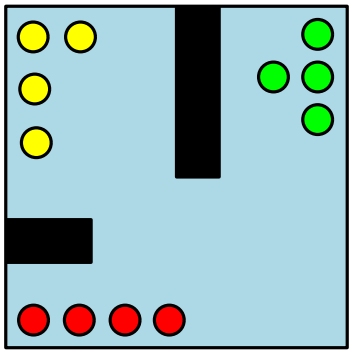

Figure 1: The motion planning problem

today. As mentioned in [20], the industrial revolution saw the development of many

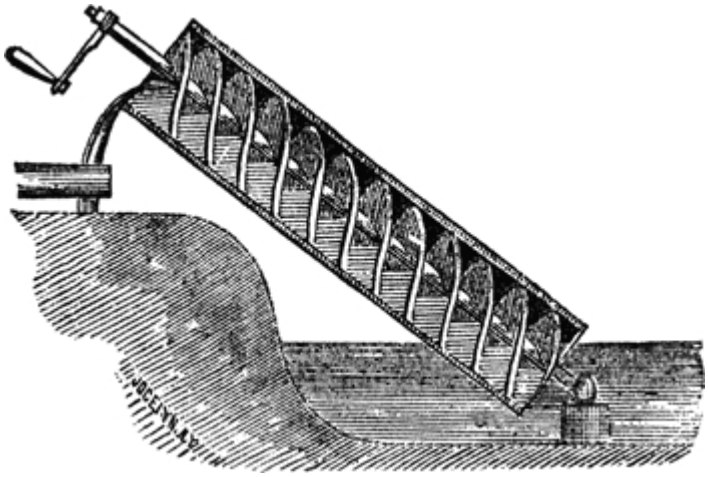

Figure 2: Archimedes' screw

important linkages. A famous example is James Watt's linkage (see Figure 3) which solves the problem of constraining the motion of a steam engine piston to an approximate straight line. Topological robotics may be viewed as a research area continuing the historical practice of seeking mathematical solutions to practical problems arising from (and inspired by the construction of) mechanical devices.

0.1.2 Robots and autonomous guided vehicles

A robot is "a machine capable of carrying out a complex series of actions automatically, especially one programmable by a computer" [55]. The word "robot" was first introduced in 1920 by the Czech author Karel Čapek in his play "Rossum's Universal Robots"; he attributes the origin of the word to his brother Josef Čapek

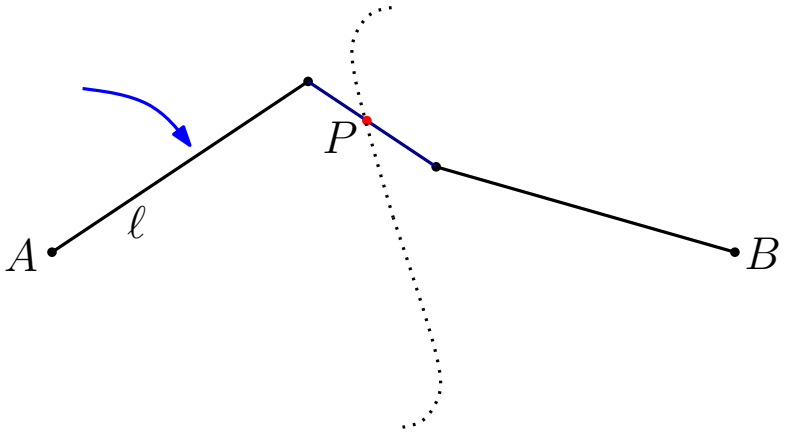

Figure 3: Watt's linkage: points A and B are fixed, bar ℓ rotates around A, and the motion of P approximates a straight line

[55, 57]. The word "robota" literally means "work" or "labour", and metaphorically "drudgery" or "hard work" in Czech [53, 55, 57]. The term "robotics" was coined by Isaac Asimov in 1940 [53] and is now viewed as "the branch of technology that deals with the design, construction, operation and application of robots" [55]. An excellent publication illustrating the multidisciplinary nature of modern robotics is the Springer Handbook of Robotics [53] (see also [37]).

An important class of robots is the so-called *autonomous guided vehicles* (also called *automated* or *automatic* guided vehicles – all abbreviated to "AGVs"). An AGV is a mobile driverless robot (see Figure 4)[2] generally used in large warehouses or factories for transporting materials within the facility [37, 39, 52, 58]. The motion of an AGV is usually constrained to a *guidepath network* consisting of electric wires, magnetic tape or laser reflectors [39, 52, 58]. In this context the term "autonomous" means "not dependent upon any link to the outside world" [48, §1]. In practical terms, this means that AGVs carry an onboard power supply and computer and are "not remote-controlled by a human, but interact with [their] environment ... and determine [their] motion without external intervention" [48, §1]. Scheduling the collision-free motion of AGVs is an important problem of practical robotics [39]. In the next subsection, we summarise how topological methods have been used to

[2]Images: public domain, courtesy of Transbotics Corporation and Hi-Tech Robotic Systemz Ltd.

Figure 4: Examples of AGVs: an outdoor laser-guided vehicle on the left, and an indoor vehicle following a magnetic strip on the factory floor on the right

model certain aspects of this problem. An excellent survey of the application of configuration spaces in industrial robotics has been written by A. Abrams and R. Ghrist [4].

0.1.3 Configuration spaces of graphs

We now discuss the role of topology in the problems of practical robotics mentioned in §0.1.1 and §0.1.2. Consider the engineering problem of safely organising multiple AGVs moving without collisions on a fixed guidepath network. This problem has been studied from a topological viewpoint by R. Ghrist in [33] (see also the expository paper [34]) and by R. Ghrist and D. Koditschek in [35, 36]. Configuration spaces of graphs arise intrinsically in this context. Indeed, the natural model is to assume that the AGV guidepath network is a graph Γ; then the space of all collision-free positions of n AGVs is precisely the n–point configuration space of Γ, namely

$$F(\Gamma, n) := \{(x_1, \ldots, x_n) \in \Gamma^n : x_i \neq x_j \text{ for } i \neq j\},$$

topologised as a subspace of the product Γ^n. In papers [35] and [36], R. Ghrist and D. Koditschek introduce the use of vector fields to construct control schemes which

safely organise AGV motion on a planar graph.

Many interesting and relevant topological properties of $F(\Gamma, n)$ have recently been discovered. For example, R. Ghrist proves in [33, Theorem 3.3] that $F(\Gamma, n)$ deformation retracts onto a finite CW complex of dimension V, where V is the number of essential vertices ($\mu(v) \geq 3$) in Γ. A similar result was proved independently by J. Świątkowski in [54, Theorem 0.1], where the author shows that the homological dimension of the *unordered* n–point configuration space $F(\Gamma, n)/S_n$ is bounded above by V. (Here, the symmetric group S_n acts freely on $F(\Gamma, n)$ by permuting coordinates). An important result of R. Ghrist [33, Theorem 3.1] states that the configuration space $F(\Gamma, n)$ is aspherical. More general configuration spaces have recently been studied by A. Abrams, D. Gay and V. Hower; in [3, Theorems 1,2] the authors explicitly determine the homotopy type of the following *discretised configuration space* of Δ^n:

$$D_k(\Delta^n) = \{\sigma_1 \times \cdots \times \sigma_k : \{\overline{\sigma}_i\} \text{ are pairwise disjoint closed cells in } \Delta^n\}.$$

(Here Δ^n is the standard n–simplex.)

In the special case when Γ is a tree T, the configuration space $F(T, n)$ of n points on T has been studied by M. Farber in [19]. This paper describes an explicit motion planning algorithm in $F(T, n)$ and computes the topological complexity (see [20, §4.2] for definitions) of $F(T, n)$, also in terms of V. Configuration spaces of trees have also been studied by other authors. For example, D. Farley and L. Sabalka [26, 28] computed the fundamental group of the (unordered) n–point configuration space of a tree (the *tree braid group*), using a discrete version of Morse theory due to R. Forman [29]. Moreover, D. Farley has computed the homology of tree braid groups in paper [24]. Presentations for the cohomology rings of tree braid groups are also described in work of D. Farley [25] and D. Farley and L. Sabalka [27].

Such *braid groups* are also investigated in work of A. Abrams, see [1, Chapter 3] and [2] (see also P. Prue and T. Scrimshaw's paper [51]). The case of braid groups of general graphs has been studied from a motion planning viewpoint by V. Kurlin [44]. Interesting computations of the braid groups of specific graphs have been carried out by M. Doig [17], F. Connolly and M. Doig [11] and A. Neels and S. Privitera [47]. An important recent paper by Ki Hyoung Ko and Hyo Won Park provides general

formulae for the first homology group of the n–point unordered configuration space of a graph (see [42, Theorem 3.16]).

Many significant results have been obtained for the case $n = 2$, when the configuration space models the collision-free motion of two particles on a graph. For example, in paper [19] M. Farber explicitly describes the topology of $F(T, 2)$ for a tree T. In his book (see [20, §2.3]) M. Farber computes the Euler characteristic $\chi(F(\Gamma, 2))$ for a general graph Γ, making use of an elegant theorem of S. Gal (see [30, Theorem 2]).[3] This result was also obtained by K. Barnett and M. Farber using a different method, see [7, Corollary 1.2]. Furthermore, in paper [7] the authors describe explicit generators for the second homology group $H_2(F(\Gamma, 2), \mathbb{Z})$. Paper [7] also contains information on the cohomology algebra $H^*(F(\Gamma, 2), \mathbb{Q})$ for any regular planar graph Γ (see also K. Barnett's thesis [6]). The results of [7] are continued by M. Farber and E. Hanbury in paper [22], in which the authors determine the Betti numbers of $F(\Gamma, 2)$ for a large class of graphs. D. Farley and L. Sabalka have studied explicit examples of graph braid groups on $n = 2$ strands, see [28, §5, §6]. Importantly, Ki Hyoung Ko and Hyo Won Park [42, Theorem 3.25] have shown that $H_1(F(\Gamma, 2))$ is free for any finite connected graph Γ and have computed $\operatorname{rk} H_1(F(\Gamma, 2))$ explicitly in terms of graph-theoretic invariants.

0.1.4 Metric graphs

A *metric graph* is a connected graph in which each edge e is labelled by a positive number $\ell_e > 0$. Such a labelling induces a metric on the graph, where the distance between two points is the length of the shortest arc connecting them (see §1.2 and §1.3 for full details). Metric graphs play an important role in this thesis (described in §0.2). They have also been studied in various other contexts. For example, A. Georgakopoulos [31] has related certain topologies on infinite graphs to the metric topology induced by an edge-labelling. In paper [32], the same author uses metric graphs to model electrical networks. In this case the label of each edge is interpreted

[3] This remarkable theorem provides an explicit formula for the *Euler-Gal power series* $\mathfrak{eu}_X(t) := \sum_{n=0}^{\infty} \frac{t^n}{n!}\chi(F(X, n))$ of a finite polyhedron X in terms of local topological properties of X.

as its electrical resistance. Moreover, O. Mermoud and M. Steiner [46] view labelled graphs as point sets in some fixed Euclidean space with given distances between certain pairs of points, and study the space of all possible realisations up to isometry. In paper [15], B. Demir, A. Deniz and S. Koçak show that under certain assumptions, two metric graphs which are sufficiently close (with respect to some metric) are actually equivalent as graphs. We also mention the beautiful expository paper by M. Baker and X. Faber [5], in which the authors study a special Laplacian operator on a metric graph.

0.1.5 The main problem and related topics

In this thesis, we study configuration spaces of thick particles on a metric graph. This means that we view the moving particles as metric balls of some positive radius $r > 0$, instead of modelling them as zero-size points. It has been recognised in the literature that regarding the moving objects as points is not completely realistic from a modelling viewpoint. For example, in the context of modelling robots moving on a factory floor, A. Abrams and R. Ghrist [4] acknowledge that "Of course, since the robots are not truly points, and since no control algorithm implementation is of infinite precision, we require that the control path reside outside of a neighborhood of the diagonal Δ in $(\mathbb{R}^2)^N$." Further, in paper [23], M. Farber, M. Grant and S. Yuzvinsky compute the topological complexity (see [20, §4.2]) of the n–point configuration space of $\mathbb{R}^k - F$, where F is a finite set of points and $k \in \{2, 3\}$. In [23, §1], the authors write "We believe that the conclusions of this paper will remain valid in a more general and realistic situation when the objects and the obstacles are represented by small balls, possibly of different radii, and the control requirements are to avoid tangencies between objects and obstacles." In this thesis we investigate how some of these issues may be addressed by replacing zero-size point particles with metric balls of positive radius.

There has also been fascinating recent progress with similar problems in a different context. For example, M. Kahle has constructed stable configurations of n discs of radius $r = O(1/n)$ in the unit square $[0, 1] \times [0, 1]$. As mentioned by P. Diaconis [16, §4], the problem of packing solid discs in a box is motivated by the study

of phase transitions in statistical mechanics. M. Kahle's result [41, Theorem 1.2] has consequences for the *Metropolis algorithm*, which is an algorithm for randomly packing discs in (for example) the unit square.

0.2 The main objects of study

In this section we briefly introduce the configuration spaces $\{F_r(\Gamma, 2)\}_{r>0}$ of two thick particles moving on a metric graph Γ. These are our main objects of study and the aim of this thesis is to study their topology.

Throughout this thesis, we work with a finite, connected graph Γ with edge set $E(\Gamma) \neq \emptyset$. We assume that there is a map $\ell : E(\Gamma) \to (0, \infty)$ labelling the edges of Γ by positive numbers, see Figure 5. Such a labelling induces a metric $d : \Gamma \times \Gamma \to \mathbb{R}$,

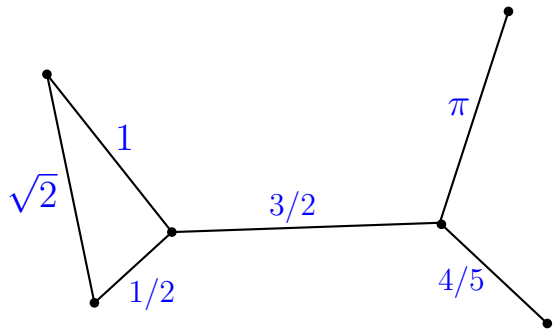

Figure 5: Labelling the edges of Γ

where $d(x, y)$ is the length of the shortest path[4] in Γ joining x and y.

Definition 0.2.1 (Thick-particle configuration space)**.** For $r > 0$, we define

$$F_r(\Gamma, 2) := \{(x, y) \in \Gamma \times \Gamma : d(x, y) \geq 2r\} = d^{-1}([2r, \infty)).$$

In other words, $F_r(\Gamma, 2)$ is the configuration space of two thick particles (robots) of radius r moving on Γ, see Figure 6. Varying the radius r of these particles gives a family of spaces $\{F_r(\Gamma, 2)\}_{r>0}$. We view $F_r(\Gamma, 2)$ as a model for the collision-free motion of two robots on the guidepath network Γ. Each robot is modelled as a metric ball of radius r, and tangencies between the robots are permitted. The following list

[4]Full details of this construction are given in Chapter 1, see §1.2 and §1.3.

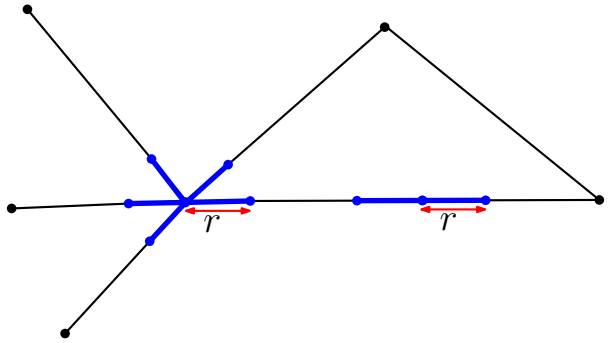

Figure 6: Two objects of radius r moving on Γ

suggested by M. Farber [21] provides several important questions about the family $\{F_r(\Gamma, 2)\}_{r>0}$.

(i) For which values of r is $F_r(\Gamma, 2)$ nonempty?

(ii) For which values of r is $F_r(\Gamma, 2)$ path-connected? For a given Γ and r, how many path-components does $F_r(\Gamma, 2)$ have?

(iii) Is there an r_0 such that for all $0 < r < r_0$, the space $F_r(\Gamma, 2)$ is homotopy equivalent to the configuration space $F(\Gamma, 2)$ of two zero-size particles?

(iv) Are there intervals (a, b) such that the homotopy type of $F_r(\Gamma, 2)$ is constant for $r \in (a, b)$?

(v) Study "phase transitions"; that is, critical values of the radius r at which the homotopy type of $F_r(\Gamma, 2)$ changes.

Answering these questions forms the basis of this thesis. We begin in Chapter 2 by developing our main tools; this development extends the work of M. Bestvina and N. Brady [8] (see also [9]). In Chapter 3 we answer questions (i) and (iv). In Chapter 3 we also investigate problem (v) by using the tools from Chapter 2; we study the change in homotopy type of $F_r(\Gamma, 2)$ as r ranges over an interval (a, b) containing precisely one critical value R.

In Chapter 5 we answer (ii) in the form of an algorithm for computing the number of path-components of $F_r(\Gamma, 2)$ given r and (Γ, ℓ). We provide a solution to (iii) together with some more general material in Chapter 4.

The theory developed in Chapter 2 applies in more general contexts than those arising from problems (i)–(v). This motivated an additional problem as follows:

(vi) Study the configuration spaces $\{F_r(\Gamma, n)\}_{r>0}$, where $n \geq 3$. (These spaces model the collision-free motion of n robots of radius r moving on a metric graph Γ).

Using the tools developed in Chapter 2, we investigate some properties of the family $\{F_r(\Gamma, n)\}_{r>0}$ (for fixed $n \geq 3$) in Chapter 6.

0.2.1 Notation

Throughout this thesis the symbol $\cong$ stands for a homeomorphism and the symbol $\simeq$ stands for a homotopy equivalence. The interior of a set A in a topological space $(X, \mathcal{T})$ is denoted by A°. The terminology "closed unit interval" means the topological space $[0, 1]$ equipped with the standard metric topology. We use the notation $b_0(X)$ for the 0th Betti number of a space X (the number of path-components of X). A discrete space containing $m \geq 0$ points is denoted by Q_m.

0.3 Thesis structure

In this final section of the introduction, we describe the structure of this thesis. The chapter dependency is shown in the graph below.

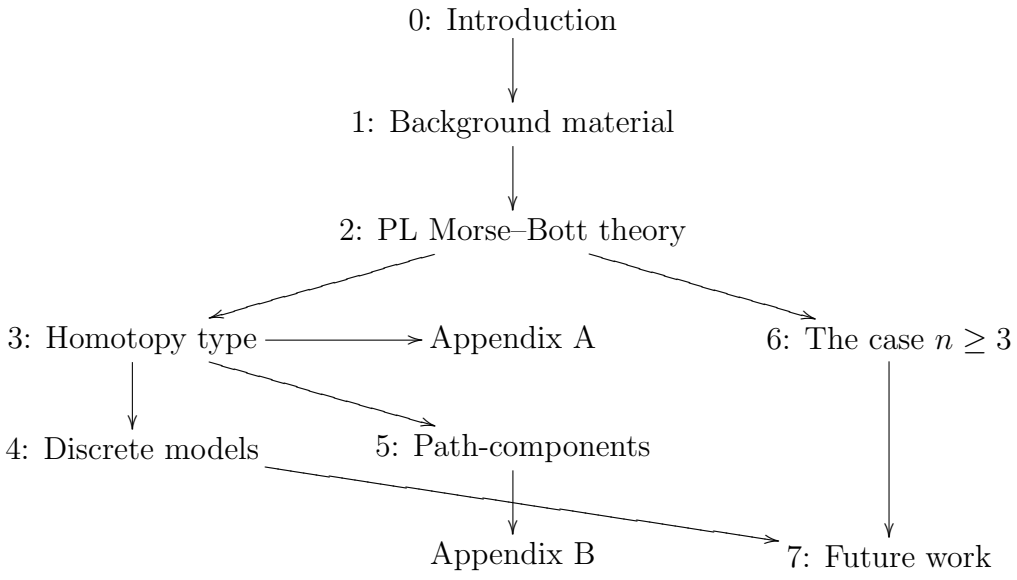

In §0.2 we introduced the thick particle configuration spaces $\{F_r(\Gamma, 2)\}_{r>0}$, the main objects of study in this thesis. We cover the necessary background material on labelled graphs and metric geometry in Chapter 1. This includes the basic definitions from graph theory (see §1.1) and the construction of the induced metric on a connected graph with positive edge labels (see §1.2 and §1.3). In §1.4 and §1.5 we discuss certain important classes of paths, define basic operations on a labelled graph, and formulate a version of the triangle inequality for labelled graphs. This inequality is needed in Chapters 2, 3, 4 and 6.

In Chapter 2 we develop a piecewise linear (PL) Morse–Bott theory (see §2.1) for affine polytope complexes (APCs), extending the work of Bestvina and Brady (see [8, 9]) who developed a PL Morse theory for affine Morse functions defined on APCs. PL Morse–Bott theory is our main tool for studying the topology of the configuration spaces mentioned in this thesis. In §2.2 we verify that the metric $d : \Gamma \times \Gamma \to \mathbb{R}$ on a metric graph is an affine Morse–Bott function, so that we may apply our PL Morse–Bott theory to this metric.

Once the basic tools have been established in Chapter 2, we begin our study of the family $\{F_r(\Gamma, 2)\}_{r>0}$ in Chapter 3 by studying the homotopy type of $F_r(\Gamma, 2)$; this depends on the size parameter $r > 0$. The main result of this chapter is that there are finitely many *critical values* (see Definitions 3.2.1) where the homotopy type of $F_r(\Gamma, 2)$ changes, see Theorem 3.2.3. This theorem also describes each of these critical values in terms of metric properties of the graph, thereby providing an upper bound for the number of critical values in terms of the metric data. We then turn our attention to analysing the change in homotopy type of $F_r(\Gamma, 2)$ as r varies over an interval containing exactly one critical value. In §3.2 we apply PL Morse–Bott theory to compute the relative homology groups of the pair $(F_a(\Gamma, 2), F_b(\Gamma, 2))$, where the interval (a, b) contains exactly one critical value. In Appendix A we discuss how Theorem 3.2.3 may be derived directly by constructing an explicit deformation retraction.

In Chapter 4 we study *discrete models* for the configuration spaces $\{F_r(\Gamma, 2)\}_{r>0}$. A discrete model for $F_r(\Gamma, 2)$ is a finite CW complex homotopy equivalent to $F_r(\Gamma, 2)$. We show that for sufficiently small $r > 0$, $F_r(\Gamma, 2)$ is homotopy equivalent to the

usual two-point configuration space $F(\Gamma, 2)$, see Theorem 4.1.6. This result is obtained by defining a CW complex which is a deformation retract of both spaces. We then introduce a CW complex $D_r(\Gamma, 2)$ and show that for each r, there is a subdivision of Γ such that $F_r(\Gamma, 2)$ deformation retracts onto $D_r(\Gamma, 2)$ (see Theorem 4.2.4). This shows that for each $r > 0$, $F_r(\Gamma, 2)$ has a discrete model which may be constructed explicitly from Γ (possibly after further subdivision of Γ).

In Chapter 5 we study the path-connectivity of the spaces $\{F_r(\Gamma, 2)\}_{r>0}$. We begin in §5.1 by reviewing the path-connectivity of the 2–point configuration space $F(\Gamma, 2)$. After this, we develop an algorithm in §5.3 for computing $b_0(F_r(\Gamma, 2))$ given Γ and r. The theoretical basis of this algorithm is provided by the general tools developed in Chapter 2. To illustrate the general complexity of the family $\{F_r(\Gamma, 2)\}_{r>0}$ we refer to Example 5.3.12, where applying the algorithm from §5.3 shows that $b_0(F_r(\Gamma, 2))$ need not be a monotone (or even unimodal) function of r. Section §5.4 contains further examples of applying the algorithm to specific labelled graphs. In Appendix B, we provide an implementation of the algorithm (written in GNU Octave) applied to trees. The main results from Chapters 2, 3 and 5 are contained in paper [14].

In Chapter 6 we study properties of the family of thick particle configuration spaces $\{F_r(\Gamma, n)\}_{r>0}$ for a general $n \geq 3$. These configuration spaces model the collision-free motion of n AGVs of radius $r > 0$ moving on a metric graph Γ. As in the previous chapters, our tool is the PL Morse–Bott theory developed in Chapter 2. We study the analogues of Theorem 3.2.3 and Theorem 4.1.6 for the general case of n thick particles on a metric graph.

Finally, in Chapter 7 we discuss some possibilities for future work. These mainly consist of unsolved problems arising from studying the family $\{F_r(\Gamma, n)\}_{r>0}$ in the general case when $n \geq 3$. Moreover, we present some ideas for studying different but related configuration spaces arising from specific practical contexts, together with some ideas for extending the work in Chapter 4.

Chapter 1

Background material on labelled graphs

In this chapter we introduce the necessary definitions and background material on labelled graphs. The main result is that a labelling of the edges of a graph by positive numbers induces a metric, see Theorem 1.3.3. We begin in §1.1 with the basic definitions, and proceed in §1.2 and §1.3 with the construction of the metric. In §1.4 we discuss special types of paths and their relationships to the induced metric. Finally in §1.5 we define the basic operations of subdivision and amalgamation in a labelled graph and state a version of the triangle inequality for labelled graphs. In particular, this inequality is required in Chapter 4 to ensure that a certain deformation retraction is well-defined.

1.1 Basic definitions from graph theory

Throughout the thesis, we study the topology of configuration spaces of thick particles on a graph. We begin by giving the requisite definitions and notation from graph theory. The main references are the textbooks by A. Hatcher [38], W. Massey [45] and D. Burago, Y. Burago and S. Ivanov [10].

Definitions 1.1.1. A topological space Γ is a *graph* if there exists (a) a discrete

space X^0; (b) a collection of closed unit intervals $\{I_\beta\}_{\beta\in\mathcal{A}}$, and (c) a map

$$\phi := \coprod_{\beta\in\mathcal{A}} \phi_\beta : \coprod_{\beta\in\mathcal{A}} \partial I_\beta \to X^0$$

such that Γ is the adjunction space

$$\Gamma = X^0 \sqcup_\phi \coprod_{\beta\in\mathcal{A}} I_\beta,$$

see Figure 1.1. Let $p : X^0 \amalg_{\beta\in\mathcal{A}} I_\beta \to \Gamma$ denote the quotient map. The elements of the set $\Gamma^{(0)} := p(X^0)$ are called the *vertices* of Γ, and the sets $\{p(I_\beta^\circ)\}_{\beta\in\mathcal{A}}$ are called the *edges* of Γ. The graph Γ is *finite* if X^0 and $\mathcal{A}$ are both finite sets.

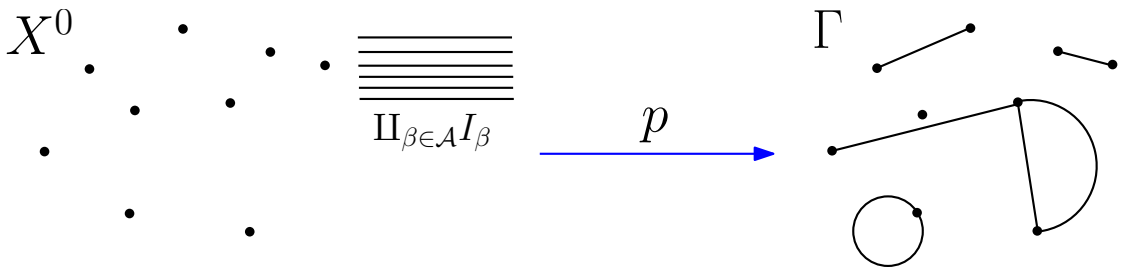

Figure 1.1: Γ is a quotient of $X^0 \amalg_{\beta\in\mathcal{A}} I_\beta$ obtained by identifying the endpoints of each interval I_β with points of X^0

Remark 1.1.2. A graph is a 1–dimensional CW complex. The 0–cells are the vertices, and the open 1–cells are the edges.

Definitions 1.1.3.

1. We also use the notation $V(\Gamma)$ and $E(\Gamma)$ for the sets of vertices and edges of Γ, respectively.

2. If $e = p(I_\beta^\circ)$ then we use the notation $\partial_0 e := p(\phi_\beta(0))$ and $\partial_1 e := p(\phi_\beta(1))$ for the *endpoints* of e. The topological boundary $\partial e = \overline{e} \setminus e$ of e is equal to $\{\partial_0 e, \partial_1 e\}$ and is contained in $V(\Gamma)$. A *closed edge* is the closure $\overline{e}$ of an edge e.

3. A vertex $v \in E(\Gamma)$ is *incident* to an edge $e \in E(\Gamma)$ (or vice-versa) if $v \in \partial e$. Edges $e, f \in E(\Gamma)$ are incident if $\partial e \cap \partial f \neq \emptyset$.

4. An edge $e \in E(\Gamma)$ such that $\partial_0 e = \partial_1 e$ is called a *loop*. If $e, f \in E(\Gamma)$ satisfy $\partial e = \partial f$ and $|\partial e| = |\partial f| = 2$, then e and f are said to be *multiple edges*.

5. A graph that has no loops or multiple edges is said to be *simple*. This is equivalent to the condition that Γ is a one-dimensional simplicial complex. Indeed, Γ is simple if and only if every edge has two endpoints and no two edges have the same set of endpoints.

6. Given a vertex $v \in V(\Gamma)$, the *degree* of v is

$$\mu(v) := |\{e \in E(\Gamma) : \partial_0 e = v\}| + |\{e \in E(\Gamma) : \partial_1 e = v\}|.$$

   Note that loops incident to v contribute 2 to $\mu(v)$. A vertex v is *isolated* if $\mu(v) = 0$, *free* if $\mu(v) = 1$, *non-essential* if $\mu(v) = 2$ and *branched* if $\mu(v) \geq 3$. If $x \in \Gamma \setminus V(\Gamma)$, then we set $\mu(x) = 2$.

7. A *subgraph* of Γ is a CW subcomplex of Γ.

8. A *cycle* is a subgraph homeomorphic to S^1. We use the notation $Z(\Gamma)$ for the set of cycles in Γ.

9. A basis $\mathcal{B}$ for the topology $\mathcal{T}$ on Γ is described as follows. A subset $G \subset \Gamma$ lies in $\mathcal{B}$ if and only if it contains a point x such that (G, x) is homeomorphic to the wedge sum $\bigvee_{\mu(x)}([0,1), 0)$, see Figure 1.2. This includes the case when x lies in an edge and $\mu(x) = 2$; in this case $G \cong [0,1) \vee [0,1)$ is a copy of $(0,1)$.

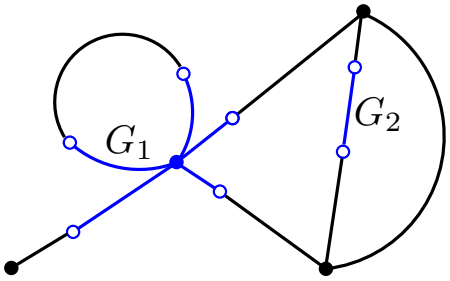

Figure 1.2: Examples of basis elements $G_1, G_2 \in \mathcal{B}$

Remark 1.1.4. Unless otherwise stated, all graphs are assumed to contain at least one edge and be finite and connected.

Example 1.1.5. Let Γ be the following subspace of $\mathbb{R}^2$.

Γ

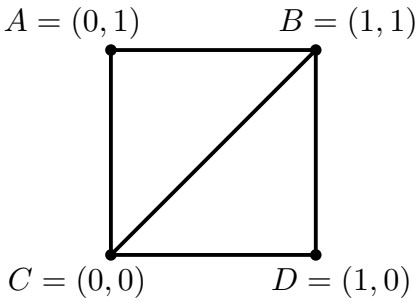

This space has a graph structure as follows. In the notation of Definitions 1.1.1, let $X^0 = \{A, B, C, D\}$, a discrete set of four points. Set $\mathcal{A} = \{1, 2, 3, 4, 5\}$ and define the map

$$\phi = \coprod_{j=1}^{5} \phi_j : \coprod_{j=1}^{5} \partial I_j \to X^0$$

by

$$\begin{aligned}
\phi_1(0) &= A, \quad \phi_1(1) = B, \\
\phi_2(0) &= A, \quad \phi_2(1) = C, \\
\phi_3(0) &= C, \quad \phi_3(1) = B, \\
\phi_4(0) &= B, \quad \phi_4(1) = D, \\
\phi_5(0) &= C, \quad \phi_5(1) = D.
\end{aligned}$$

It follows that Γ is the adjunction space $X^0 \sqcup_\phi \coprod_{j=1}^{5} I_j$. In this case, Γ is a simple graph with four vertices and five edges. There are two non-essential vertices and two branched vertices.

We continue with the definitions. Definition 1.1.6 is given in [7, §1] and will be needed in this thesis when we study discrete models in Chapter 4.

Definition 1.1.6 (Support)**.** Let Γ be a graph and let $x \in \Gamma$. The *support* of x is the smallest subgraph of Γ containing x, namely

$$\operatorname{supp}(x) := \begin{cases} \{x\}, & \text{if } x \in V(\Gamma), \\ \overline{e}, & \text{if } x \in e \text{ and } e \text{ is an edge of } \Gamma. \end{cases}$$

Definition 1.1.7 (Star)**.** Any point $x \in \Gamma$ has a neighbourhood U_x homeomorphic to the cone over a discrete set of $\mu(x)$ points. Such a neighbourhood of x will be referred to as a *star neighbourhood of* x, see Figure 1.3.

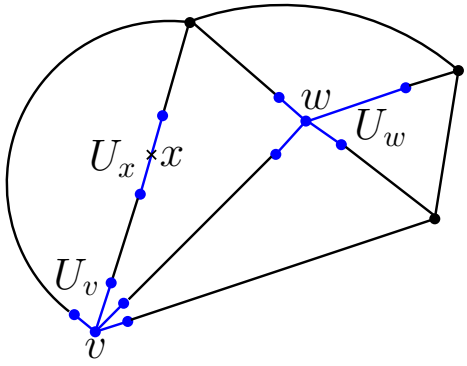

Figure 1.3: Star neighbourhoods U_x, U_v, U_w in Γ

Labelled graphs have an important role in this thesis.

Definition 1.1.8 (Labelled graph)**.** A labelled graph is a pair (Γ, ℓ) comprising a graph Γ together with a map $\ell : E(\Gamma) \to (0, \infty)$ assigning a positive number $\ell(e)$ to each edge $e \in E(\Gamma)$.

Example 1.1.9. Let Γ be the graph shown in Figure 1.4. There are six edges $e_1, \ldots, e_6$ comprising $E(\Gamma)$. The map $\ell : E(\Gamma) \to (0, \infty)$ is given by $\ell(e_1) = \ell(e_3) = 1$, $\ell(e_2) = 1/2$, $\ell(e_4) = 3/2$, $\ell(e_5) = \sqrt{2}$ and $\ell(e_6) = 5/6$.

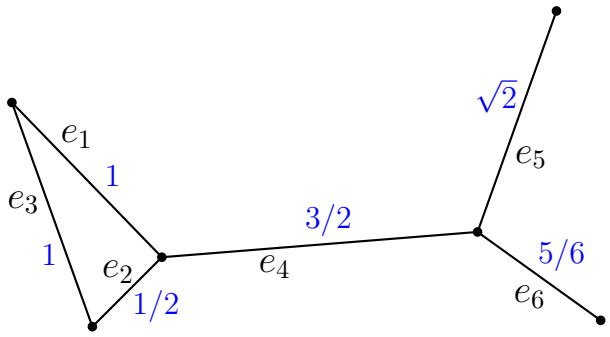

Figure 1.4: Assigning a label to each edge

In §1.2 and §1.3 we show that any labelled graph (Γ, ℓ) has an induced metric $d : \Gamma \times \Gamma \to \mathbb{R}$.

1.2 The length of an edgepath

In this section we begin by defining a metric on each edge of a labelled graph (Γ, ℓ). We then define an edgepath sequence in a graph and show how to define its length.

Definition 1.2.1. Let e be an edge of Γ. There are two cases, namely when $\overline{e}$ is homeomorphic to $[0,1]$ and when it is homeomorphic to S^1.

1. Suppose that $\overline{e}$ is homeomorphic to $[0,1]$. Let $T : \overline{e} \to [0,1]$ be the homeomorphism such that $T(\partial_0 e) = 0$, $T(\partial_1 e) = 1$ and $e \ni y \mapsto T(y) \in (0,1)$ is the identity map $\mathrm{id} : e \to (0,1)$. We define $\rho_{\overline{e}} : \overline{e} \times \overline{e} \to \mathbb{R}$ by

$$\rho_{\overline{e}}(x,y) = \ell(e)|T(x) - T(y)|, \quad \forall x, y \in \overline{e},$$

   where $\ell(e)$ is the label of the edge e.

2. Suppose that e is a loop. Let $T : \overline{e} \to S^1$ be the homeomorphism such that $T(\partial_0 e) = 1$ and $T(w) = e^{2\pi i w}$, for all $y \in e = (0,1)$. We define $\rho_{\overline{e}} : \overline{e} \times \overline{e} \to \mathbb{R}$ by

$$\rho_{\overline{e}}(x,y) = \frac{\ell(e)}{2\pi} \min\left\{|\arg T(x) - \arg T(y)|, 2\pi - |\arg T(x) - \arg T(y)|\right\},$$

   with the convention that $\arg z \in [0, 2\pi)$ for $z \in S^1$. That is, we define $\rho_{\overline{e}}(x,y)$ to be the length of the shorter of the two arcs joining $T(x)$ and $T(y)$ in a circle with circumference $\ell(e)$, see Figure 1.5.

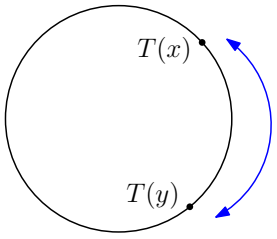

Figure 1.5: The shorter of the two arcs joining $T(x)$ and $T(y)$

Definition 1.2.2. An *edgepath sequence* is a finite sequence of points of Γ,

$$\mathbf{x} = (x_0, x_1, x_2, \ldots, x_n), \quad n \geq 1,$$

such that for each $i \in \{0, 1, \ldots, n-1\}$, there is a unique edge e_i such that $x_i, x_{i+1} \in \overline{e}_i$.

Example 1.2.3. On the left of Figure 1.6, (x_0, x_1, x_2, x_3) is not an edgepath sequence because $x_1, x_2 \in \overline{e}_1, \overline{e}_2$ and $e_1 \neq e_2$. On the right of Figure 1.6, $(x_0, \ldots, x_4)$ is an edgepath sequence.

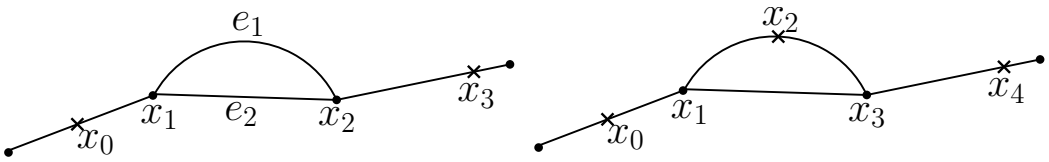

Figure 1.6: A sequence which is not an edgepath sequence and one that is

Definition 1.2.4. The *length* of an edgepath sequence $\mathbf{x} = (x_0, \ldots, x_n)$ is

$$L_{\mathbf{x}} := \sum_{i=0}^{n-1} \rho_{\overline{e}_i}(x_i, x_{i+1}).$$

Example 1.2.5. Consider the edgepath sequence $\mathbf{x} = (x_0, x_1, \ldots, x_9)$ in Figure 1.7. We have $L_{\mathbf{x}} = 1 + 4 \times 1/2 + 1 + 2 + 2 \times 1 = 8$.

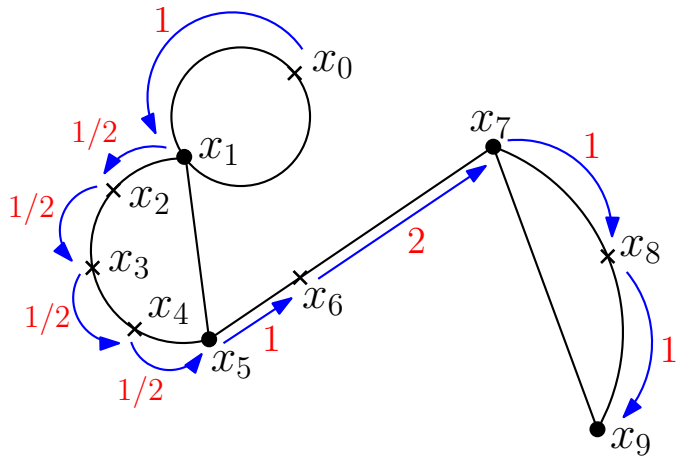

Figure 1.7: The length of an edgepath sequence

1.3 The induced metric

We proceed with the construction of the metric d induced on Γ by an edge-labelling $\ell : E(\Gamma) \to (0, \infty)$.

Remark 1.3.1. Since Γ is path-connected, it has the following property: for any $x, y \in \Gamma$ there is an edgepath sequence $\mathbf{x} = (x_0, x_1, \ldots, x_n)$ with $x_0 = x$ and $x_n = y$. Let $P(x, y)$ be the set of all such edgepath sequences.

Definition 1.3.2. For any $x, y \in \Gamma$, the set $\{L_{\mathbf{x}} : \mathbf{x} \in P(x, y)\}$ is nonempty and bounded below by zero. We define $d : \Gamma \times \Gamma \to \mathbb{R}$ by $d(x, y) := \inf\{L_{\mathbf{x}} : \mathbf{x} \in P(x, y)\}$.

Theorem 1.3.3. *The map $d : \Gamma \times \Gamma \to \mathbb{R}$ is a metric.*

Proof. From the definition, $d(x, y) \geq 0$ for all $x, y \in \Gamma$. If $x = y$, then $\mathbf{x} = (x, y)$ is an edgepath sequence with $L_{\mathbf{x}} = 0$, so $d(x, y) = 0$. Assume that $x \neq y$. We distinguish four cases.

(i) If $x, y \in V(\Gamma)$, then $L_{\mathbf{x}} \geq \min_{e \in E(\Gamma)} \ell(e)$ for all $\mathbf{x} \in P(x, y)$.

(ii) If one of x, y is a vertex and the other is not, say $x \in V(\Gamma)$ and $y \in e$, then $L_{\mathbf{x}} \geq \rho_{\overline{e}}(y, \partial e) > 0$ for all $\mathbf{x} \in P(x, y)$.

(iii) If x, y lie in distinct edges e, f, respectively, then $L_{\mathbf{x}} \geq \rho_{\overline{e}}(x, \partial e) + \rho_{\overline{f}}(y, \partial e) > 0$ for all $\mathbf{x} \in P(x, y)$.

(iv) If x, y lie in the same edge e, then

$$L_{\mathbf{x}} \geq \min\{\rho_{\overline{e}}(x, y), \rho_{\overline{e}}(x, \partial e) + \rho_{\overline{e}}(y, \partial e)\} > 0, \quad \forall \mathbf{x} \in P(x, y).$$

In all cases we obtain $d(x, y) > 0$. To prove symmetry, first define

$$\mathbf{x}^t := (x_n, x_{n-1}, \ldots, x_1, x_0)$$

whenever $\mathbf{x} = (x_0, \ldots, x_n)$ is an edgepath sequence. Then $\mathbf{x} \in P(x, y)$ if and only if $\mathbf{x}^t \in P(y, x)$, and

$$L_{\mathbf{x}^t} = \sum_{i=0}^{n-1} \rho_{\overline{e}_i}(x_{i+1}, x_i) = \sum_{i=0}^{n-1} \rho_{\overline{e}_i}(x_i, x_{i+1}) = L_{\mathbf{x}},$$

from the symmetry of each $\rho_{\bar{e}_i}$. This gives

$$\begin{aligned} d(x,y) &= \inf\{L_{\mathbf{x}} : \mathbf{x} \in P(x,y)\} = \inf\{L_{\mathbf{x}^t} : \mathbf{x} \in P(x,y)\} \\ &= \inf\{L_{\mathbf{w}} : \mathbf{w} \in P(y,x)\} = d(y,x). \end{aligned}$$

To prove the triangle inequality, let

$$\mathbf{x}_1 = (x_0, \ldots, x_n) \in P(x,y), \quad \mathbf{x}_2 = (y_0, \ldots, y_m) \in P(y,z)$$

be arbitrary. Define

$$\mathbf{x}_1 : \mathbf{x}_2 := (x_0, x_1, \ldots, x_n, y_0, y_1, \ldots, y_m);$$

then $\mathbf{x}_1 : \mathbf{x}_2 \in P(x,z)$ and

$$d(x,z) \leq L_{\mathbf{x}_1:\mathbf{x}_2} = L_{\mathbf{x}_1} + L_{\mathbf{x}_2}.$$

Taking the infimum over all $\mathbf{x}_1 \in P(x,y)$ and then over all $\mathbf{x}_2 \in P(y,z)$ gives $d(x,z) \leq d(x,y) + d(y,z)$. □

This metric induces a topology $\tau(d)$ on Γ, so it is natural to ask if it is related to the CW topology. The answer is given by the following statement.

Proposition 1.3.4. *If (Γ, ℓ) is a finite, connected labelled graph then the* CW *topology $\mathcal{T}$ coincides with the metric topology $\tau(d)$.*

Proof. We show that a basis for $\tau(d)$ is contained in $\mathcal{T}$, and vice-versa. For $\mathcal{T}$, we use the basis $\mathcal{B}$ from Definitions 1.1.3, see Figure 1.2. For $\tau(d)$ we use the basis $\mathcal{B}_d$ comprising the balls $B_r(x)$ for $x \in \Gamma$ and $r > 0$.

(i) To show that $\mathcal{B}_d \subseteq \mathcal{T}$, fix $x \in \Gamma$, and define

$$r(x) := \begin{cases} \frac{1}{2} \min\{\ell(e) : e \in E(\Gamma),\ x \in \partial e\}, & \text{if } x \in V(\Gamma), \\ d(x, V(\Gamma)), & \text{if } x \notin V(\Gamma), \end{cases}$$

see Figure 1.8. For any $0 < r < r(x)$, the pair $(B_r(x), x)$ is homeomorphic to $\bigvee_{\mu(x)}([0,1), 0)$ and thus $B_r(x) \in \mathcal{B}$.

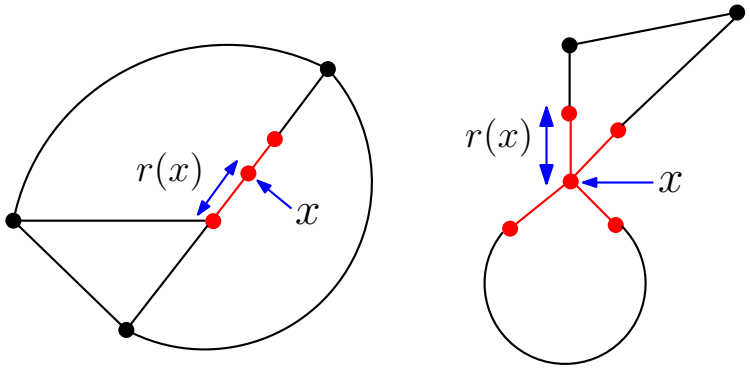

Figure 1.8: The definition of $r(x)$

(ii) We now show that $\mathcal{B} \subseteq \tau(d)$. Let $G \in \mathcal{B}$ and choose $x \in G$ such that $(G, x) \cong \bigvee_{\mu(x)}([0,1), 0)$. If $\mu(x) = 2$, then G is a copy of $(0,1)$ and contains a metric ball around each of its points. If $\mu(x) \neq 2$, then $x \in V(\Gamma)$. For any $y \in G \setminus \{x\}$ we have $\mu(y) = 2$ and so G contains a metric ball around y. If $y = x$ then we set $r := \min_{p \in \partial G} d(x, p)$ to obtain $B_r(x) \subseteq G$, see Figure 1.9. Hence G is $\tau(d)$–open.

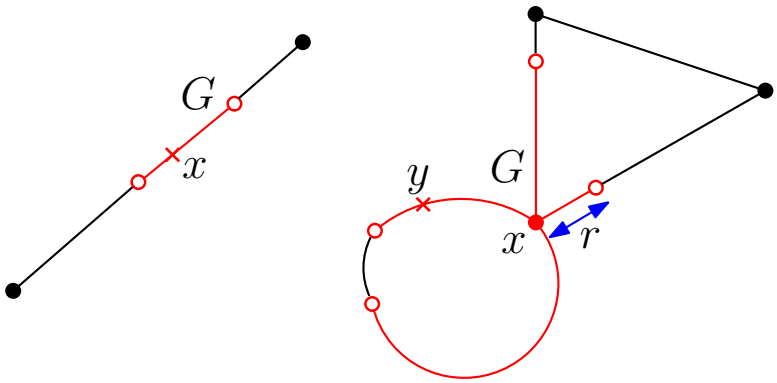

Figure 1.9: Sets $G \in \mathcal{B}$, a typical $y \in G$ and the definition of r if $y = x$

□

Corollary 1.3.5. *Any two labellings $\ell_1, \ell_2 : E(\Gamma) \to (0, \infty)$ induce homeomorphic metric spaces (Γ, d_1), (Γ, d_2).*

Remark 1.3.6. These metric spaces need not be isometric – for example, consider two distinct labellings of $\Gamma = [0,1]$ with its minimal graph structure.

1.4 Special paths and further metric properties

In this section we introduce terminology for different types of paths and then mention some interesting properties of the induced metric on a labelled graph (Γ, ℓ).

Definition 1.4.1. Let (Y, ρ) be a metric space. A path $c : [0,1] \to Y$ has *constant speed* if

$$\rho(c(s), c(t)) = \rho(c(0), c(1))|s - t|, \quad \forall s, t \in [0,1].$$

Definitions 1.4.2. Let (Γ, ℓ) be a labelled graph.

1. If $x, y \in \overline{e}$ and e is not a loop, then denote the unique constant-speed path in $(\overline{e}, \rho_{\overline{e}})$ from x to y by $p_{(x,y)} : [0,1] \to (\overline{e}, \rho_{\overline{e}})$.

2. If e is a loop and $\rho_{\overline{e}}(x, y) \neq \ell(e)/2$, then there is a unique constant-speed path $p_{(x,y)}$ in $(\overline{e}, \rho_{\overline{e}})$ from x to y (following the shorter of the two geodesic arcs). If $\rho_{\overline{e}}(x, y) = \ell(e)/2$, then there are exactly two constant-speed paths in $(\overline{e}, \rho_{\overline{e}})$ from x to y. Let $p_{(x,y)}$ denote the path that traverses $\overline{e}$ in the anticlockwise direction.

We now define the path induced by an edgepath sequence.

Definitions 1.4.3. Let $\mathbf{x} = (x_0, x_1, \ldots, x_n)$ be an edgepath sequence. The *path* $\gamma_{\mathbf{x}} : [0,1] \to \Gamma$ *induced by* $\mathbf{x}$ is the concatenation

$$p_{(x_0,x_1)} \cdot p_{(x_1,x_2)} \cdot \ldots \cdot p_{(x_{n-1},x_n)} : [0,1] \to \Gamma,$$

using the interval $[t_i, t_{i+1}] \subset [0,1]$ for $p_{(x_i,x_{i+1})}$, where

$$t_k := \frac{1}{L_{\mathbf{x}}} \sum_{j=0}^{k-1} \rho_{\overline{e}_j}(x_j, x_{j+1}),$$

provided that $L_{\mathbf{x}} \neq 0$. If $L_{\mathbf{x}} = 0$, then $\gamma_{\mathbf{x}}$ is the constant path with value x_0. The *length* of $\gamma_{\mathbf{x}}$ is $L(\gamma_{\mathbf{x}}) := L_{\mathbf{x}}$.

A path $c : [0,1] \to \Gamma$ is an *edgepath* if there is an edgepath sequence $\mathbf{x}$ such that $\gamma_{\mathbf{x}} = c$. An edgepath $\gamma_{\mathbf{x}}$, where $\mathbf{x} = (x_0, \ldots, x_n)$, is *minimal-length* if $L(\gamma_{\mathbf{x}}) = d(x_0, x_n)$.

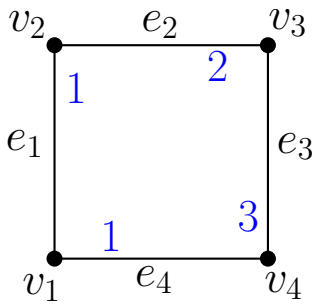

Figure 1.10: The labelled graph structure on Γ

Example 1.4.4. Let Γ be the boundary of the unit square $[0,1] \times [0,1]$ with the labelled graph structure shown in Figure 1.10. Consider the edgepath sequence $\mathbf{x} = (v_1, v_2, v_3, v_4)$. We have $L_{\mathbf{x}} = 6$ and the path $\gamma_{\mathbf{x}}$ induced by $\mathbf{x}$ is the concatenation

$$p_{(v_1,v_2)} \cdot p_{(v_2,v_3)} \cdot p_{(v_3,v_4)} : [0,1] \to \Gamma,$$

where we use $[0, 1/6]$ for $p_{(v_1,v_2)}$, $[1/6, 1/2]$ for $p_{(v_2,v_3)}$ and $[1/2, 1]$ for $p_{(v_3,v_4)}$. This gives the formula

$$\gamma_{\mathbf{x}}(t) = \begin{cases} (0, 6t), & t \in [0, 1/6], \\ (3t - 1/2, 1), & t \in [1/6, 1/2], \\ (1, 2 - 2t), & t \in [1/2, 1]. \end{cases}$$

Moreover $L(\gamma_{\mathbf{x}}) = 6 \neq 1 = d(v_1, v_4)$, so $\gamma_{\mathbf{x}}$ is not minimal-length. On the other hand, if $\mathbf{y} = (v_1, v_4)$, then $\gamma_{\mathbf{y}}(t) = (t, 0)$ for all $t \in [0, 1]$ and $\gamma_{\mathbf{y}}$ is minimal-length since $L(\gamma_{\mathbf{y}}) = 1 = d(v_1, v_4)$.

We now define a *circuit*. These are used in the proof of Theorem 4.2.4.

Definition 1.4.5. A *circuit* is the image of a path $\gamma_{\mathbf{x}}$ induced by an edgepath sequence $\mathbf{x} = (x_0, \ldots, x_n)$ such that $x_0, \ldots, x_n \in V(\Gamma)$, $x_0 = x_n$ and such that any given vertex appears at most twice in the sequence $x_0, \ldots, x_n$.

We also have the following simple result which states that the infimum in Definition 1.3.2 is achieved.

Lemma 1.4.6. *For all $x, y \in \Gamma$ there is an edgepath sequence $\mathbf{x} = (x, \ldots, y)$ such that $L_{\mathbf{x}} = d(x, y)$.*

Proof. Choose edges e, f such that $x \in \overline{e}$ and $y \in \overline{f}$. For each $v \in \partial e$ and $w \in \partial f$, consider the edgepath sequences $\mathbf{x}(v,w) = (v, \ldots, w)$ with vertex entries. Since Γ is finite, these yield finitely many values $L_{\mathbf{x}(v,w)}$, at least one of which is $d(v,w)$. Hence, there are finitely many values $L_{(x):\mathbf{x}(v,w):(y)}$ as v, w range over $\partial e, \partial f$ respectively, and together with $\rho_{\overline{e}}(x,y)$ if $e = f$, at least one of these is $d(x,y)$. □

Corollary 1.4.7. *For any $x, y \in \Gamma$ there is a minimal-length edgepath from x to y.*

The following lemma is used in various contexts throughout the thesis.

Lemma 1.4.8. *A minimal-length edgepath has constant speed.*

Proof. Let $\mathbf{x} = (x_0, x_1, \ldots, x_n)$ be an edgepath sequence such that $c = \gamma_{\mathbf{x}} : [0,1] \to \Gamma$ is minimal-length. Seeking a contradiction, assume that c does not have constant speed, so that there exist $s, t \in [0,1]$, $s < t$, such that

$$d(c(s), c(t)) \neq d(c(0), c(1))|s - t|.$$

Since

$$d(c(s), c(t)) \leq |s - t| L(\gamma_{\mathbf{x}}) = |s - t| d(c(0), c(1)),$$

we obtain $d(c(s), c(t)) < |s - t| d(c(0), c(1))$. Now choose edgepath sequences

$$\mathbf{y}_1 := (x_0, x_1, \ldots, x_p, c(s)), \quad \mathbf{y}_2 := (c(s), x_{p+1}, \ldots, x_q, c(t)),$$

and $\mathbf{y}_3 := (c(t), x_{q+1}, \ldots, x_n)$ such that $L(\gamma_{\mathbf{x}}) = L_{\mathbf{y}_1} + L_{\mathbf{y}_2} + L_{\mathbf{y}_3}$, see Figure 1.11. We have

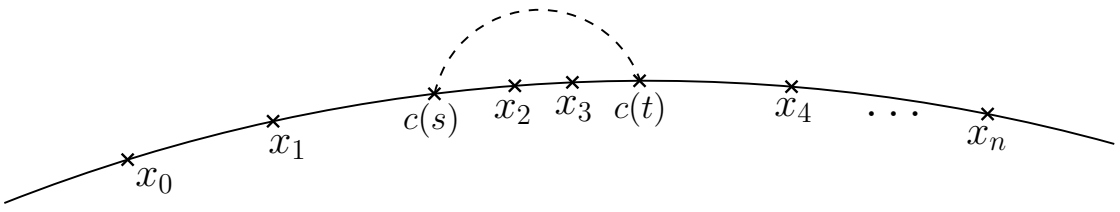

Figure 1.11: Construction of $\mathbf{y}_1$,$\mathbf{y}_2$ and $\mathbf{y}_3$

$$L_{\mathbf{y}_2} = |s - t| L(\gamma_{\mathbf{x}}) = |s - t| d(c(0), c(1)) > d(c(s), c(t)),$$

so

$$\begin{aligned} d(c(0), c(1)) = L(\gamma_{\mathbf{x}}) &= L_{\mathbf{y}_1} + L_{\mathbf{y}_2} + L_{\mathbf{y}_3} \\ &> d(c(0), c(s)) + d(c(s), c(t)) + d(c(t), c(1)) \\ &\geq d(c(0), c(1)). \end{aligned}$$

□

We finish this section with two metric properties.

Lemma 1.4.9. (Γ, d) *is complete.*

Proof. $(\Gamma, \mathcal{T})$ is compact since it is a finite CW complex. Proposition 1.3.4 implies that $(\Gamma, \tau(d))$ is compact. A compact metric space is complete. □

Definition 1.4.10. A metric space (Y, ρ) has the *midpoint property* if for all $x, y \in Y$ there exists $z \in Y$ such that $\rho(z, x) = \rho(z, y) = \frac{1}{2}\rho(x, y)$.

Lemma 1.4.11. (Γ, d) *has the midpoint property.*

Proof. Let $x, y \in \Gamma$ be distinct, and let $\gamma : [0, 1] \to \Gamma$ be a minimal-length edgepath from x to y (such a path exists by Corollary 1.4.7). Lemma 1.4.8 shows that

$$d(\gamma(s), \gamma(t)) = d(\gamma(0), \gamma(1))|t - s|, \quad \forall s, t \in [0, 1].$$

Taking $z = \gamma(1/2)$ we obtain $d(z, x) = \frac{1}{2}d(x, y) = d(z, y)$. □

1.5 Basic operations and the cycle inequality

In this section we describe the procedures of subdivision and amalgamation in a labelled graph. Subdivision is the procedure of inserting vertices to create additional edges, and amalgamation is the procedure of removing non-essential vertices. We then define a version of the triangle inequality for a labelled graph, which we call the cycle inequality.

1.5.1 Subdivision

The subdivision procedure for a labelled graph is similar to that given in [1, Definition 2.3] for graphs.

Definitions 1.5.1. Let $e \in E(\Gamma)$ and let $y \in e$. The labelled graph (Γ_s, ℓ_s) *obtained from* (Γ, ℓ), e *and* y *by subdivision* is defined as follows.

(i) If $\overline{e}$ is homeomorphic to $[0,1]$, then $V(\Gamma_s) = V(\Gamma) \cup \{y\}$ and $E(\Gamma_s) = (E(\Gamma) - \{e\}) \cup \{f, g\}$, where the new edges f and g satisfy $\partial_0 f = \partial_0 e$, $\partial_1 f = y = \partial_0 g$, and $\partial_1 g = \partial_1 e$. The labels of f and g are $\ell_s(f) = \rho_{\overline{e}}(\partial_0 e, y)$ and $\ell_s(g) = \rho_{\overline{e}}(y, \partial_1 e)$, and $\ell_s(h) = \ell(h)$ for all $h \in E(\Gamma) - \{e\}$.

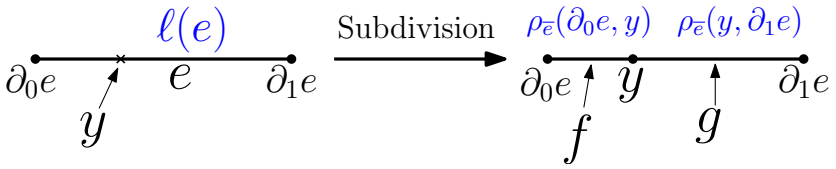

(ii) If e is a loop, then Γ_s has the same vertices and edges as in case (i). Let $T : \overline{e} \to S^1$ be the unique homeomorphism such that $T(\partial_0 e) = 1$ and $T(w) = e^{2\pi i w}$ for all $w \in e = (0,1)$. If $\arg T(y) \in [0, \pi)$ then we set $\ell_s(f) = \rho_{\overline{e}}(\partial_0, y)$ and $\ell_s(g) = \ell(e) - \rho_{\overline{e}}(\partial_0, y)$. If $\arg T(y) \in [\pi, 2\pi)$, then we set $\ell_s(f) = \ell(e) - \rho_{\overline{e}}(\partial_0, y)$ and $\ell_s(g) = \rho_{\overline{e}}(\partial_0, y)$, see Figure 1.12.

A *subdivision* of (Γ, ℓ) is a labelled graph obtained by subdividing (Γ, ℓ) finitely many times.

We have the following simple but important observation about subdivision.

Lemma 1.5.2. *Suppose that* (Γ_s, ℓ_s) *is a subdivision of* (Γ, ℓ). *If* d_s *and* d *are the induced metrics on* Γ_s *and* Γ, *respectively, then* (Γ_s, d_s) *and* (Γ, d) *are isometric.*

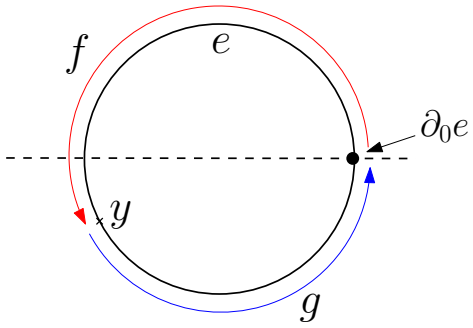

Figure 1.12: Subdividing a loop: $\arg T(w) \in [0, \pi)$ above the horizontal line, and $\arg T(w) \in [\pi, 2\pi)$ below

1.5.2 Amalgamation

Amalgamation is the procedure of removing non-essential vertices ($\mu(v) = 2$) from a labelled graph.

Definitions 1.5.3. Let v be a non-essential vertex with distinct incident edges $e \neq f$. The labelled graph (Γ_a, ℓ_a) *obtained from* (Γ, ℓ) *and* v *by amalgamation* is defined as follows. We set $V(\Gamma_a) = V(\Gamma) - \{v\}$ and $E(\Gamma_a) = (E(\Gamma) - \{e, f\}) \cup \{g\}$, where $\partial_0 g, \partial_1 g$ are the unique elements of $\partial e - \{v\}$ and $\partial f - \{v\}$, respectively. Further, $\ell_a(g) = \ell(e) + \ell(f)$ and $\ell_a(h) = \ell(h)$ for all $h \in E(\Gamma) - \{e, f\}$, see the following diagram.

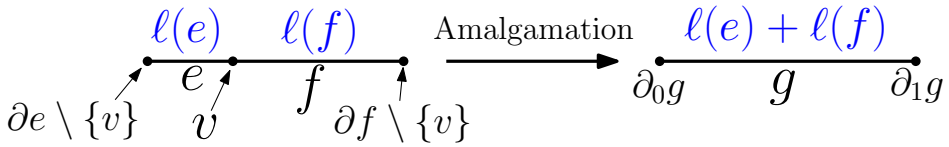

An *amalgam* of (Γ, ℓ) is a labelled graph obtained from (Γ, ℓ) by performing finitely many amalgamations.

We also have the analogue of Lemma 1.5.2 for amalgamation.

Lemma 1.5.4. *Suppose that* (Γ_a, ℓ_a) *is an amalgam of* (Γ, ℓ). *If* d_a *and* d *are the induced metrics on* Γ_a *and* Γ, *respectively, then* (Γ_a, d_a) *and* (Γ, d) *are isometric.*

1.5.3 The cycle inequality

In this subsection we define the cycle inequality for a simple labelled graph. We first make the following observation.

Lemma 1.5.5. *Let (Γ, ℓ) be a labelled graph. There exists a subdivision (Γ_s, ℓ_s) such that Γ_s is simple.*

Proof. A loop e may be removed by inserting two new vertices into e. Let $v, w \in V(\Gamma)$ be distinct, and suppose that there are exactly $N > 1$ edges $e_1, \ldots, e_N$ with boundary $\{v, w\}$. Insert a new vertex into e_j for each $j \in \{1, \ldots, N-1\}$. This removes the multiple edges connecting v and w. Since Γ is finite, there are only finitely many loops and multiple edges to be removed. □

Notation 1.5.6. If Γ is simple, then each cycle is the union at least three closed edges. If $C \in Z(\Gamma)$, then we use the notation $C = (e_1, \ldots, e_K)$ to indicate that $C = \bigcup_{j=1}^{K} \overline{e}_j$ and that edge e_j is incident to edges e_{j+1} and e_{j-1}, for $1 \leq j \leq K$, subscripts being taken modulo K, see Figure 1.13.

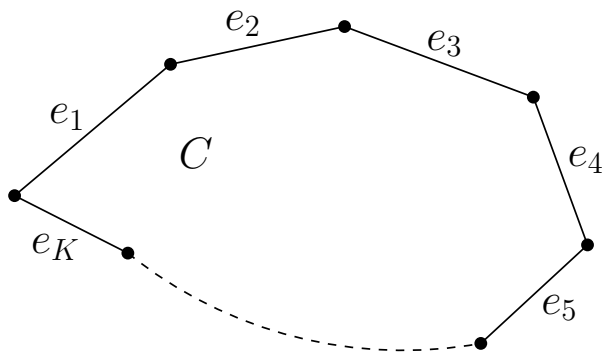

Figure 1.13: A cycle $C = (e_1, \ldots, e_K)$ in a simple graph

Definition 1.5.7 (Cycle inequality)**.** Let (Γ, ℓ) be a simple labelled graph. A cycle $C = (e_1, \ldots, e_K)$ *satisfies the cycle inequality* if

$$\ell(e_j) \leq \sum_{\substack{1 \leq k \leq K \\ k \neq j}} \ell(e_k), \quad \forall j \in \{1, \ldots, K\}.$$

(Γ, ℓ) *satisfies the cycle inequality* if every cycle $C \in Z(\Gamma)$ satisfies the cycle inequality.

We now give an equivalent condition for the cycle inequality to be satisfied in terms of the induced metric. For $e \in E(\Gamma)$, we use the notation $d_{\overline{e}}$ for the metric on $\overline{e}$ obtained by restricting d to $\overline{e} \times \overline{e}$.

Proposition 1.5.8. *A simple labelled graph (Γ, ℓ) satisfies the cycle inequality if and only if $d_{\overline{e}} = \rho_{\overline{e}}$ for each $e \in E(\Gamma)$.*

Proof. Suppose that $d_{\overline{e}} \neq \rho_{\overline{e}}$ for some $e \in E(\Gamma)$. Then there exist $x, y \in \overline{e}$ such that $d_{\overline{e}}(x, y) < \rho_{\overline{e}}(x, y)$. Write $\partial e = \{v, w\}$ and assume without loss of generality that v, w, x, y are as in the following diagram (otherwise, interchange x and y).

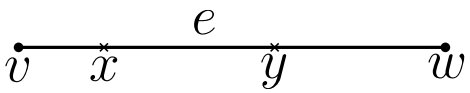

Since $d(x, y) < \rho_{\overline{e}}(x, y)$, there exist $e_1, \ldots, e_N \in E(\Gamma)$ such that $C = (e, e_1, \ldots, e_N) \in Z(\Gamma)$ and

$$\ell(e_1) + \cdots + \ell(e_N) + \rho_{\overline{e}}(v, x) + \rho_{\overline{e}}(y, w) < \rho_{\overline{e}}(x, y).$$

This implies

$$\begin{aligned} \ell(e_1) + \cdots + \ell(e_N) &\leq \ell(e_1) + \cdots + \ell(e_N) + \rho_{\overline{e}}(v, x) + \rho_{\overline{e}}(y, w) \\ &< \rho_{\overline{e}}(x, y) \leq \ell(e), \end{aligned}$$

so C does not satisfy the cycle inequality. Conversely, assume that the cycle inequality fails for some cycle $C = (e_1, \ldots, e_K)$. This means that

$$\ell(e_j) > \sum_{\substack{1 \leq k \leq K \\ k \neq j}} \ell(e_k),$$

for some $j \in \{1, \ldots, K\}$. Write $\partial e_j = \{v, w\}$, and let $\mathbf{x} = (v, \ldots, w)$ be the sequence comprising the vertices in C in cyclic order starting with v and finishing with w. This is an edgepath sequence since Γ has no multiple edges. We have $L_{\mathbf{x}} = \sum_{\substack{1 \leq k \leq K \\ k \neq j}} \ell(e_k)$, so

$$\rho_{\overline{e}_j}(v, w) = \ell(e_j) > L_{\mathbf{x}} \geq d(v, w) = d_{\overline{e}_j}(v, w),$$

showing that $d_{\overline{e}_j} \neq \rho_{\overline{e}_j}$. □

Corollary 1.5.9. *If (T, ℓ) is a labelled tree with induced metric d, then $d_{\overline{e}} = \rho_{\overline{e}}$ for each $e \in E(T)$.*

Proof. T contains no cycles, so trivially satisfies the cycle inequality. □

We conclude this section by showing that a labelled graph satisfies the cycle inequality given sufficient subdivision.

Lemma 1.5.10. *Any labelled graph* (Γ, ℓ) *admits a subdivision satisfying the cycle inequality.*

Proof. In view of Lemma 1.5.5, it may be assumed that Γ is simple. Suppose that $C = (e_1, \ldots, e_K)$ does not satisfy the cycle inequality. This means that there exists $j \in \{1, \ldots, K\}$ such that

$$\ell(e_j) > \sum_{\substack{1 \leq k \leq K \\ k \neq j}} \ell(e_k).$$

Choose $N \in \mathbb{N}$ such that

$$\frac{1}{N} \leq \frac{1}{2\ell(e_j)} \sum_{k=1}^{K} \ell(e_k).$$

Now form a subdivision of (Γ, ℓ) by inserting $(N-1)$ equally-spaced vertices into edge e_j, so that the N new edges each have label $\ell(e_j)/N$. We obtain

$$\frac{\ell(e_j)}{N} \leq \sum_{\substack{1 \leq k \leq K \\ k \neq j}} \ell(e_k) + (N-1)\frac{\ell(e_j)}{N},$$

so the failure of the cycle inequality for C on e_j has been eliminated. Repeat this procedure for each edge of C on which the cycle inequality fails. Finally, repeat the whole process for each cycle which does not satisfy the cycle inequality. There are finitely many cycles, so the result is a subdivision of (Γ, ℓ) which satisfies the cycle inequality. □

Chapter 2

PL Morse–Bott theory

We begin by developing our main tool for studying configuration spaces of thick particles on graphs. This tool is a suitably modified version of the piecewise linear (PL) Morse theory developed by M. Bestvina and N. Brady (see [8, §2] and the expository paper [9]), which we call PL Morse–Bott theory. The main results of this thesis in Chapters 3 and 5, as well as the results in Chapter 6, all follow from application of this theory.

In §2.1, we extend Bestvina and Brady's PL Morse theory to apply to a larger class of functions, which we call *affine Morse–Bott* functions. We then verify in §2.2 that the induced metric d on a metric graph belongs to this class. This enables us to apply the general results from §2.1 to d and obtain information about the preimages $\{d^{-1}([y,\infty))\}_{y>0}$ (which are precisely the thick particle configuration spaces $\{F_r(\Gamma,2)\}_{r>0}$, see §0.2). We apply the results of §2.1 in Chapter 3, see §3.2.

2.1 Developing PL Morse–Bott theory

In this section we establish PL Morse–Bott theory, the main mathematical tool of this thesis. We begin with the basic definitions and examples, extending the original results due to M. Bestvina and N. Brady [8, §2] on PL Morse theory to the Morse–Bott case. The difference is that we allow our functions to be constant on cells of positive dimension. This is the reason for choosing the terminology "Morse–Bott".

2.1.1 Definitions and examples

Definition 2.1.1 (see [9], Definition 2.1)**.** An *affine polytope complex of dimension* $m \geq 1$ is a CW complex X in which each closed cell F is equipped with a *characteristic function* $\chi_F : C_F \to X$ such that:

(i) C_F is a convex polyhedral cell in $\mathbb{R}^m$ for each F;

(ii) χ_F is an embedding for each closed cell F;

(iii) the restriction of χ_F to any face of C_F coincides with the characteristic function of another cell precomposed with an affine homeomorphism of $\mathbb{R}^m$.

(An *affine homeomorphism* of $\mathbb{R}^m$ is a map $h : \mathbb{R}^m \to \mathbb{R}^m$ of the form $h(\mathbf{x}) = A\mathbf{x}+\mathbf{b}$, for some invertible matrix $A \in \mathbb{R}^{m\times m}$ and $\mathbf{b} \in \mathbb{R}^m$).

Example 2.1.2. The space X shown in Figure 2.1 is an affine polytope complex of dimension three.

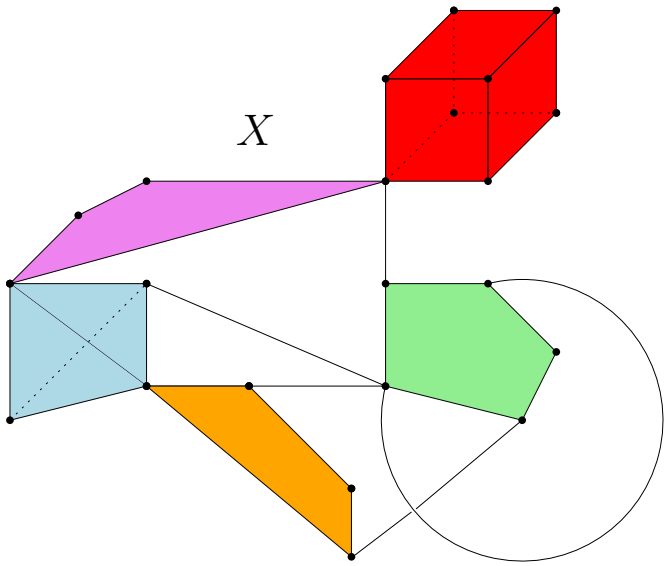

Figure 2.1: An example of an affine polytope complex

Let X be an affine polytope complex of dimension m.

Definition 2.1.3. A continuous map $f : X \to \mathbb{R}$ is an *affine Morse–Bott function* if $f \circ \chi_F : C_F \to \mathbb{R}$ extends to an affine function $\mathbb{R}^m \to \mathbb{R}$ for each cell $F \subset X$.

Remarks 2.1.4. We emphasise that $f \circ \chi_F$ may be constant on a cell $F \subset X$ with $\dim F > 0$. The set of all affine Morse–Bott functions $X \to \mathbb{R}$ forms a vector space over $\mathbb{R}$. In particular, if f is an affine Morse–Bott function then so is $-f$.

Let $f : X \to \mathbb{R}$ be an affine Morse–Bott function.

Definition 2.1.5. A cell F of X is *critical* if f is constant on F.

Remark 2.1.6. In particular, all 0–cells of X are critical.

Definition 2.1.7. A number $R \in \mathbb{R}$ is a *critical level* of f if there exists a cell F of X on which f is constant with value R.

Definition 2.1.8. The union of all critical cells is the *critical subcomplex* of f, and is denoted by $C(f)$.

Remarks 2.1.9.

(i) If f is constant on an open cell $e \subset X$, then by continuity f is constant on $\overline{e}$. Hence, $C(f)$ is indeed a subcomplex of X.

(ii) $C(f) = \amalg_R C(f, R)$ is the disjoint union of the subcomplexes $C(f, R)$, where R ranges over all critical levels of f and $C(f, R)$ is the union of all critical cells K such that $f|_K \equiv R$.

(iii) Writing $C(f) = \amalg_{\alpha \in A} Z_\alpha$ as the union of its connected components refines the decomposition from (ii), that is, for each $\alpha \in A$ there is a critical level R such that $Z_\alpha \subset C(f, R)$.

Definition 2.1.10. A non-critical cell K of X is *descending* if $f|_K$ achieves its maximum on a subcomplex of $K \cap C(f)$.

Notation 2.1.11. If $f : X \to \mathbb{R}$ is an affine Morse–Bott function and $c \in \mathbb{R}$, we write $X^c := f^{-1}((-\infty, c])$.

Example 2.1.12. Consider the affine polytope complex X and the function $f : X \to \mathbb{R}$ shown in Figure 2.2. The space X has one 3–cell K, a 2–cell H and two 1–cells e_1 and e_2. We see that f is an affine Morse–Bott function on X. The critical cells

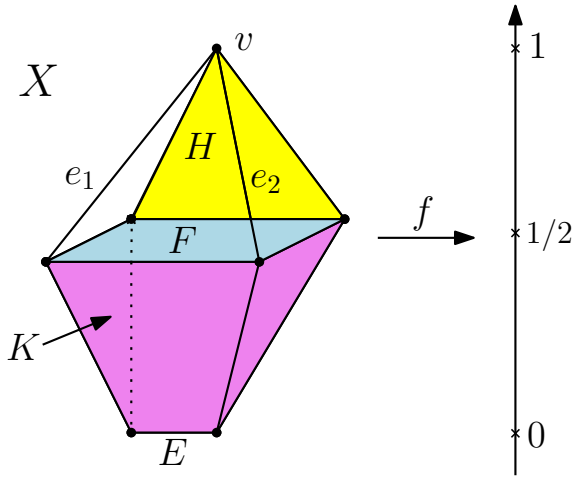

Figure 2.2: The function $f : X \to \mathbb{R}$

are v (a 0–cell), F (a 2–cell in the boundary of K) and E (a 1–cell in the boundary of K). The critical levels are 0 (from E), 1/2 (from F) and 1 (from v). The critical subcomplex is $C(f) = E \sqcup F \sqcup v$, and $C(f,0) = E$, $C(f,1/2) = F$, $C(f,1) = v$. The descending cells are H ($f|_H$ achieves its maximum on $v \subset H \cap C(f)$), e_1 and e_2 ($f|_{e_j}$ achieves its maximum on $v \subset e_j \cap C(f)$, $j = 1, 2$) and K ($f|_K$ achieves its maximum on $F \subset K \cap C(f)$).

2.1.2 Descending sets and links

We now define the descending set $D_\downarrow(Z_\alpha)$ and the descending link $\mathrm{Lk}_\downarrow(Z_\alpha)$ of a connected component Z_α of the critical subcomplex $C(f)$. Suppose that $f|_{Z_\alpha} \equiv R$. Choose $S < R$ such that the interval $[S, R)$ does not contain any critical level of f.

Definition 2.1.13. The *descending set* $D_\downarrow(Z_\alpha)$ of Z_α is

$$D_\downarrow(Z_\alpha) := f^{-1}([S,R]) \cap \bigcup K,$$

where the union is taken over the cells K of X such that $f|_K$ achieves its maximum on $K \cap Z_\alpha$.

Remark 2.1.14. $D_\downarrow(Z_\alpha)$ is a closed subspace of X containing Z_α.

Definition 2.1.15. The descending link $\mathrm{Lk}_\downarrow(Z_\alpha)$ of Z_α is

$$\mathrm{Lk}_\downarrow(Z_\alpha) := f^{-1}(\{S\}) \cap \bigcup K = f^{-1}(\{S\}) \cap D_\downarrow(Z_\alpha).$$

Remark 2.1.16. Definitions 2.1.13 and 2.1.15 are independent (up to homeomorphism) of the choice of S (provided $[S, R)$ contains no critical level of f), because each cell of X is PL homeomorphic to a convex polyhedron in $\mathbb{R}^m$.

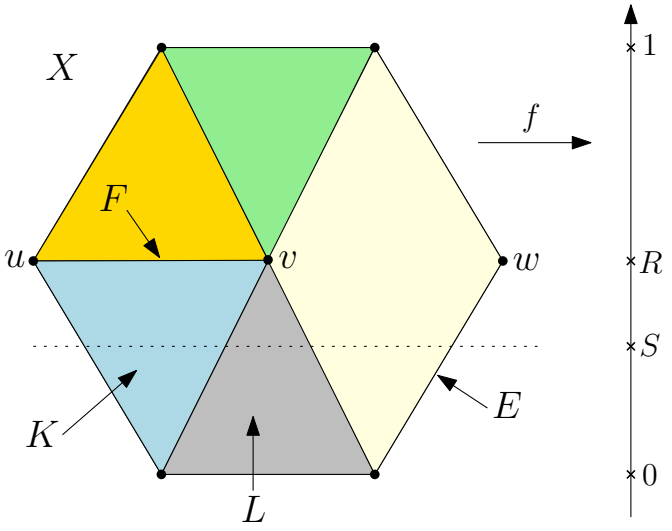

Figure 2.3: The hexagon X

Example 2.1.17. Consider the hexagon X shown in Figure 2.3, comprising seven 0–cells, eleven 1–cells and five 2–cells. Let $f : X \to [0, 1]$ be the height function as shown. The subcomplex $C(f, R)$ has two connected components $Z_1 = F$ and $Z_2 = \{w\}$. The descending set $D_\downarrow(Z_1)$ and the descending link $\mathrm{Lk}_\downarrow(Z_1)$ are the following subsets of $K \cup L$:

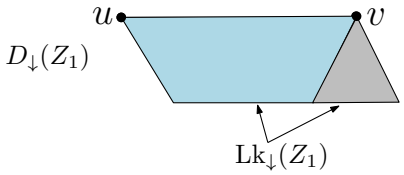

On the other hand, $D_\downarrow(Z_2) \subset E$ is an interval, and $\mathrm{Lk}_\downarrow(Z_2)$ is a single point.

Lemma 2.1.18. *There is a deformation retraction of $D_\downarrow(Z_\alpha)$ onto Z_α.*

Proof. The proof is very similar to that of [9, Proposition 2.4]. For $j \in \{0, \dots, m\}$, let

$$A_j := Z_\alpha \cup (D_\downarrow(Z_\alpha) \cap X^{(j)}),$$

where $X^{(j)}$ is the j–skeleton of X. In particular, $A_0 = Z_\alpha$ and $A_m = D_\downarrow(Z_\alpha)$. It suffices to show that A_j deformation retracts onto A_{j-1} for each $j \in \{1, \dots, m\}$.

Let L be a descending j–cell. Identify L with the convex j–cell C_L in $\mathbb{R}^m$ via the characteristic map $\chi_L : C_L \to L$. By possibly precomposing with a partial affine homeomorphism of $\mathbb{R}^m$, it may be assumed that f is a height function on L (since f is not constant on L). Then $f^{-1}([S,R]) \cap L$ may be identified with a convex polytope K in $\mathbb{R}^m$, and $f^{-1}(\{S\}) \cap L$ is the lower face of K. The set $f^{-1}(\{R\}) \cap L$ is a convex polyhedron of dimension strictly smaller than $\dim K$. The polytope K has the following property: there is a deformation retraction of K onto its boundary ∂K minus the lower $(j-1)$–dimensional face. Combining these deformation retractions over all such j–cells L of X gives a deformation retraction of A_j onto A_{j-1}. □

Example 2.1.19. Consider the hexagon from Figure 2.3. The steps of the deformation retraction of $D_\downarrow(Z_1)$ onto Z_1 from Lemma 2.1.18 are shown as follows.

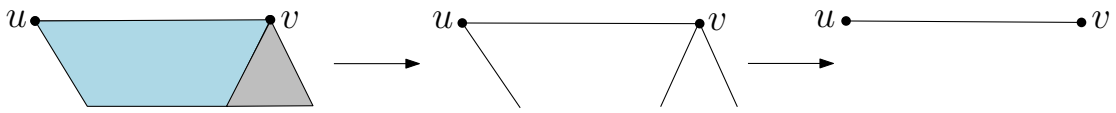

Cell structure

The descending link $\mathrm{Lk}_\downarrow(Z_\alpha)$ of a connected component Z_α of $C(f)$ may be equipped with a cell structure as follows. For each $j \in \{0, 1, \ldots, m-1\}$, the j–cells of $\mathrm{Lk}_\downarrow(Z_\alpha)$ are the connected components of the intersection

$$\mathrm{Lk}_\downarrow(Z_\alpha) \cap \bigcup (K^{(j+1)} \setminus K^{(j)}),$$

where $K^{(\ell)}$ is the ℓ–skeleton of K. Here, the union is over the cells K of X such that $f|_K$ achieves its maximum on $K \cap Z_\alpha$.

There is also a surjection

$$h_\alpha : \mathrm{Lk}_\downarrow(Z_\alpha) \to Z_\alpha$$

defined inductively on the skeleta of $\mathrm{Lk}_\downarrow(Z_\alpha)$ as follows.

(i) Let v be a vertex of $\mathrm{Lk}_\downarrow(Z_\alpha)$. There exists a unique 1–cell of X connecting v to a vertex v' in Z_α (this 1–cell is unique because there are no critical levels of f in the interval $[S,R)$). Define $h_\alpha(v) = v'$.

(ii) The map h_α is cellular, and on each j–cell of $\mathrm{Lk}_\downarrow(Z_\alpha)$, h_α is either constant or maps linearly onto a cell of Z_α of dimension at most j.

In general, the map $h_\alpha : \mathrm{Lk}_\downarrow(Z_\alpha) \to Z_\alpha$ satisfies the following property. The descending set $D_\downarrow(Z_\alpha)$ is a copy of the mapping cylinder $M(h_\alpha)$, with base $f^{-1}(\{S\}) \cap D_\downarrow(Z_\alpha) = \mathrm{Lk}_\downarrow(Z_\alpha)$ and top $f^{-1}(\{R\}) \cap D_\downarrow(Z_\alpha) = Z_\alpha$.

Example 2.1.20. Let T be the solid tetrahedron in Figure 2.4. It is an affine polytope complex with four 0–cells, six 1–cells, four 2–cells and one 3–cell K. Let $f : T \to \mathbb{R}$ be the affine Morse–Bott height function as shown. The critical subcomplex $C(f)$ has three components, one of which is $Z_1 = C(f, R) = F$. The descending link $\mathrm{Lk}_\downarrow(Z_1)$ is a 2–dimensional convex polyhedron with four vertices $v_1, \ldots, v_4$, four 1–cells $e_1, \ldots, e_4$ and one 2–cell. The map $h_1 : \mathrm{Lk}_\downarrow(Z_1) \to Z_1$ is specified as follows: h_1 maps $\overline{e}_1$ to v and $\overline{e}_2$ to w, whereas $\overline{e}_3$, $\overline{e}_4$ and every segment parallel to $\overline{e}_3, \overline{e}_4$ is mapped linearly onto F.

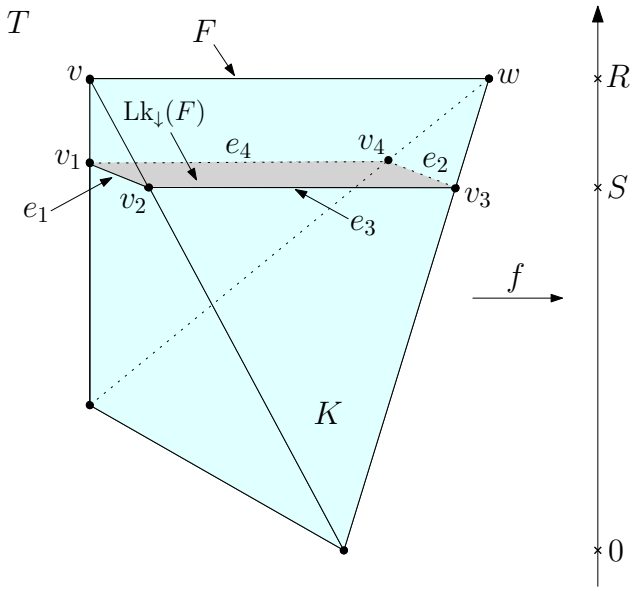

Figure 2.4: The solid tetrahedron T

2.1.3 Morse–Bott theory for affine polytope complexes

Let $f : X \to \mathbb{R}$ be an affine Morse–Bott function. We now study the homotopy type of the sets $\{X^c\}_{c\in\mathbb{R}}$. First, we consider the case when there are no critical levels in an interval.

Proposition 2.1.21. *Let $R < R'$ be such that there are no critical levels of $f : X \to \mathbb{R}$ in the interval $(R, R']$. Then $X^{R'}$ deformation retracts onto X^R.*

Proof. For $j \in \{0, 1, \ldots, m\}$, let

$$A_j = X^R \cup (X^{R'} \cap X^{(j)}),$$

so that $A_0 = X^R$ and $A_m = X^{R'}$. It suffices to show that A_j deformation retracts onto A_{j-1} for each $j \in \{1, \ldots, m\}$. Consider a j–cell L of X such that $L \cap f^{-1}((R, R']) \neq \emptyset$. Identify L with the convex j–cell C_L in $\mathbb{R}^m$ via the characteristic map $\chi_L : C_L \to L$. By possibly precomposing with a partial affine homeomorphism of $\mathbb{R}^m$, it may be assumed that f is a height function on L (since f is not constant on L). Then $f^{-1}([R, R']) \cap L$ may be identified with a convex polytope K in $\mathbb{R}^m$. The set $f^{-1}(\{R'\}) \cap L$ is the top face of the polytope K. The set $f^{-1}(\{R\}) \cap L$ is a convex polyhedron of dimension strictly smaller than $\dim K$. The polytope K has the following property: there is a deformation retraction of K onto its boundary ∂K minus the top $(j-1)$–dimensional face. Combining these deformation retractions over all j–cells L of X with $L \cap f^{-1}((R, R']) \neq \emptyset$ gives a deformation retraction of A_j onto A_{j-1}. □

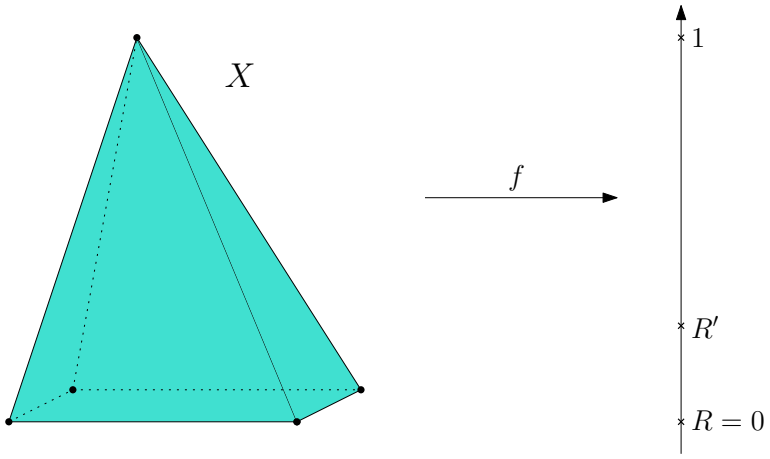

Figure 2.5: The pyramid X and the affine Morse–Bott function f

Example 2.1.22. Consider the solid pyramid X in Figure 2.5. It is an affine polytope complex with five 0–cells, eight 1–cells, five 2–cells and one 3–cell. Let $f : X \to \mathbb{R}$ be the affine Morse–Bott function as shown. Here $R' \in (0, 1)$, and the

base of X is at level $R = 0$. In this case, $\dim X = 3$ and the steps of the deformation retraction from Proposition 2.1.21 are shown in Figure 2.6.

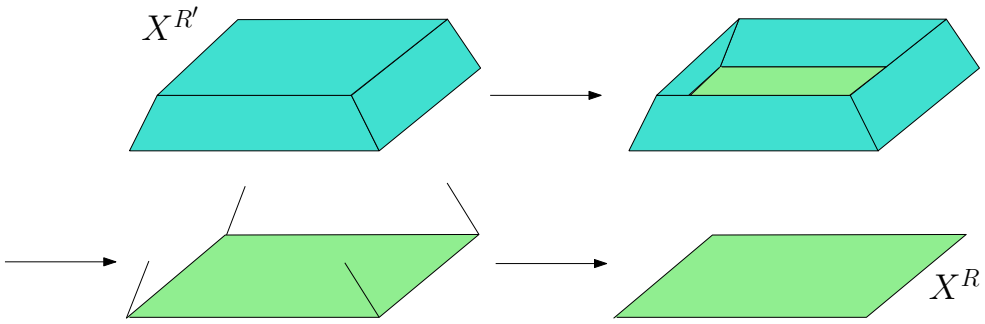

Figure 2.6: The steps of the deformation retraction from Proposition 2.1.21

We now consider the case when there is exactly one critical level in an interval. Let $a < R < b$ be such that R is the only critical level of f in $[a, b]$, and write $C(f, R) = \amalg_{i=1}^{n} Z_i$ as the disjoint union of its connected components.

Proposition 2.1.23. *(X^b, X^a) is homotopy equivalent to the pair (Q, X^a), where $Q \subset X^R$ is the space obtained from X^a by attaching the mapping cylinders $\{M(h_i) = D_{\downarrow}(Z_i)\}_{i=1}^{n}$ as follows:[1] for each $i \in \{1, \ldots, n\}$, identify the copies of $\mathrm{Lk}_{\downarrow}(Z_i)$ contained in $M(h_i)$ and X^a.*

Proof. In view of Proposition 2.1.21, X^b deformation retracts onto X^R. It suffices to show that $f^{-1}([a, R])$ deformation retracts onto its subspace $Q \cap f^{-1}([a, R])$. For $j \in \{0, 1, \ldots, m\}$, let

$$A_j = (Q \cup X^{(j)}) \cap f^{-1}([a, R]),$$

so that $A_0 = Q \cap f^{-1}([a, R])$ and $A_m = f^{-1}([a, R])$. Again, we show that A_j deformation retracts onto A_{j-1} for each $j \in \{1, \ldots, m\}$. Let L be a j–cell of X such that $f^{-1}([a, R]) \cap L \neq \emptyset$ and L does not contain a $(j-1)$–cell of $C(f, R)$ in its boundary. Identify L with the convex polyhedral cell C_L in $\mathbb{R}^m$; it may be assumed that f is a height function on L. Then $f^{-1}([a, R]) \cap L$ is a j–dimensional convex polytope in $\mathbb{R}^m$, with top face $f^{-1}(\{R\}) \cap L$ not a cell of $C(f, R)$. There is a deformation retraction of this polytope onto its boundary minus the top face. Hence, A_j deformation retracts onto A_{j-1}. □

[1] The mapping cylinder $M(h_i)$ is equal to $D_{\downarrow}(Z_i)$ up to canonical homeomorphism.

Example 2.1.24. Consider the Morse–Bott function $f : X \to [0,1]$ from Figure 2.3. Let $a < R < b$ be as shown in Figure 2.7. The subcomplex $C(f,R)$ has two connected components $Z_1 = F$ and $Z_2 = \{w\}$. The mapping cylinders $M(h_1)$ and $M(h_2)$ coincide with $D_\downarrow(Z_1)$ and $D_\downarrow(Z_2)$, respectively. The space X^b deformation retracts onto X^R, and the pair (X^R, X^a) deformation retracts onto (Q, X^a) as in Figure 2.8.

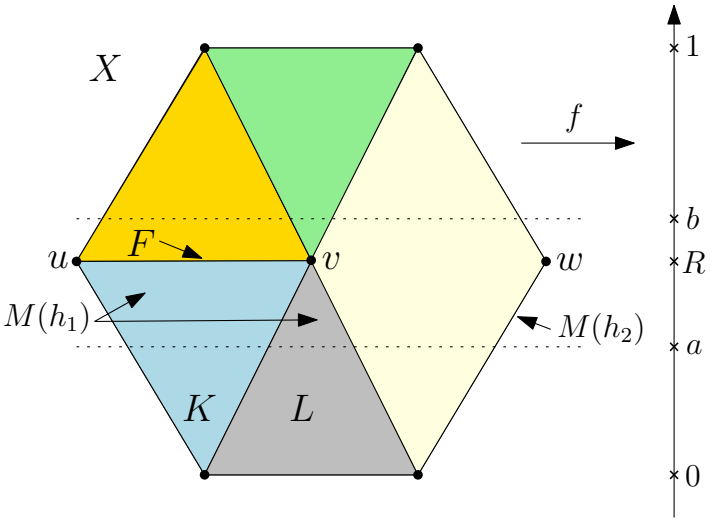

Figure 2.7: The mapping cylinders $M(h_1)$ and $M(h_2)$

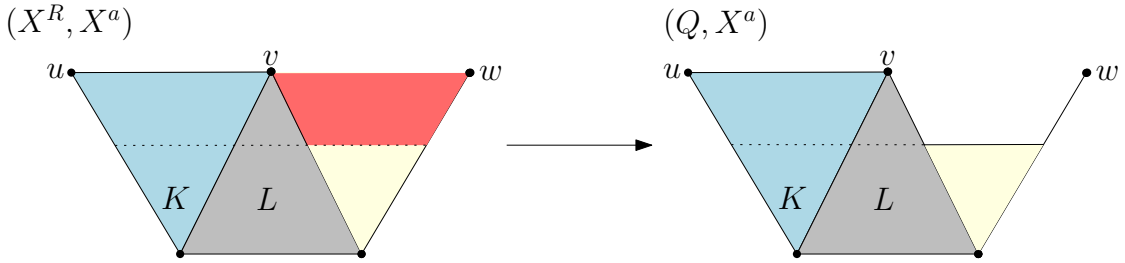

Figure 2.8: Deformation retraction of (X^R, X^a) onto (Q, X^a)

Remark 2.1.25. There are analogues of Propositions 2.1.21 and 2.1.23 for the family $\{X_c\}_{c\in\mathbb{R}}$, where $X_c := f^{-1}([c,\infty))$ for each $c \in \mathbb{R}$. In fact, if $f : X \to \mathbb{R}$ is an affine Morse–Bott function on X, then so is $-f : X \to \mathbb{R}$.

Corollary 2.1.26. *Assume that $C(f,R) = Z$ is connected, and let $h : \mathrm{Lk}_\downarrow(Z) \to Z$ be the map defined in §2.1.2 (in particular, $M(h) = D_\downarrow(Z)$). Then the inclusion $(M(h), \mathrm{Lk}_\downarrow(Z)) \hookrightarrow (X^b, X^a)$ induces homology isomorphisms.*

Proof. The map $(Q, X^a) \hookrightarrow (X^b, X^a)$ is a homotopy equivalence from Proposition 2.1.23. By excision, the inclusion $(M(h), \mathrm{Lk}_\downarrow(Z)) \hookrightarrow (Q, X^a)$ induces isomorphisms on homology. □

Corollary 2.1.27. *Under the assumptions of Corollary 2.1.26,*

$$\begin{aligned}\operatorname{rk} H_j(X^b, X^a) = &\operatorname{rk}\operatorname{coker}[\iota_* : H_j(\mathrm{Lk}_\downarrow(Z)) \to H_j(D_\downarrow(Z))] \\ &+ \operatorname{rk}\ker[\iota_* : H_{j-1}(\mathrm{Lk}_\downarrow(Z)) \to H_{j-1}(D_\downarrow(Z))]\end{aligned}$$

for each $j \geq 0$.

Proof. By replacing $H_j(X^b, X^a)$ with $H_j(D_\downarrow(Z), \mathrm{Lk}_\downarrow(Z))$, the long exact sequence of the pair $(D_\downarrow(Z), \mathrm{Lk}_\downarrow(Z)) = (M(h), \mathrm{Lk}_\downarrow(Z))$ becomes

$$\begin{aligned}\cdots \to H_j(\mathrm{Lk}_\downarrow(Z)) \xrightarrow{\iota_*} H_j(D_\downarrow(Z)) \to H_j(X^b, X^a) \\ \to H_{j-1}(\mathrm{Lk}_\downarrow(Z)) \xrightarrow{\iota_*} H_{j-1}(D_\downarrow(Z)) \to \dots\end{aligned}$$

□

Remark 2.1.28. Now suppose that $C(f, R) = \amalg_{i=1}^n Z_i$ has n connected components $Z_1, \dots, Z_n$. The analogues of Corollaries 2.1.26 and 2.1.27 are as follows.

(i) The inclusion $\amalg_{i=1}^n (M(h_i), \mathrm{Lk}_\downarrow(Z_i)) \hookrightarrow (X^b, X^a)$ induces isomorphisms on homology.

(ii) For each $j \geq 1$,

$$\begin{aligned}\operatorname{rk} H_j(X^b, X^a) = \sum_{i=1}^n (&\operatorname{rk}\operatorname{coker}[\iota_* : H_j(\mathrm{Lk}_\downarrow(Z_i)) \to H_j(D_\downarrow(Z_i)] \\ &+ \operatorname{rk}\ker[\iota_* : H_{j-1}(\mathrm{Lk}_\downarrow(Z_i)) \to H_{j-1}(D_\downarrow(Z_i))])\,.\end{aligned}$$

2.2 The metric is an affine Morse–Bott function

In this section we verify that the metric d is an affine Morse–Bott function on $\Gamma \times \Gamma$ (see §1.3 for the definition of the metric d on an edge-labelled graph). This enables us to apply the general statements from §2.1 and obtain information on the homotopy type of the configuration spaces $\{F_r(\Gamma, 2)\}_{r>0}$ (we perform this application in Chapter 3, see §3.2).

With respect to some CW decomposition of $\Gamma \times \Gamma$, we need to show that:

(i) $\Gamma \times \Gamma$ is an affine polytope complex, and

(ii) for each closed cell F of $\Gamma \times \Gamma$, the composition

$$d \circ \chi_F : C_F \to \mathbb{R}$$

extends to an affine map $\mathbb{R}^2 \to \mathbb{R}$. Here, $\chi_F : C_F \to F$ is a characteristic function of F (see Definition 2.1.1), and C_F is a convex polyhedral cell in $\mathbb{R}^2$ of dimension $\dim F$.

In the remainder of this section we verify the following statement.

Proposition 2.2.1. *The product* CW *structure on* $\Gamma \times \Gamma$ *admits a subdivision such that (i) and (ii) hold.*

Proof. Since Γ is simple, it is a cube complex of dimension one. Hence, the product $\Gamma \times \Gamma$ is a cube complex of dimension two. Any finite-dimensional cube complex is an APC,[2] so $\Gamma \times \Gamma$ is an APC with respect to the product CW structure. Hence (i) holds.

We now show that $\Gamma \times \Gamma$ admits a subdivision such that (ii) holds. We recall from §1.1 that in a simple graph, we have an identification $\psi_e : \overline{e} \to [0, 1]$ of each closed edge $\overline{e}$ with $[0, 1]$. For $i \in \{0, 1\}$, we write $\partial_i e = \psi_e^{-1}(\{i\})$ (see Definitions 1.1.3). A closed 2–cell F of $\Gamma \times \Gamma$ has the form $F = \overline{e} \times \overline{f}$, where e and f are edges. Set $C_F = [0, 1] \times [0, 1]$ and $\chi_F(i, j) = (\partial_i e, \partial_j f)$ for all $i, j \in \{0, 1\}$. If $e = f$, then since the cycle inequality is satisfied, $d|_F$ has the form

$$d(x, y) = \ell(e) \, |\psi_e(x) - \psi_e(y)| \,, \quad (x, y) \in F,$$

[2] See the remarks after [9, Definition 2.1].

where $\ell(e)$ is the label of e. In this case, add a diagonal 1–cell to $F = \overline{e} \times \overline{e}$ as shown in Figure 2.9, creating two triangular 2–cells F_1 and F_2. If $\chi_{F_j} : C_{F_j} \to F_j$ is a characteristic function of F_j for $j \in \{1, 2\}$, then $d \circ \chi_{F_j}$ extends to an affine map $\mathbb{R}^2 \to \mathbb{R}$, for $j \in \{1, 2\}$, see Figure 2.10. Now assume that e and f are distinct.

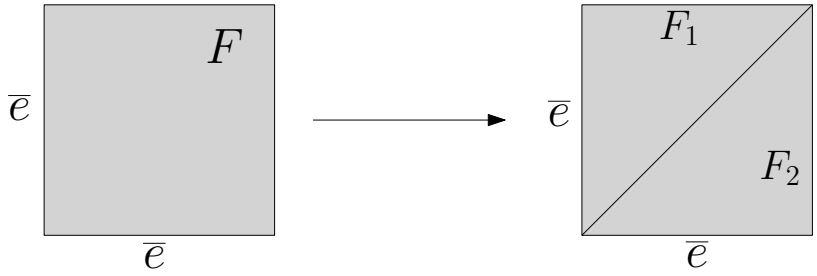

Figure 2.9: Subdividing a diagonal 2–cell $F = \overline{e} \times \overline{e}$

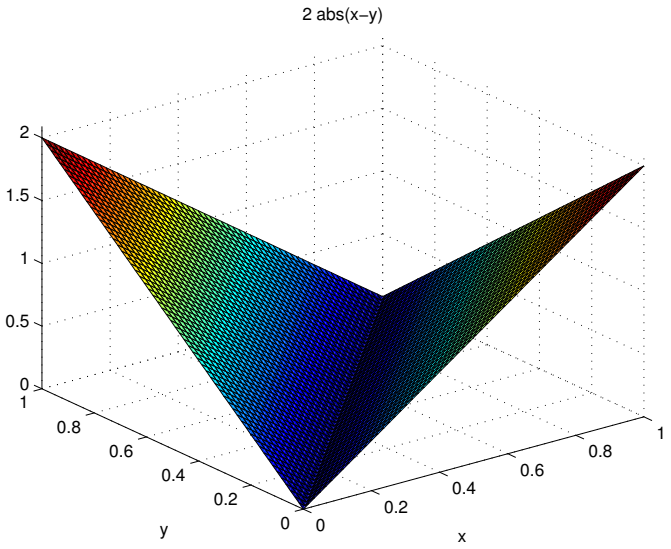

Figure 2.10: The metric d on a diagonal 2–cell $F = \overline{e} \times \overline{e}$ with $\ell(e) = 2$

There are several cases to consider, arising from the positions of minimal-length edgepaths joining points of $\overline{e}$ to points of $\overline{f}$.

Case 1. Suppose that there exist vertices $v \in \partial e$ and $w \in \partial f$ such that every minimal-length edgepath from $\overline{e}$ to $\overline{f}$ passes through v and w, see Figure 2.11. Let $a := d(\overline{e}, \overline{f})$ be the distance between $\overline{e}$ and $\overline{f}$. Without loss of generality, assume that $\partial_1 e = v$ and $\partial_0 f = w$. Then

$$d(\chi_F(0,0)) = a + \ell(e), \;\; d(\chi_F(1,0)) = a,$$

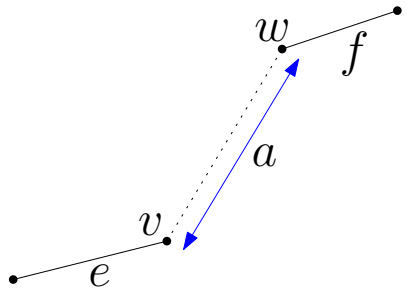

Figure 2.11: The situation in Case 1

$$d(\chi_F(0,1)) = a + \ell(e) + \ell(f), \;\; d(\chi_F(1,1)) = a + \ell(f)$$

and $d \circ \chi_F$ extends to an affine map $\mathbb{R}^2 \to \mathbb{R}$, see Figures 2.12 and 2.13.

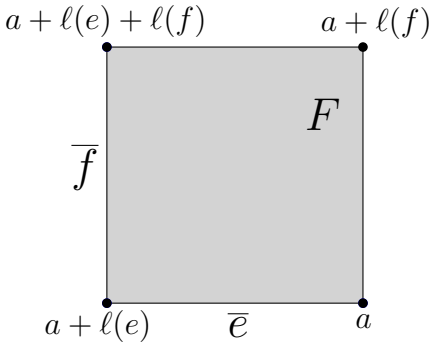

Figure 2.12: $d \circ \chi_F$ extends to an affine map $\mathbb{R}^2 \to \mathbb{R}$

Case 2. Now suppose that we are not in Case 1. This means that for all $v \in \partial e$ and $w \in \partial f$ there is a minimal-length edgepath from $\overline{e}$ to $\overline{f}$ not containing v or not containing w. We identify three subcases illustrated in Figures 2.14, 2.17 and 2.20.

(i) Assume that there is a vertex $v \in \partial e$ such that every minimal-length edgepath from $\overline{e}$ to $\overline{f}$ passes through v, see Figure 2.14 (the argument is the same if there is a vertex $w \in \partial f$ such that every minimal-length edgepath from $\overline{e}$ to $\overline{f}$ passes through w). Write $a = d(v, \partial_0 f)$ and $b = d(v, \partial_1 f)$. By assumption, there is a point $x \in f$ such that

$$d(v, \partial_0 f) + d(\partial_0 f, x) = d(x, \partial_1 f) + d(\partial_1 f, v).$$

Moreover,

$$d(\chi_F(0,0)) = a + \ell(e), \quad d(\chi_F(1,0)) = a$$

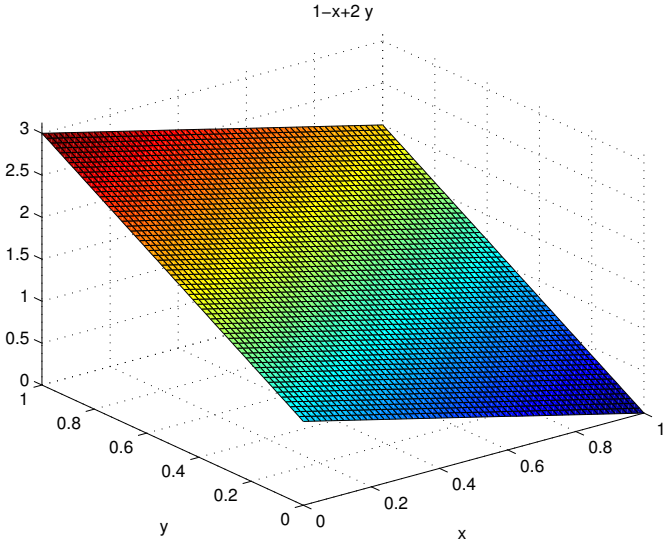

Figure 2.13: The graph of $d \circ \chi_F$ with $a = 0$, $\ell(e) = 1$ and $\ell(f) = 2$

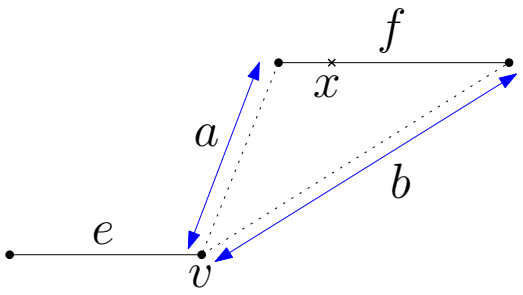

Figure 2.14: Case 2(i)

and

$$d(\chi_F(0,1)) = b + \ell(e), \quad d(\chi_F(1,1)) = b.$$

The line $\overline{e} \times \{x\}$ separates F into two closed 2–cells F_1 and F_2. If $j \in \{1,2\}$ and $\chi_{F_j} : C_{F_j} \to F_j$ is a characteristic function of F_j, then $d \circ \chi_{F_j}$ extends to an affine map $\mathbb{R}^2 \to \mathbb{R}$, see Figures 2.15 and 2.16.

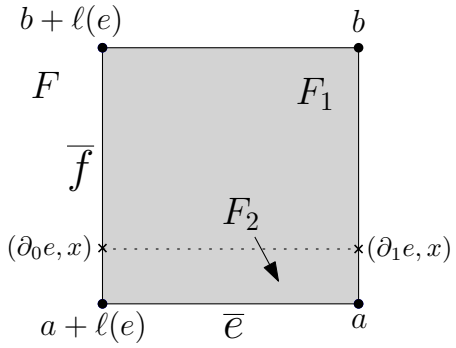

Figure 2.15: The separating line $\overline{e} \times \{x\}$

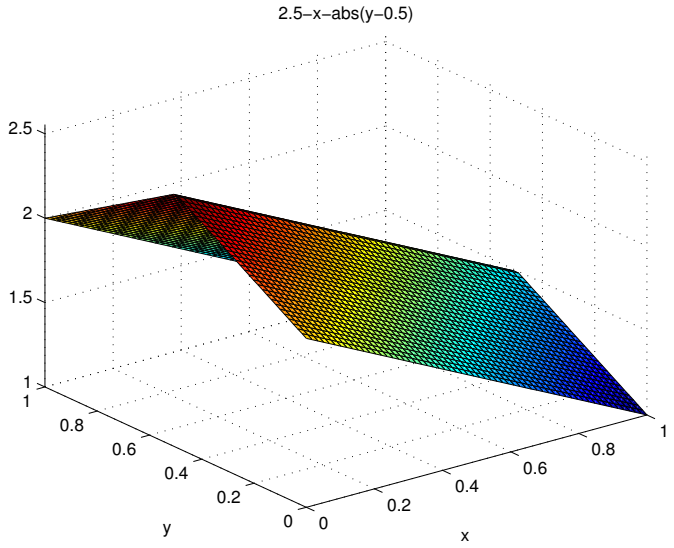

Figure 2.16: The graph of $d \circ \chi_F$ with $a = b = 1$ and $\ell(e) = \ell(f) = 1$

(ii) We now assume that (i) does not hold, and that all minimal-length edgepaths from $\partial_0 e$ to $\partial_0 f$ are disjoint from all minimal-length edgepaths from $\partial_1 e$ to $\partial_1 f$. Write $a = d(\partial_0 e, \partial_0 f)$ and $b = d(\partial_1 e, \partial_1 f)$. Without loss of generality, there is a point $x \in \overline{e}$ equidistant to $\partial_0 f$ along two distinct edgepaths, see Figure 2.17.

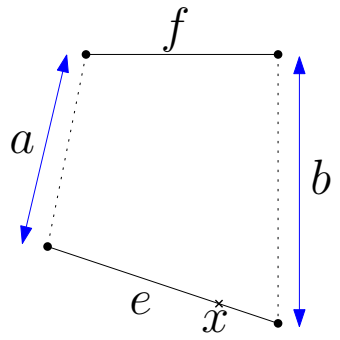

Figure 2.17: Case 2(ii)

We have $d(\chi_F(0,0)) = a$ and $d(\chi_F(1,1)) = b$. There is also a diagonal line in F on which d is constant with value $(\ell(e)+\ell(f)+a+b)/2$. This line separates F into two closed 2–cells F_1 and F_2. If $j \in \{1,2\}$ and $\chi_{F_j} : C_{F_j} \to F_j$ is a characteristic function of F_j, then $d \circ \chi_{F_j}$ extends to an affine map $\mathbb{R}^2 \to \mathbb{R}$, see Figures 2.18 and 2.19.

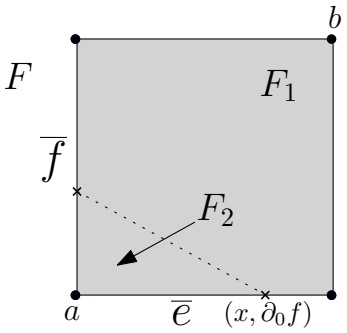

Figure 2.18: The separating line on which d is constant

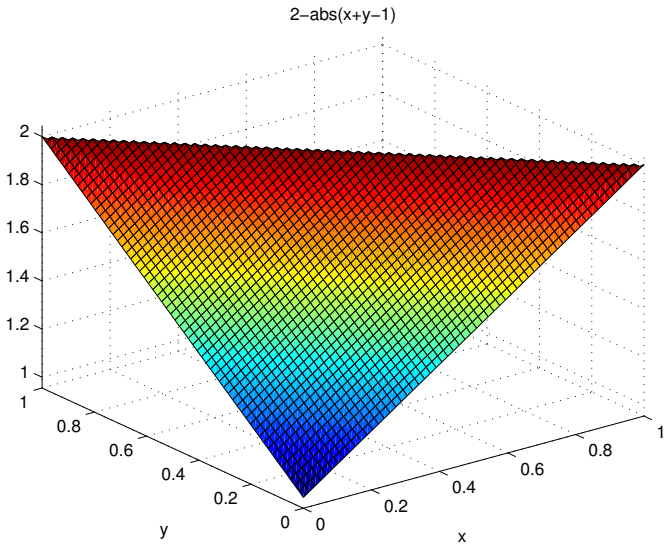

Figure 2.19: The graph of $d \circ \chi_F$ with $a = b = 1$ and $\ell(e) = \ell(f) = 1$; it is symmetric about $y = 1 - x$

(iii) Finally, we assume that (i) does not hold and that at least one minimal-length edgepath from $\partial_0 e$ to $\partial_0 f$ intersects a minimal-length edgepath from $\partial_1 e$ to $\partial_1 f$, see Figure 2.20. There are points $x \in e$, $y \in f$ equidistant from the intersection of these edgepaths (otherwise we are in Case 2(i)). The lines $\{x\} \times \overline{f}$ and $\overline{e} \times \{y\}$ separate F into four closed 2–cells F_1, F_2, F_3, F_4. If $j \in \{1, 2, 3, 4\}$ and χ_{F_j} is a characteristic function of F_j, then $d \circ \chi_{F_j}$ extends to an affine map $\mathbb{R}^2 \to \mathbb{R}$, see Figure 2.21. The graph of $d \circ \chi_{F_j}$ resembles the graph in Case 1 (Figure 2.13) for each $j \in \{1, 2, 3, 4\}$.

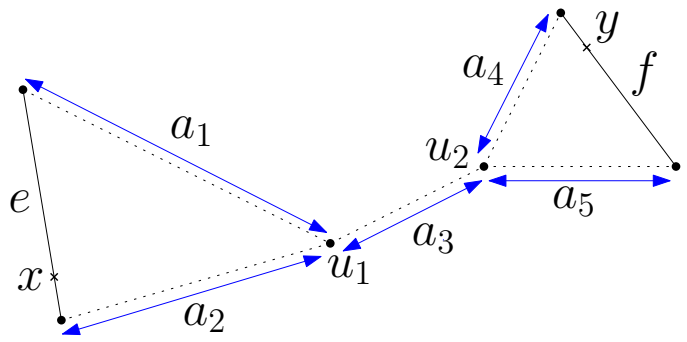

Figure 2.20: Case 2(iii)

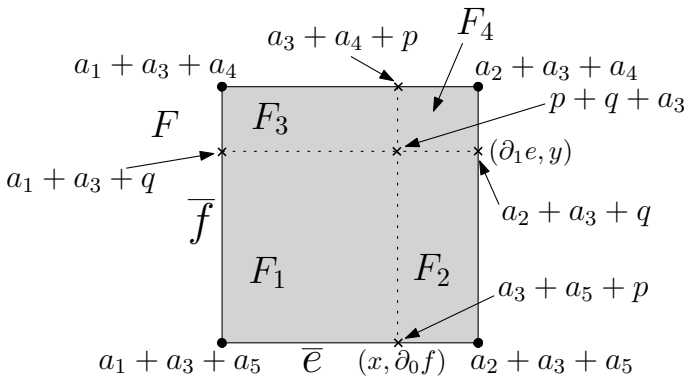

Figure 2.21: The graph of d in Case 2(iii). Here, $p = (a_1 + a_2 + \ell(e))/2$ and $q = (a_4 + a_5 + \ell(f))/2$.

Finally, we note that under the subdivisions in Figure 2.9 and all subcases of Case 2 (see Figures 2.15, 2.18 and 2.21) $\Gamma \times \Gamma$ remains an affine polytope complex. This establishes Proposition 2.2.1. □

Chapter 3

Homotopy type of the configuration spaces $\{F_r(\Gamma, 2)\}_{r>0}$

In this chapter we study the homotopy type of the thick particle configuration space $F_r(\Gamma, 2)$ as r varies. The main result is an upper bound for the number of critical values of r where a homotopy type change occurs, see Theorem 3.2.3. This is achieved by describing each critical value explicitly in terms of metric properties of the graph Γ.

We begin in §3.1 by recalling the definition of the thick particle configuration spaces $\{F_r(\Gamma, 2)\}_{r>0}$ and discussing some basic properties and examples. Next, in §3.2 we apply the PL Morse–Bott theory developed in §2.1 and obtain the main result of this chapter, Theorem 3.2.3. In §3.2 we also address the important question of how the homotopy type of $F_r(\Gamma, 2)$ changes as r ranges over an interval containing exactly one critical value. The PL Morse–Bott theory from §2.1 provides a general answer to this question, which we quantify in §3.2 by calculating the ranks of the relative homology groups of the pair $(F_a(\Gamma, 2), F_b(\Gamma, 2))$, where the interval (a, b) contains exactly one critical value.

3.1 Definitions and examples

We first recall the definitions from §0.2. We work with a finite, connected graph Γ and a labelling $\ell : E(\Gamma) \to (0, \infty)$ of the edges of Γ. Such a labelling induces a

metric d on Γ, where $d(x, y)$ is the length of the shortest path connecting the points x and y. The details of this construction are in Chapter 1, see §1.2 and §1.3. The main definitions are as follows.

Definition 3.1.1. The *two-point configuration space of* Γ is

$$F(\Gamma, 2) := \{(x, y) \in \Gamma \times \Gamma : x \neq y\}.$$

Equivalently, $F(\Gamma, 2) = d^{-1}((0, \infty)) = \Gamma \times \Gamma \setminus \Delta$, where Δ is the diagonal in $\Gamma \times \Gamma$.

Definition 3.1.2. For $r > 0$, we define

$$F_r(\Gamma, 2) := \{(x, y) \in \Gamma \times \Gamma : d(x, y) \geq 2r\}.$$

Remark 3.1.3. We observe that $F(\Gamma, 2) = \bigcup_{r>0} F_r(\Gamma, 2)$.

In the context of topological robotics, $F_r(\Gamma, 2)$ models the collision-free motion of two robots of radius r on Γ such that tangencies between the robots are permitted. We need only consider sufficiently small values of r, as the following lemma shows.

Lemma 3.1.4. *Let* $R := \frac{1}{2} \operatorname{diam} \Gamma$. *We have* $F_r(\Gamma, 2) \neq \emptyset \iff r \in (0, R]$.

Proof. If $r > R$ and $(x, y) \in F_r(\Gamma, 2)$, then $d(x, y) \geq 2r > 2R$, a contradiction. Thus $F_r(\Gamma, 2) = \emptyset$ for all $r > R$. Conversely, $\Gamma \times \Gamma$ is compact and d is continuous, so there exists $(x, y) \in \Gamma \times \Gamma$ such that $d(x, y) = \operatorname{diam} \Gamma$. Hence $(x, y) \in F_R(\Gamma, 2)$ and so $F_r(\Gamma, 2) \neq \emptyset$ for any $r \in (0, R]$. □

We now discuss examples of the families $\{F_r(\Gamma, 2)\}_{r>0}$. These examples illustrate the general phenomenon that for a given graph Γ, the configuration space $F_r(\Gamma, 2)$ assumes only finitely many homotopy types as r varies over $\left(0, \frac{1}{2} \operatorname{diam} \Gamma\right]$.

Example 3.1.5. Let $\Gamma = [0, 1]$ have the graph structure with two vertices $0, 1$ and one edge $e = (0, 1)$, the latter equipped with label 1.

(Γ, ℓ) 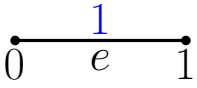

For $r \in (0, 1/2)$, $F_r(\Gamma, 2)$ comprises two triangles, see Figure 3.1. Moreover,

$$F_{1/2}(\Gamma, 2) = \{(0, 1), (1, 0)\}$$

is a two-point space and $F_r(\Gamma, 2) = \emptyset$ for $r > 1/2$.

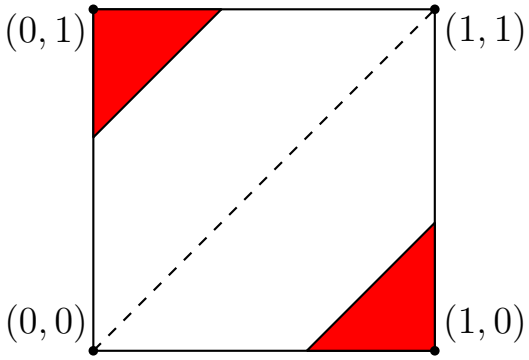

Figure 3.1: The configuration space $F_r(\Gamma, 2)$ for $r \in (0, 1/2)$

Example 3.1.6. Let $\Gamma = S^1$ have the graph structure with one vertex v and one edge e, the latter given label 1. For $x \neq y$, $d(x, y)$ is equal to the length of the shorter of the two arcs joining x and y, see Figure 3.2. With this metric, the diameter of

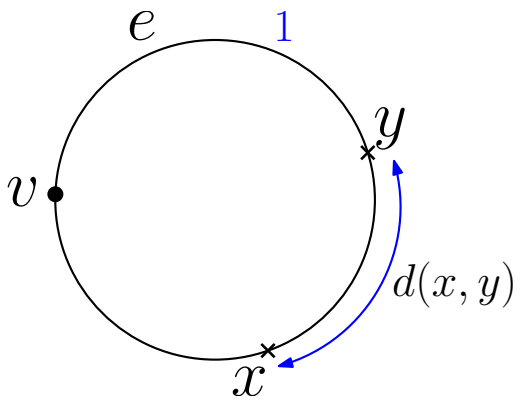

Figure 3.2: The metric on S^1

Γ is 1/2. For each $r \in (0, 1/4]$, the configuration space $F_r(S^1, 2)$ has the homotopy type of S^1. To see this, consider $S^1 \subset \mathbb{C}$ as the unit complex numbers; the metric is

$$d(z_1, z_2) = \frac{1}{2\pi} \min\{|\arg z_1 - \arg z_2|, 2\pi - |\arg z_1 - \arg z_2|\}, \quad \text{for } z_1, z_2 \in S^1,$$

where we take $\arg z \in [0, 2\pi)$ for $z \in S^1$. For $r \in (0, 1/4]$, define

$$h : F_r(S^1, 2) \to S^1 \times (S^1 \setminus B_{2r}(1))$$

by

$$h(z_1, z_2) = (z_1, z_2/z_1), \quad \forall (z_1, z_2) \in F_r(S^1, 2).$$

Here, $B_{2r}(1)$ is an open ball of radius $2r$ about $1 \in S^1$. It is easy to check that h is a homeomorphism, using the property that $d(\omega z_1, \omega z_2) = d(z_1, z_2)$ for any

$\omega, z_1, z_2 \in S^1$. Therefore $F_r(S^1, 2)$ is homeomorphic to $S^1 \times (S^1 \setminus B_{2r}(1))$, and so is homotopy equivalent to S^1, since $S^1 \setminus B_{2r}(1)$ is contractible.

Example 3.1.7. Let Γ be the Y–graph comprising three edges e_1, e_2, e_3 incident to a central vertex v, and assume that all three edges have label 1.

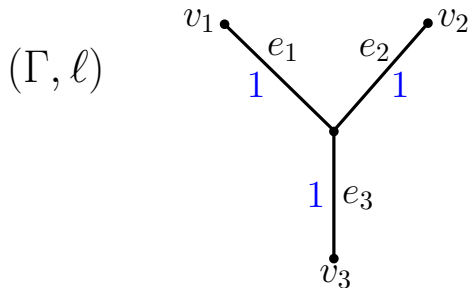

The configuration space $F(\Gamma, 2)$ is described by Abrams and Ghrist in their expository paper [4, Example 1], see also [33, Lemma 1.1]. It embeds in $\mathbb{R}^3$ as shown in Figure 3.3. The base comprises the six 2–cells $\overline{e}_i \times \overline{e}_j$, for $i \neq j$. The remaining six triangles (of length and height 1) come from removing the diagonals from the three squares $\overline{e}_i \times \overline{e}_i$, $i = 1, 2, 3$. The vertex in the centre is missing, and the dashed lines on the six triangles represent the missing diagonal Δ of $\Gamma \times \Gamma$. For $r \in (0, 1/2)$, the corresponding configuration space $F_r(\Gamma, 2)$ is shown in Figure 3.4. The hole in the centre has been replaced with a missing hexagon, and the six triangular fins now have length and height $1 - 2r$. When $r = 1/2$, the six triangular fins have shrunk to the six non-convex points on the outer boundary of the base, see Figure 3.5. For values of $r \in (1/2, 1)$, $F_r(\Gamma, 2)$ is disconnected, with six path-components, see Figure 3.6. Finally when $r = 1$, the space $F_r(\Gamma, 2)$ comprises six points, namely the convex points on the outer boundary of the base, see Figure 3.7.

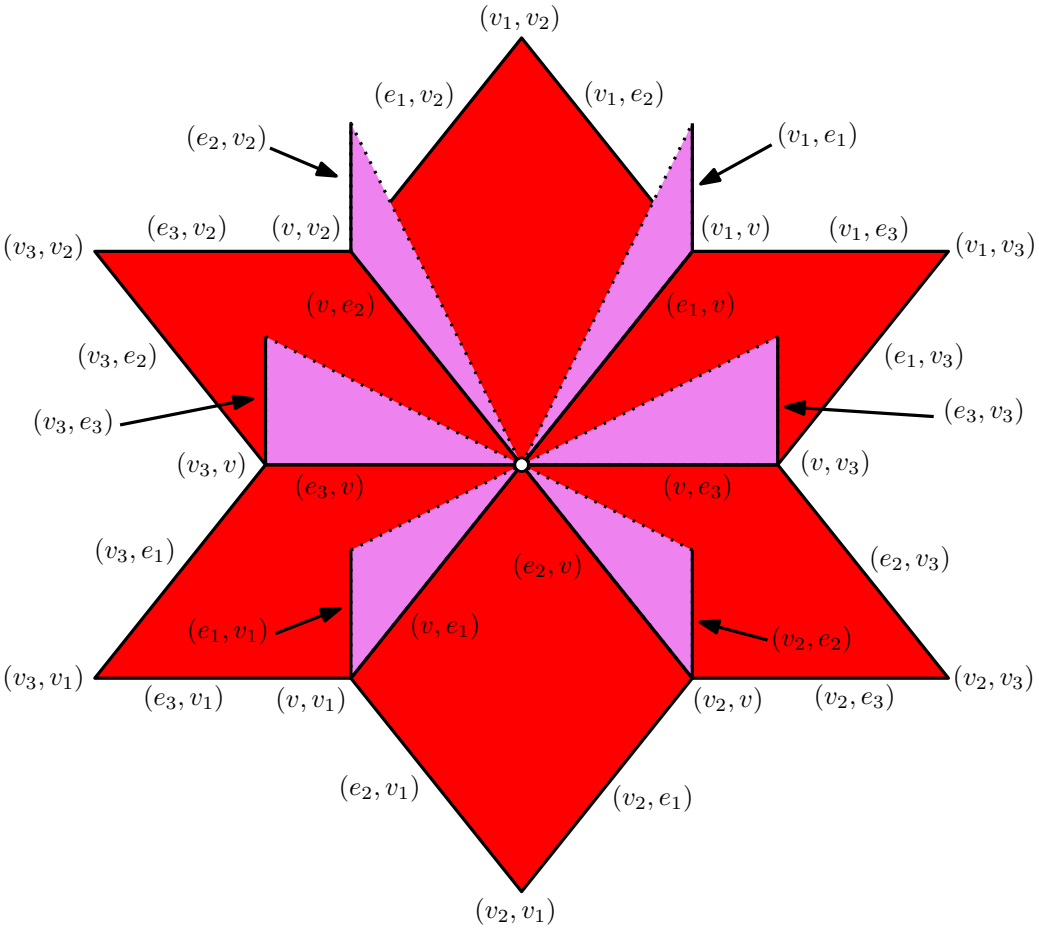

Figure 3.3: The configuration space $F(\Gamma, 2)$

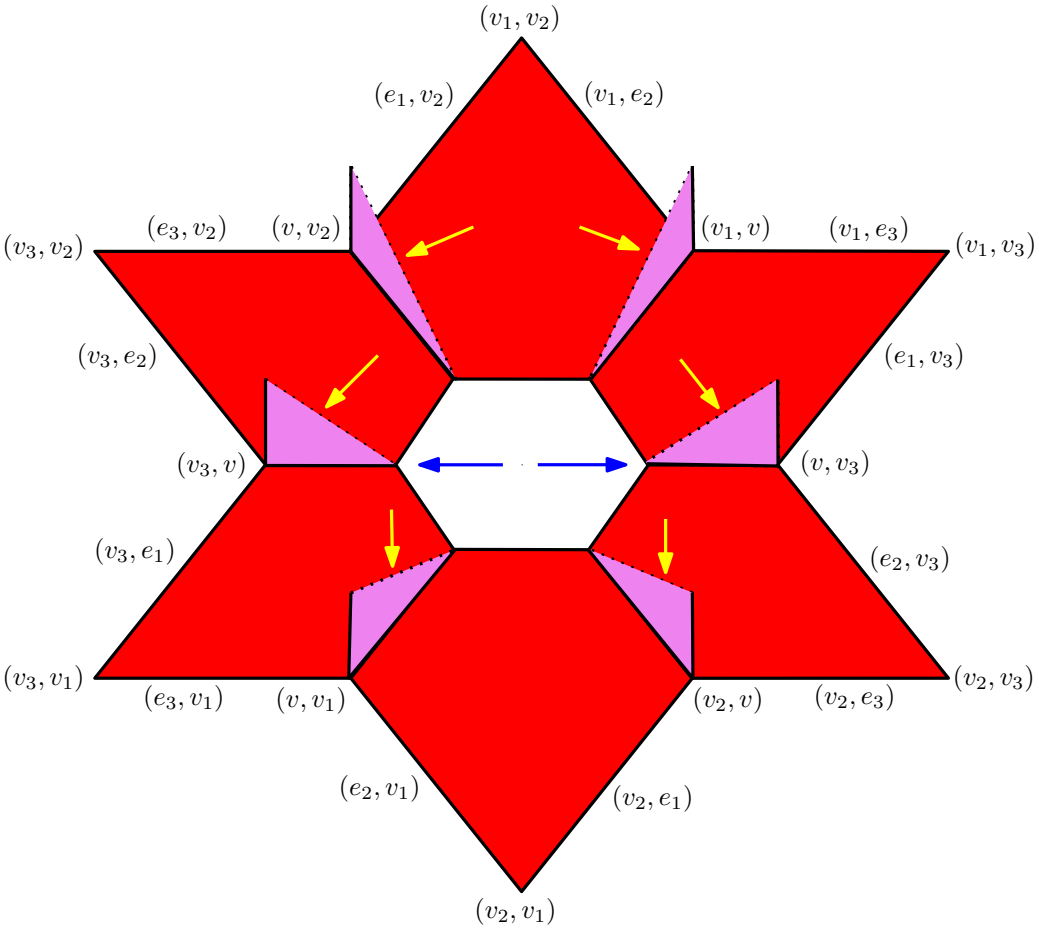

Figure 3.4: The configuration space $F_r(\Gamma, 2)$ for $r \in (0, 1/2)$

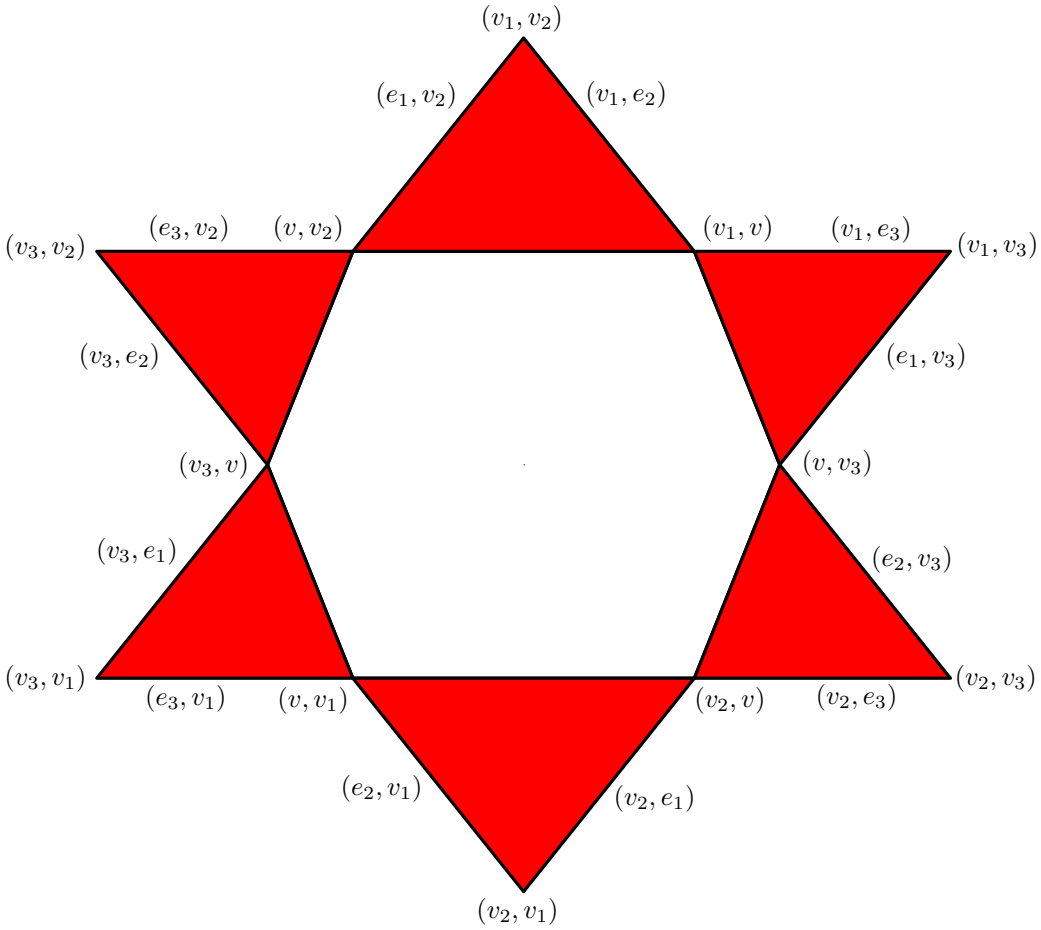

Figure 3.5: The configuration space $F_{1/2}(\Gamma, 2)$

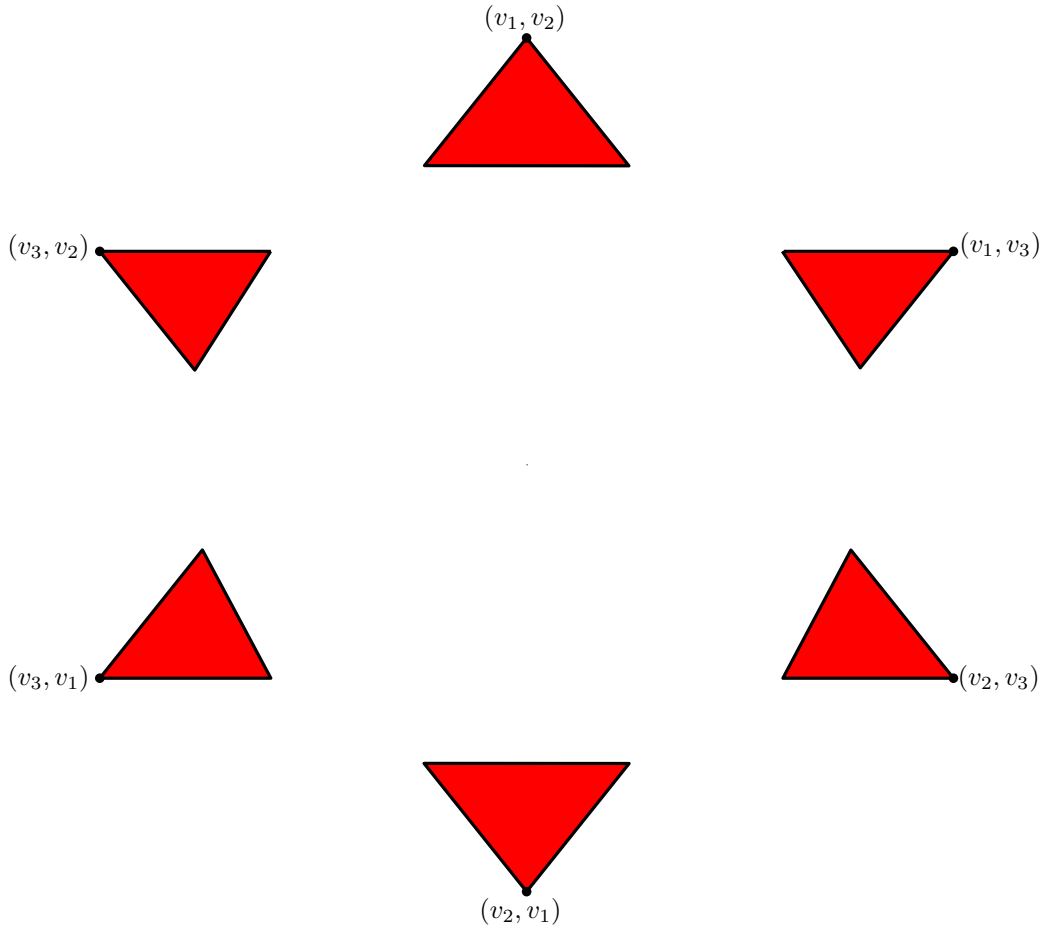

Figure 3.6: The configuration space $F_r(\Gamma, 2)$ for $r \in (1/2, 1)$

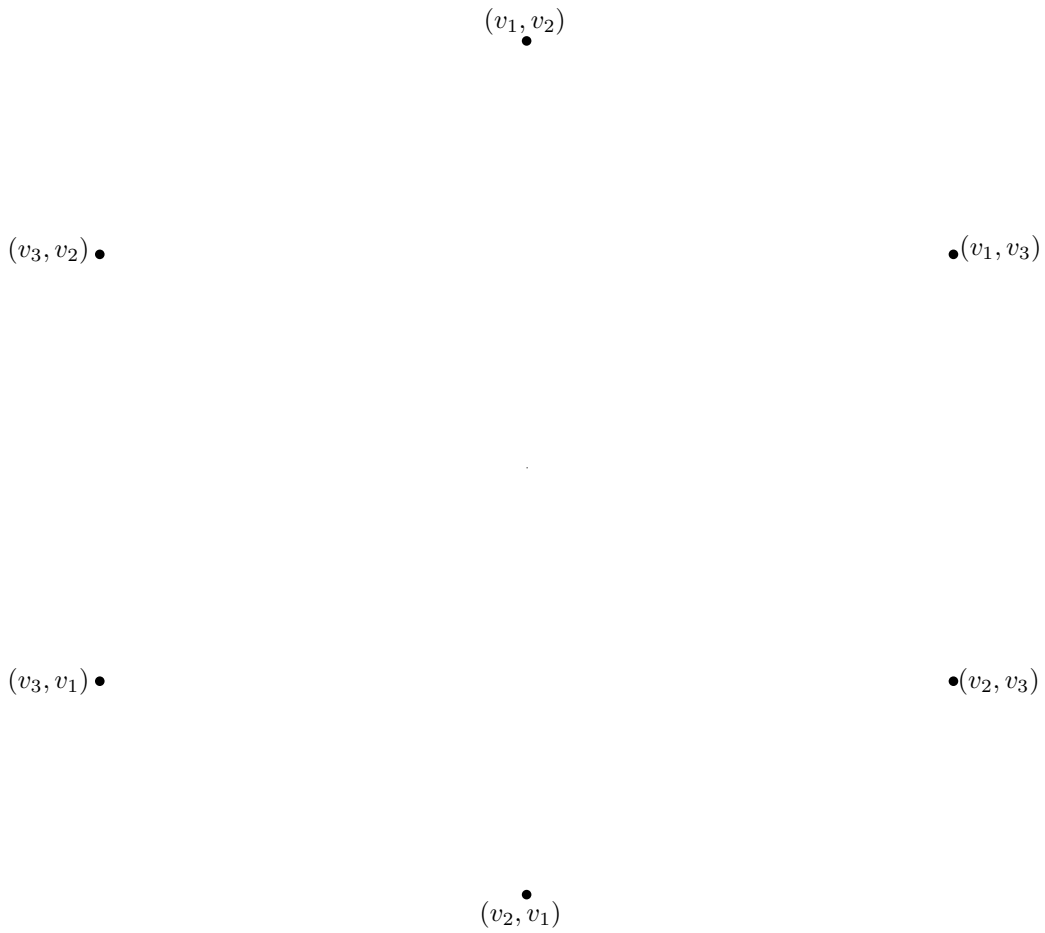

Figure 3.7: The space $F_1(\Gamma, 2)$

Example 3.1.8. (see [33, Example 4]). Let $P = S^1 \vee [0,1]$ be the P–graph shown in Figure 3.8. Since P is the quotient of the Y–graph (see Example 3.1.7) obtained by

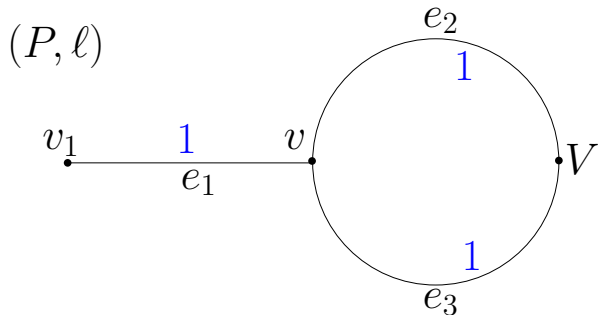

Figure 3.8: The labelling on the P–graph

identifying two free vertices, we can obtain $F(P,2)$ by performing the appropriate identifications on the configuration space $F(Y,2)$, where Y is the Y–graph (see Figure 3.3). This computation was first performed by R. Ghrist, see [33, Example 4].

Starting from the Y–graph, we identify the vertices v_2 and v_3 to form the P–graph. To obtain $F(P,2)$ from $F(Y,2)$, we implement the following six edge identifications:

- identify (v_2, e_1) with (v_3, e_1) and identify (e_1, v_2) with (e_1, v_3);
- identify (v_2, e_2) with (v_3, e_2) and identify (e_2, v_2) with (e_2, v_3);
- identify (v_2, e_3) with (v_3, e_3) and identify (e_3, v_2) with (e_3, v_3).

This gives the space shown in Figure 3.9; it deformation retracts onto a graph homotopy equivalent to $S^1 \vee S^1 \vee S^1$. We write $V = \{v_2, v_3\}$ for the vertex of the P–graph obtained by identifying v_2 and v_3 in the Y–graph.

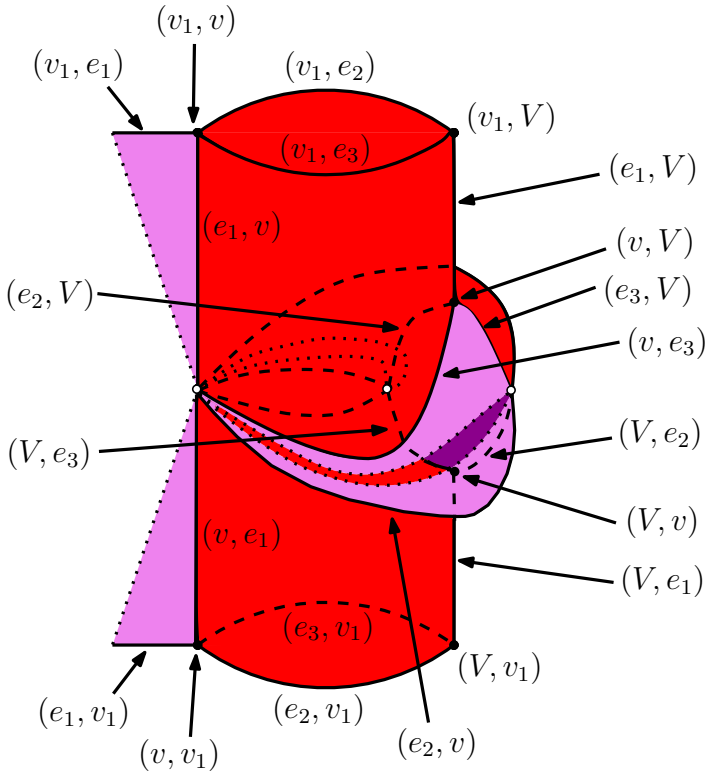

Figure 3.9: The configuration space $F(P, 2)$

Given the space $F(P, 2)$, we now deduce the structure of the thick particle configuration spaces $\{F_r(P, 2)\}_{r>0}$. Firstly, as r ranges over $(0, 1/2)$, the triangular fins of $F(P, 2)$ become smaller and the three holes expand in size. For $r \in (0, 1/2)$, the configuration space $F_r(P, 2)$ is homotopy equivalent to the space shown in Figure 3.10, and thus $F_r(P, 2) \simeq S^1 \vee S^1 \vee S^1$.

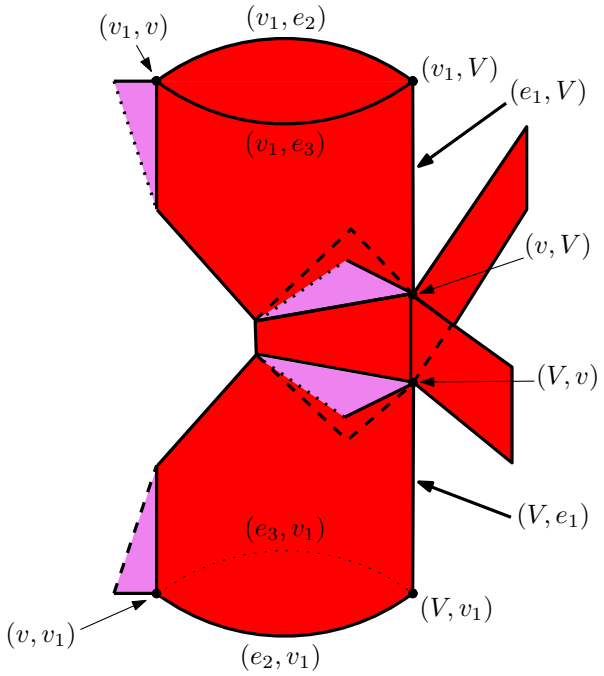

Figure 3.10: A space homotopy equivalent to $F_r(P, 2)$ when $r \in (0, 1/2)$

When $r = 1/2$, the triangular fins have disappeared and the holes have expanded to reach the pairs of vertices at distance one apart (namely (v_1, v), (v, v_1), (V, v) and (v, V)), see Figure 3.11. Next, for $r \in (1/2, 1)$, the configuration space $F_r(P, 2)$ is disconnected with two contractible components, as shown on the left of Figure 3.12. Finally, $F_1(P, 2)$ comprises the two vertex pairs (v_1, v_2) and (v_2, v_1), and $F_r(P, 2) = \emptyset$ for $r > 1$.

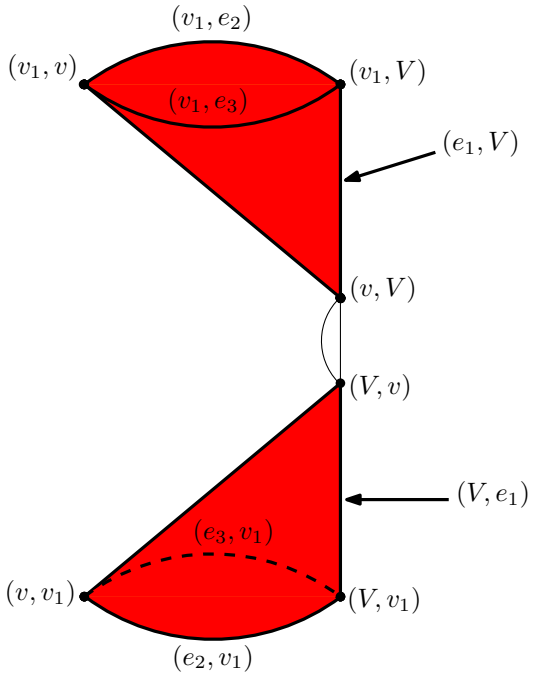

Figure 3.11: The space $F_{1/2}(P, 2)$

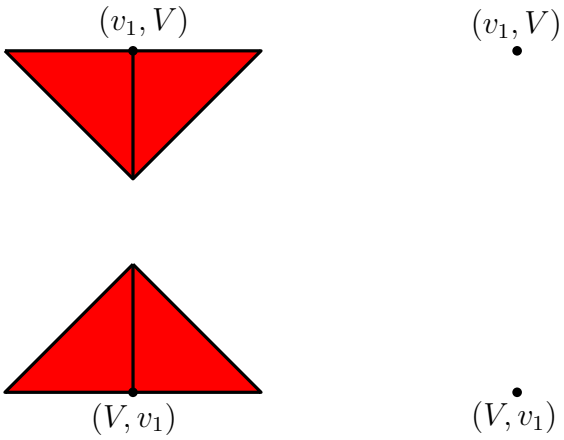

$F_r(P, 2)$ for $r \in (1/2, 1)$ The space $F_1(P, 2)$

Figure 3.12: The spaces $F_r(P, 2)$ for $r \in (1/2, 1]$

Remark 3.1.9. If we wish to study the collision-free motion of two robots of *different* radii $r_1, r_2 > 0$ on a metric graph Γ, then a suitable configuration space is

$$F_{r_1,r_2}(\Gamma, 2) := \{(x, y) \in \Gamma \times \Gamma : d(x, y) \geq r_1 + r_2\},$$

see Figure 3.13. However, $F_{r_1,r_2}(\Gamma, 2)$ is actually equal to the thick particle config-

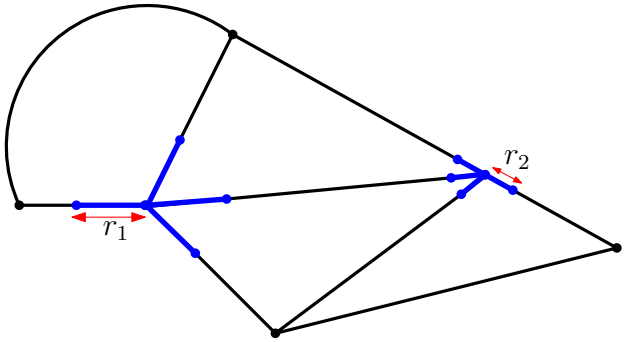

Figure 3.13: Two robots of different radii $r_1, r_2 > 0$

uration space $F_{(r_1+r_2)/2}(\Gamma, 2)$, so it suffices to study the family $\{F_r(\Gamma, 2)\}_{r>0}$. I am grateful to M. Farber and V. Kurlin for raising this question.

3.2 Critical values and homology groups

In this section we apply the PL Morse–Bott theory from §2.1 to obtain information on the homotopy type of the configuration spaces $\{F_r(\Gamma, 2)\}_{r>0}$. From Proposition 2.2.1, d is an affine Morse–Bott function on $\Gamma \times \Gamma$ with respect to a suitable CW structure. Since $F_r(\Gamma, 2) = d^{-1}([2r, \infty))$, we work with the sublevel sets of $g := -d$, which is also an affine Morse–Bott function (see Remark 2.1.4).

3.2.1 Critical values of the family $\{F_r(\Gamma, 2)\}_{r>0}$

In this subsection we define the critical values of the family $\{F_r(\Gamma, 2)\}_{r>0}$, and derive an upper bound for the number of critical values in terms of metric properties of Γ (see Theorem 3.2.3).

Definitions 3.2.1 (Regular and critical values)**.** A number $R > 0$ is a *regular value* of the family $\{F_r(\Gamma, 2)\}_{r>0}$ if there is an open set $U_R \subset (0, \infty)$ containing R such that $F_{r_2}(\Gamma, 2)$ is a deformation retract of $F_{r_1}(\Gamma, 2)$ for all $r_1, r_2 \in U_R$ with $r_1 \leq r_2$. A number $R > 0$ is a *critical value* of $\{F_r(\Gamma, 2)\}_{r>0}$ if it is not a regular value.

Examples 3.2.2.

1. Let $\Gamma = [0, 1]$ be the labelled graph from Example 3.1.5. We see that $F_s(\Gamma, 2)$ is a deformation retract of $F_r(\Gamma, 2)$ for all $r, s \in (0, 1/2]$ with $r \leq s$. In particular

$F_{1/2}(\Gamma, 2) = \{(0,1),(1,0)\} = Q_2$ is a deformation retract of $F_r(\Gamma, 2)$ for all $r \in (0, 1/2]$, and $F_r(\Gamma, 2) = \emptyset$ for all $r > 1/2$. Hence $r = 1/2$ is the only critical value of the family $\{F_r(\Gamma, 2)\}_{r>0}$; all other numbers $r > 0$ are regular values.

2. Let $\Gamma = S^1$ be the circle from Example 3.1.6. Then $F_s(\Gamma, 2)$ is a deformation retract of $F_r(\Gamma, 2)$ for all $r, s \in (0, 1/4]$ such that $r \leq s$. We have $F_r(\Gamma, 2) \simeq S^1$ for all $r \in (0, 1/4]$, and $F_r(\Gamma, 2) = \emptyset$ for all $r > 1/4$. Hence, $r = 1/4$ is the only critical value of the family $\{F_r(\Gamma, 2)\}_{r>0}$.

3. Let Γ be the Y–graph from Example 3.1.7. Here, $F_s(\Gamma, 2) \simeq S^1$ is a deformation retract of $F_r(\Gamma, 2)$ for all $r, s \in (0, 1/2]$ with $r \leq s$. For $r, s \in (1/2, 1]$ with $r \leq s$, $F_r(\Gamma, 2)$ deformation retracts onto $F_s(\Gamma, 2) \simeq Q_6$. We have $F_r(\Gamma, 2) = \emptyset$ for all $r > 1$. Hence, the critical values of the family $\{F_r(\Gamma, 2)\}_{r>0}$ are $1/2$ and 1; all other numbers $r > 0$ are regular values.

4. Let Γ be the P–graph from Example 3.1.8. We have $F_r(\Gamma, 2) \simeq S^1 \vee S^1 \vee S^1$ for all $r \in (0, 1/2]$, $F_r(\Gamma, 2) \simeq S^0$ for $r \in (1/2, 1]$ and $F_r(\Gamma, 2) = \emptyset$ for all $r > 1$. The critical values of the family $\{F_r(\Gamma, 2)\}_{r>0}$ are $1/2$ and 1; all other positive numbers are regular values.

Recall that $Z(\Gamma)$ is the set of cycles in Γ (subgraphs homeomorphic to S^1) and $\ell(C)$ is the length of $C \in Z(\Gamma)$. We also write $Z := |Z(\Gamma)|$ and $E = |E(\Gamma)|$. The following theorem is the main result of this chapter.

Theorem 3.2.3. *Each critical value of the family $\{F_r(\Gamma, 2)\}_{r>0}$ has the form*

$$\frac{1}{2}\left(\frac{1}{2}\sum_{C \in Z(\Gamma)} \varepsilon_C \ell(C) + \sum_{e \in E(\Gamma)} \varepsilon_e \ell(e)\right), \tag{1}$$

where at most two of $\varepsilon_C \in \{0, 1\}$ are non-zero and $\varepsilon_e \in \{0, 1\}$, $\forall e \in E(\Gamma)$. In particular, there are fewer than $2^E \max\{2Z(Z-1), 1\}$ critical values.

Proof. Let $\Gamma \times \Gamma$ be equipped with the subdivision from Proposition 2.2.1, so that d (and hence g) is an affine Morse–Bott function. Since $\Gamma \times \Gamma$ has finitely many cells, Proposition 2.1.21 implies that the family of sublevel sets $\{g^{-1}((-\infty, c])\}_{c \in \mathbb{R}}$ has finitely many critical values. Hence, the family $\{F_r(\Gamma, 2)\}_{r>0}$ has the same property.

To obtain formula (1), we refer to the proof of Proposition 2.2.1. Critical levels of d arising from Case 1 are contained in the set $\{d(v,w)\}_{v,w\in V(\Gamma)}$ of distances between vertices. Such distances have the form $\sum_{e\in E(\Gamma)} \varepsilon_e \ell(e)$ for some coefficients $\varepsilon_e \in \{0,1\}$.

Case 2(i) contributes critical levels of the form

$$\varepsilon_1 \ell(e) + \varepsilon_2 \ell(C),$$

for some edge e, cycle C and coefficients $\varepsilon_1, \varepsilon_2 \in \{0,1\}$, the latter not both zero. Critical levels of d arising from Case 2(ii) have the form $\ell(C)/2$ for some $C \in Z(\Gamma)$. Case 2(iii) contributes critical levels of the form

$$\frac{1}{2}(\varepsilon_1 \ell(C_1) + \varepsilon_2 \ell(C_2)) + \sum_{e\in E(\Gamma)} \varepsilon_e \ell(e)$$

for some coefficients $\varepsilon_1, \varepsilon_2, \varepsilon_e \in \{0,1\}$, not all zero, see Figure 2.21. Finally, we combine these observations to obtain formula (1). The factor of $1/2$ appears because a critical value of the family $\{F_r(\Gamma,2)\}_{r>0}$ is a critical level of d divided by two. □

Remark 3.2.4. Let Γ be the Y–graph from Example 3.1.7. Excluding numbers exceeding $\frac{1}{2}\operatorname{diam}\Gamma$ (this may be done in view of Lemma 3.1.4), formula (1) yields two possible critical values of the family $\{F_r(\Gamma,2)\}_{r>0}$, namely $1/2$ and 1. Hence part 3 of Examples 3.2.2 shows that the number of possible critical values given by (1) is exact for this graph.

Example 3.2.5. Let Γ be the 1–skeleton of the 3–simplex Δ^3, and equip each edge with label 1, see Figure 3.14. Cycles in Γ have length 3 or 4, depending

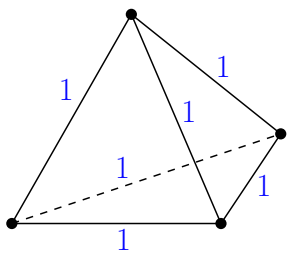

Figure 3.14: The labelled 1–skeleton of Δ^3

on the number of edges they contain. From Theorem 3.2.3, the critical values of

$\{F_r(\Gamma,2)\}_{r>0}$ have the form

$$R = \frac{1}{2}\left(\frac{1}{2}\lambda + K\right),$$

where $\lambda \in \{0,3,4,6,7,8\}$ and $K \in \{0,1,\ldots,6\}$.

Example 3.2.6. Consider the labelled graph shown below.

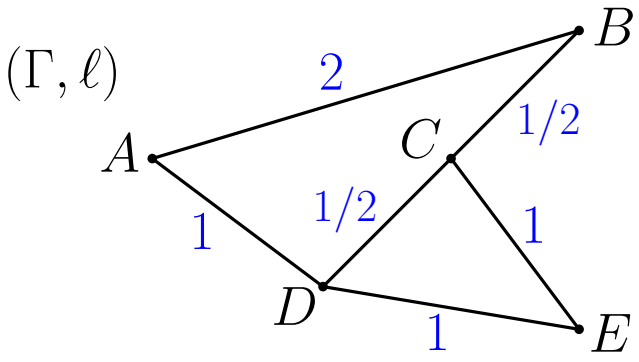

The cycles are (i) $ABCDA$, of length 4; (ii) $DCED$, of length 5/2, and (iii) $ABCEDA$, of length 11/2. Three edges have label 1, two have label 1/2, and one has label 2. From Theorem 3.2.3, each critical value of $\{F_r(\Gamma,2)\}_{r>0}$ has the form

$$R = \tfrac{1}{2}\left(\tfrac{1}{2}\lambda + K\right), \text{ where } \lambda \in \left\{0, \tfrac{5}{2}, 4, \tfrac{11}{2}, 8, 5, 11, \tfrac{13}{2}, \tfrac{19}{2}\right\},$$

and $K = \varepsilon_1 + \varepsilon_2 + \varepsilon_3 + \frac{1}{2}(\varepsilon_4 + \varepsilon_5) + 2\varepsilon_6$ for some $\varepsilon_i \in \{0,1\}$, $1 \le i \le 6$.

3.2.2 Behaviour across a critical value

We now focus on the change in homotopy type of $F_r(\Gamma,2)$ as r transits a critical value. The results of PL Morse–Bott theory (see §2.1.3) provide a complete answer to this question, which we quantify by computing $\operatorname{rk} H_k(F_a(\Gamma,2), F_b(\Gamma,2); \mathbb{Q})$ for $k = 0,1,2$ and calculating explicit generators for $H_2(F_a(\Gamma,2), F_b(\Gamma,2); \mathbb{Q})$.

The critical subcomplex, descending sets and descending links

Suppose that $0 < a < D/2 < b$ are such that D is the only critical level of the metric d in $[2a, 2b]$. Since there are no critical cells of dimension two, the critical subcomplex $C(d)$ is a graph. In particular, $C(d,D)$ is a graph. Let Z be a component of $C(d,D)$.

From the previous section (see Figures 2.15, 2.18 and 2.21) only the 0–cells of Z need be considered to determine $\mathrm{Lk}_{\downarrow}(Z)$, via the disjoint union

$$\mathrm{Lk}_{\downarrow}(Z) = \coprod_{(v,w)\in Z^{(0)}} \mathrm{Lk}_{\downarrow}(v,w).$$

Let (v,w) be a 0–cell of Z. This means that (v,w) is a vertex of $\Gamma\times\Gamma$ with respect to the subdivision from Proposition 2.2.1. The g–descending cells F such that $g|_F$ achieves its maximum on (v,w) are found as follows.

(Case 1). Suppose that both v and w are vertices of Γ. Let $e_1,\ldots,e_p$ be the edges incident to v such that $y\mapsto d(y,w)$ increases on e_i as we move away from v. Let $f_1,\ldots,f_q$ be the edges incident to w such that $y\mapsto d(y,v)$ increases on f_j as we move away from w, see Figure 3.15. Then the above cells F are the largest cells of $\Gamma\times\Gamma$ containing (v,w) and contained in the products $\overline{e}_i\times\overline{f}_j$. The subset $\mathrm{Lk}_{\downarrow}(v,w)\cap F$ of $\mathrm{Lk}_{\downarrow}(v,w)$ contained in F is shown in Figure 3.16.

Figure 3.15: Finding the g–descending cells incident to (v,w)

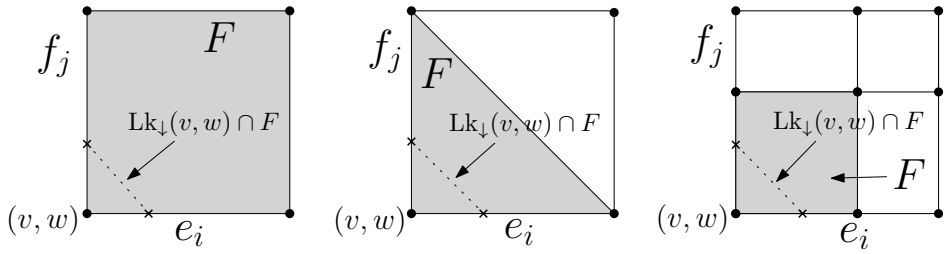

Figure 3.16: g–descending cells F incident to (v,w), with $\mathrm{Lk}_{\downarrow}(v,w)\cap F$ shown in each case

It follows that $\mathrm{Lk}_{\downarrow}(v,w) = K_{p,q}$ (the complete bipartite graph of type (p,q)), where we set $K_{0,m} := Q_m$ to be a discrete set of $m\geq 1$ points and $K_{0,0} := \emptyset$.

(Case 2). Now suppose that one of v, w is a vertex of Γ and the other is equidistant (at distance D) along at least two distinct paths, see Figure 3.17.

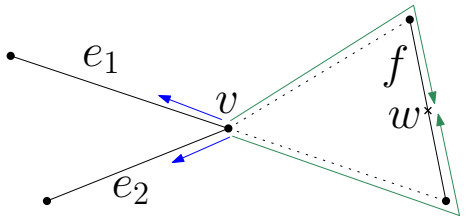

Figure 3.17: The situation in Case 2

Let $e_1, \ldots, e_m$ be the edges incident to v satisfying the same property as in Case 1 above. Then the cells F such that $g|_F$ achieves its maximum on (v, w) are precisely $\overline{e}_i \times \{w\}$, for $1 \leq i \leq m$. Hence $\mathrm{Lk}_\downarrow(v, w) = Q_m$ (a discrete set of m points). If v, w are both not vertices of Γ, then (v, w) is a vertex of the subdivision of $\Gamma \times \Gamma$ from Case 2(iii) in §2.2, see Figure 2.21. In this case $\mathrm{Lk}_\downarrow(v, w) = \emptyset$, since (v, w) is a local maximum of d.

The map $h : \mathrm{Lk}_\downarrow(Z) \to Z$

It is easy to determine the map $h : \mathrm{Lk}_\downarrow(Z) \to Z$ for Z a component of $C(d, D)$. Indeed, $\mathrm{Lk}_\downarrow(Z)$ is the disjoint union $\coprod_{(v,w)\in Z^{(0)}} \mathrm{Lk}_\downarrow(v, w)$ and for each $(v, w) \in Z^{(0)}$, $h|_{\mathrm{Lk}_\downarrow(v,w)}$ is constant with value (v, w). In particular, for $j \geq 0$,

$$\ker[h_* : H_j(\mathrm{Lk}_\downarrow(Z)) \to H_j(Z)] = H_j(\mathrm{Lk}_\downarrow(Z)) = \bigoplus_{(v,w)\in Z^{(0)}} H_j(\mathrm{Lk}_\downarrow(v, w)),$$

and

$$\mathrm{coker}[h_* : H_j(\mathrm{Lk}_\downarrow(Z)) \to H_j(Z)] = H_j(Z) \quad \text{for} \quad j \geq 1.$$

From above, $\mathrm{Lk}_\downarrow(v, w) = K_{p,q}$, where $p = p(v, w)$, $q = q(v, w) \geq 0$ are as previously defined. Thus,

$$H_j(K_{p,q}) = \begin{cases} \mathbb{Z}, & j = 0 \\ \mathbb{Z}^{(p-1)(q-1)}, & j = 1 \\ 0, & j \geq 2, \end{cases} \qquad \text{for } p, q \geq 1, \tag{1}$$

and

$$H_j(K_{0,n}) = \begin{cases} \mathbb{Z}^n, & j = 0 \\ 0, & j \geq 1, \end{cases} \qquad \text{for } n \geq 0. \tag{2}$$

Applying the main result

Let $Z_1, \ldots, Z_n$ be the components of $C(d, D)$. Applying a corollary of Proposition 2.1.23 (see Remarks 2.1.28(ii)) gives the following statement. (In the following material we write $F_s \equiv F_s(\Gamma, 2)$ for clarity.)

Theorem 3.2.7. *For each $j \geq 0$,*

$$\begin{aligned}\operatorname{rk} H_j(F_a, F_b; \mathbb{Q}) = \sum_{i=1}^{n} &(\operatorname{rk}\operatorname{coker}[(h_i)_* : H_j(\mathrm{Lk}_\downarrow(Z_i)) \to H_j(Z_i)] \\ &+ \operatorname{rk}\ker[(h_i)_* : H_{j-1}(\mathrm{Lk}_\downarrow(Z_i)) \to H_{j-1}(Z_i)])\,.\end{aligned}$$

We now analyse this statement for $j = 0, 1$ and 2 separately. When $j = 0$, we have

$$\operatorname{rk}\operatorname{coker}[(h_i)_* : H_0(\mathrm{Lk}_\downarrow(Z_i)) \to H_0(Z_i)] = \operatorname{rk} H_0(Z_i) = 1,$$

since $(h_i)_* = 0$ and Z_i is connected. Hence we find that $\operatorname{rk} H_0(F_a, F_b)$ is the number of path-components of $C(d, D)$.

For $j = 1$, we have

$$\begin{aligned}&\operatorname{rk}\operatorname{coker}[(h_i)_* : H_1(\mathrm{Lk}_\downarrow(Z_i)) \to H_1(Z_i)] + \operatorname{rk}\ker[(h_i)_* : H_0(\mathrm{Lk}_\downarrow(Z_i)) \to H_0(Z_i)] \\ &\quad = \operatorname{rk} H_1(Z_i) + \operatorname{rk} H_0(\mathrm{Lk}_\downarrow(Z_i)) \quad (\text{since } (h_i)_* = 0) \\ &\quad = \operatorname{rk} H_1(Z_i) + \sum_{(v,w)\in Z_i^{(0)}} \operatorname{rk} H_0(\mathrm{Lk}_\downarrow(v, w)).\end{aligned}$$

For each $(v, w) \in Z_i^{(0)}$, $\operatorname{rk} H_0(\mathrm{Lk}_\downarrow(v, w))$ may be computed explicitly from formulas (1) and (2). Moreover, Z_i is a connected graph, so we have an algorithm for computing $\operatorname{rk} H_1(Z_i)$ and thus also for computing $\operatorname{rk} H_1(F_a, F_b)$.

For $j = 2$, we use the facts that $H_2(Z_i) = 0$ and $(h_i)_* = 0$ to obtain

$$\begin{aligned}&\operatorname{rk}\operatorname{coker}[(h_i)_* : H_2(\mathrm{Lk}_\downarrow(Z_i)) \to H_2(Z_i)] + \operatorname{rk}\ker[(h_i)_* : H_1(\mathrm{Lk}_\downarrow(Z_i)) \to H_1(Z_i)] \\ &\quad = 0 + \operatorname{rk} H_1(\mathrm{Lk}_\downarrow(Z_i)) = \sum_{(v,w)\in Z_i^{(0)}} \operatorname{rk} H_1(\mathrm{Lk}_\downarrow(v, w)) \\ &\quad = \sum_{\substack{(v,w)\in Z_i^{(0)} \\ p(v,w),q(v,w)\geq 2}} (p(v, w) - 1)(q(v, w) - 1). \qquad (3)\end{aligned}$$

Figure 3.18: $p(v,w), q(v,w) \geq 2$

Finally, we describe explicit generators for $H_2(F_a, F_b)$. Suppose that $(v,w) \in Z_i^{(0)}$ contributes to the sum (3). We have $p(v,w), q(v,w) \geq 2$, see Figure 3.18. The g–descending link of (v,w) is $\mathrm{Lk}_\downarrow(v,w) = K_{p,q}$, see Figure 3.19. Choose the maximal

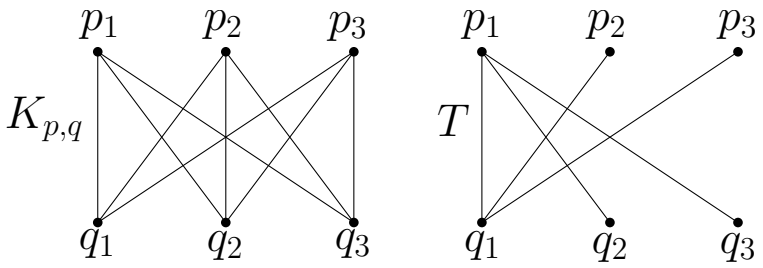

Figure 3.19: The descending link $\mathrm{Lk}_\downarrow(v,w) = K_{p,q}$ and the maximal tree T

tree T in $K_{p,q}$ as shown in Figure 3.19. There are $(p-1)(q-1)$ edges of $K_{p,q}$ not contained in T. The generators of $H_1(K_{p,q})$ are the cycles in $K_{p,q}$ defined by the sequences $(p_1, q_1, p_i, q_j, p_1)$ for $i,j \geq 2$. From the exact sequence of the pair (F_a, F_b), $H_2(F_a, F_b)$ is isomorphic to a subgroup of $H_1(F_b)$. We interpret the generators of $H_1(K_{p,q})$ as generators of $H_1(F_b)$ which lie in the kernel of the inclusion-induced homomorphism $H_1(F_b) \to H_1(F_a)$, see Figure 3.20.

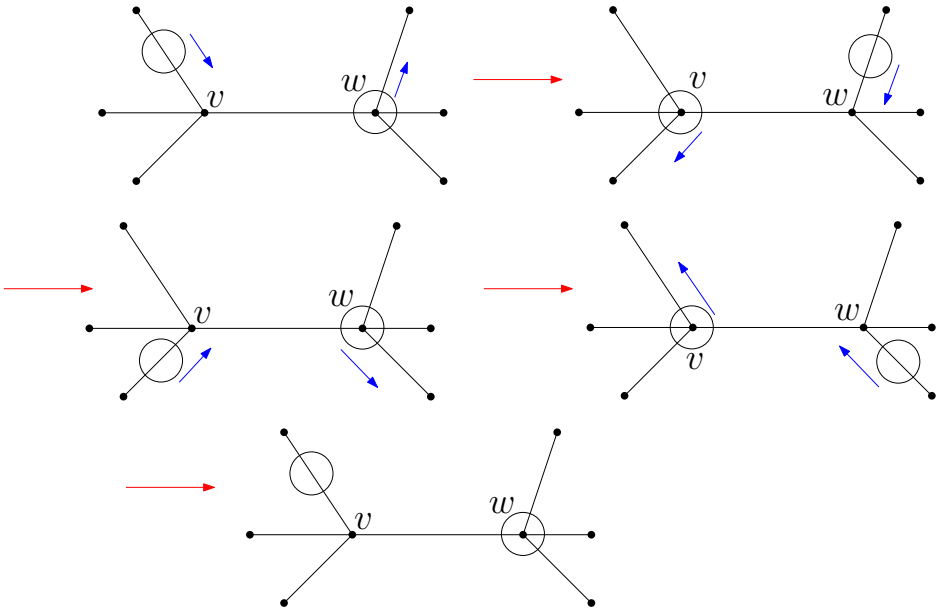

Figure 3.20: Generators of $H_1(K_{p,q})$ interpreted as cycles in $H_1(F_b)$

3.3 Further examples of applying PL Morse–Bott theory

In this section we discuss some examples of applying the theory from §2.1 to families of configuration spaces $\{F_r(\Gamma,2)\}_{r>0}$ for specific labelled graphs (Γ,ℓ).

We know from Theorem 3.2.3 and Lemma 3.1.4 that $F_r(\Gamma,2)$ assumes finitely many homotopy types as r ranges over $\left(0,\frac{1}{2}\operatorname{diam}\Gamma\right]$ and that $F_r(\Gamma,2)=\emptyset$ if and only if $r>\frac{1}{2}\operatorname{diam}\Gamma$, respectively. PL Morse–Bott theory also tells us how to compute the change in homotopy type as r passes a critical value (see Proposition 2.1.23). Referring ahead to Theorem 4.1.6, there is a homotopy equivalence $F_r(\Gamma,2)\simeq F(\Gamma,2)$ for sufficiently small r. Combining these results, we could in principle start with the space $F_R(\Gamma,2)$ for $R=\frac{1}{2}\operatorname{diam}\Gamma$ and construct a space homotopy equivalent to the 2–point configuration space $F(\Gamma,2)$. This is precisely what we do in this section.

Example 3.3.1. Let (Γ,ℓ) be the labelled Y–graph as shown, and let $\Gamma\times\Gamma$ have the product CW structure.

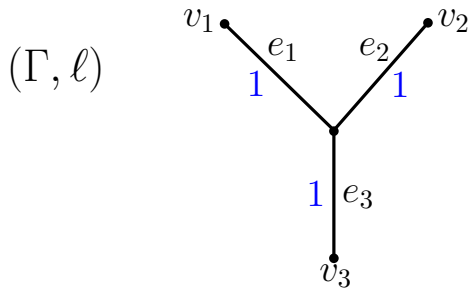

Since Γ is a tree, the metric d is an affine Morse–Bott function without any further subdivision of $\Gamma \times \Gamma$ (see the proof of Proposition 2.2.1 – for a tree we are always in Case 1). The critical levels of d are 1 and 2, corresponding to the distances between distinct vertices. We compute the homotopy type of $d^{-1}([1,\infty)) = F_{1/2}(\Gamma, 2)$ using PL Morse–Bott theory. Note that Theorem 4.1.6 shows that there is a homotopy equivalence $F_{1/2}(\Gamma, 2) \simeq F(\Gamma, 2)$. Firstly, $d^{-1}([2,\infty)) = C(d, 2)$ comprises the six points

$$\{(v_i, v_j) : i, j \in \{1, 2, 3\},\ \ i \neq j\}.$$

Moreover, $C(d, 1)$ comprises the six pairs of vertices at distance one apart:

$$C(d, 1) = \{(v, v_i), (v_i, v) : i \in \{1, 2, 3\}\}.$$

The following table shows the ascending cells incident to the cells of $C(d, 1)$. (We now work with d–ascending cells and links rather than using $g = -d$ and finding g–descending cells.)[1] We use the notation Q_m for a discrete set of m points.

Cell of $C(d,1)$	Ascending Cells	Ascending Link
(v_1, v)	$(v_1, e_2), (v_1, e_3)$	$\mathrm{Lk}_\uparrow(v_1, v) = Q_2$
(v_2, v)	$(v_2, e_1), (v_2, e_3)$	$\mathrm{Lk}_\uparrow(v_2, v) = Q_2$
(v_3, v)	$(v_3, e_1), (v_3, e_2)$	$\mathrm{Lk}_\uparrow(v_3, v) = Q_2$
(v, v_1)	$(e_2, v_1), (e_3, v_1)$	$\mathrm{Lk}_\uparrow(v, v_1) = Q_2$
(v, v_2)	$(e_1, v_2), (e_3, v_2)$	$\mathrm{Lk}_\uparrow(v, v_2) = Q_2$
(v, v_3)	$(e_1, v_3), (e_2, v_3)$	$\mathrm{Lk}_\uparrow(v, v_3) = Q_2$

The cone over Q_2 is an interval, see Figure 3.21. From this data and the statement of

[1] Ascending cells and links are defined in the obvious way, see Definition 2.1.10 and Definition 2.1.15.

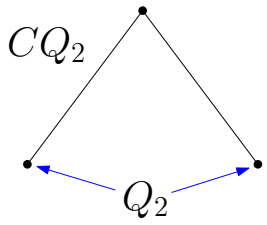

Figure 3.21: The cone CQ_2 over Q_2

Proposition 2.1.23, $F_{1/2}(\Gamma, 2)$ is homotopy equivalent to the space shown in Figure 3.22. We obtain $F_{1/2}(\Gamma, 2) \simeq S^1$ and thus $F(\Gamma, 2) \simeq S^1$.

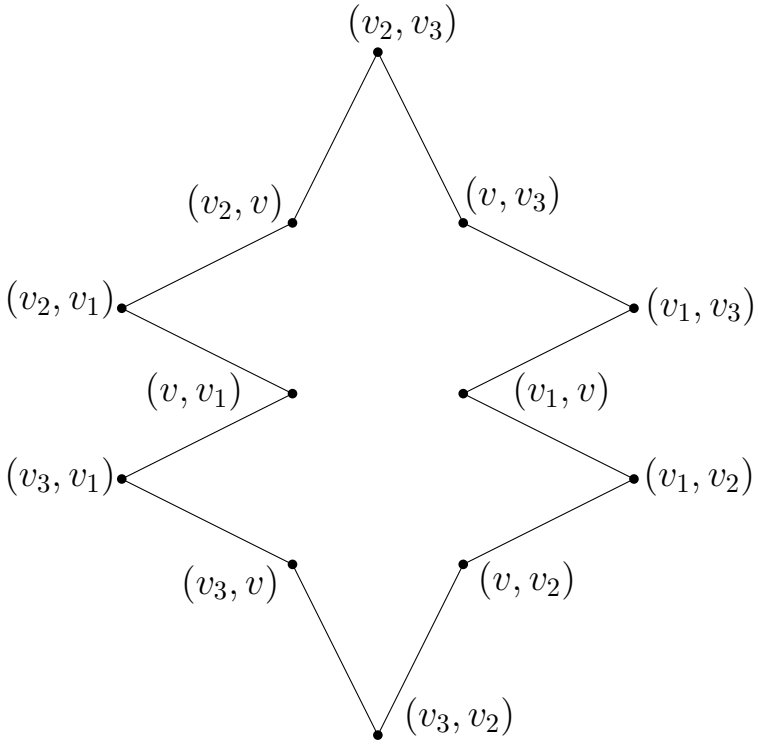

Figure 3.22: A space homotopy equivalent to $F_{1/2}(\Gamma, 2)$ when Γ is the Y–graph

Example 3.3.2. Let (Γ, ℓ) be the labelled P–graph shown in Figure 3.23. We subdivide the product CW structure on $\Gamma \times \Gamma$ so that d is an affine Morse–Bott function (see the proof of Proposition 2.2.1, Cases 1 and 2(ii)). The critical levels of d are 1/2, 1, 3/2 and 2. Since removing vertices of degree two does not change the metric space (Γ, ℓ) (see Lemma 1.5.4), Theorem 3.2.3 shows that 1/2 and 1 are the only critical values. In particular, we have a homotopy equivalence $F(\Gamma, 2) \simeq F_{1/2}(\Gamma, 2)$. We now compute the homotopy type of $F_{1/2}(\Gamma, 2)$ using PL Morse–Bott

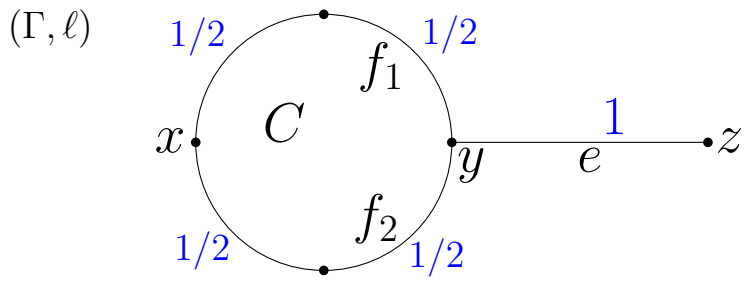

Figure 3.23: The labelling on the P–graph $\Gamma = S^1 \vee [0,1]$

theory. We have

$$C(d,2) = d^{-1}([2,\infty)) = \{(x,z),(z,x)\}.$$

Moreover, $C(d,1)$ comprises the antipodal configurations on the cycle C together with the configurations (y,z) and (z,y). The following table shows the ascending cells incident to the cells of $C(d,1)$.

Cell of $C(d,1)$	Ascending Cells	Ascending Link
(x,y)	(x,e)	$\mathrm{Lk}_\uparrow(x,y) = Q_1 = \{\star\}$
(y,x)	(e,x)	$\mathrm{Lk}_\uparrow(y,x) = Q_1 = \{\star\}$
(y,z)	$(f_1,z),(f_2,z)$	$\mathrm{Lk}_\uparrow(y,z) = Q_2$
(z,y)	$(z,f_1),(z,f_2)$	$\mathrm{Lk}_\uparrow(z,y) = Q_2$

From this data and Proposition 2.1.23, $F_{1/2}(\Gamma,2)$ is homotopy equivalent to the space shown in Figure 3.24, and hence $F(\Gamma,2) \simeq F_{1/2}(\Gamma,2) \simeq S^1 \vee S^1 \vee S^1$.

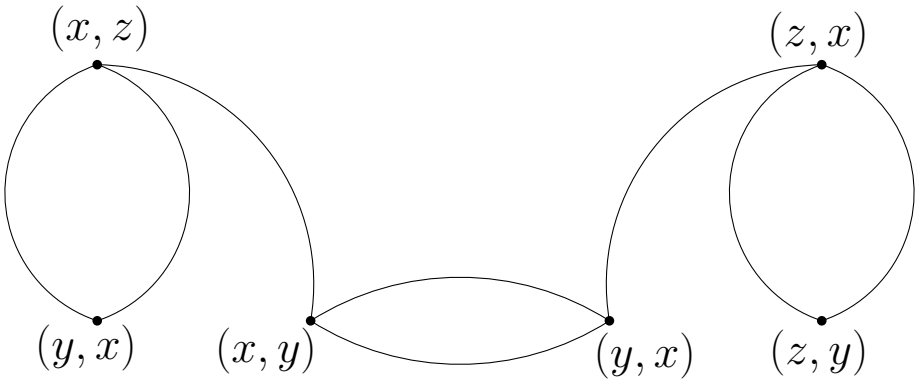

Figure 3.24: A space homotopy equivalent to $F_{1/2}(S^1 \vee [0,1],2)$

Example 3.3.3. Let (Γ,ℓ) be the labelled wedge of two circles shown in Figure 3.25. As in Example 3.3.2, we subdivide $\Gamma \times \Gamma$ so that d is piecewise affine. The

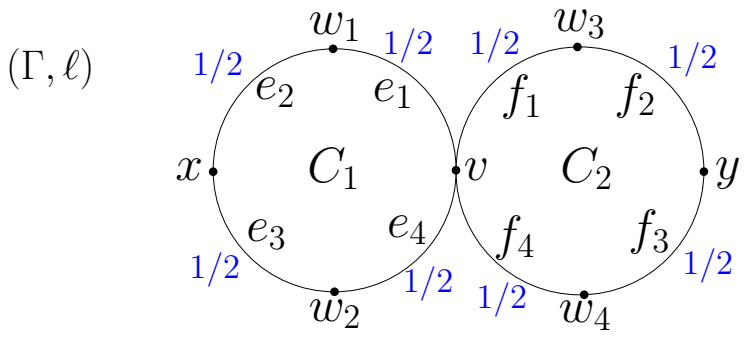

Figure 3.25: The labelling on $\Gamma = S^1 \vee S^1$

critical levels of d are $1/2$, 1, $3/2$ and 2; as in Example 3.3.2, $1/2$ and 1 are the only possible critical values and thus $F(\Gamma, 2) \simeq F_{1/2}(\Gamma, 2)$. We now compute the homotopy type of $F_{1/2}(\Gamma, 2)$ using PL Morse–Bott theory. We have

$$C(d, 2) = d^{-1}([2, \infty)) = \{(x, y), (y, x)\}.$$

Moreover, $C(d, 1)$ comprises two circles corresponding to antipodal configurations on the two cycles C_1 and C_2, together with the eight configurations

$$(w_1, w_3), (w_1, w_4), (w_2, w_3), (w_2, w_4), (w_3, w_1), (w_3, w_2), (w_4, w_1), (w_4, w_2).$$

The following table shows the ascending cells incident to the cells of $C(d, 1)$.

Cell of $C(d, 1)$	Ascending Cells	Ascending Link
(x, v)	(x, f_1), (x, f_4)	$\mathrm{Lk}_\uparrow(x, v) = Q_2$
(v, x)	(f_1, x), (f_4, x)	$\mathrm{Lk}_\uparrow(v, x) = Q_2$
(v, y)	(e_1, y), (e_4, y)	$\mathrm{Lk}_\uparrow(v, y) = Q_2$
(y, v)	(y, e_1), (y, e_4)	$\mathrm{Lk}_\uparrow(y, v) = Q_2$
(w_1, w_3)	$e_2 \times f_2$	$\mathrm{Lk}_\uparrow(w_1, w_3) = [0, 1]$
(w_1, w_4)	$e_2 \times f_3$	$\mathrm{Lk}_\uparrow(w_1, w_4) = [0, 1]$
(w_2, w_3)	$e_3 \times f_2$	$\mathrm{Lk}_\uparrow(w_2, w_3) = [0, 1]$
(w_2, w_4)	$e_3 \times f_3$	$\mathrm{Lk}_\uparrow(w_2, w_4) = [0, 1]$
(w_3, w_1)	$f_2 \times e_2$	$\mathrm{Lk}_\uparrow(w_3, w_1) = [0, 1]$
(w_3, w_2)	$f_2 \times e_3$	$\mathrm{Lk}_\uparrow(w_3, w_2) = [0, 1]$
(w_4, w_1)	$f_3 \times e_2$	$\mathrm{Lk}_\uparrow(w_4, w_1) = [0, 1]$
(w_4, w_2)	$f_3 \times e_3$	$\mathrm{Lk}_\uparrow(w_4, w_2) = [0, 1]$

Using this data and Proposition 2.1.23, $F_{1/2}(\Gamma, 2)$ is homotopy equivalent to the space shown in Figure 3.26, and hence $F(\Gamma, 2) \simeq \bigvee_{i=1}^{7} S^1$. This confirms the calculation performed in Example 4.2.3, where we obtained the homotopy equivalence $F(\Gamma, 2) \simeq \bigvee_{i=1}^{7} S^1$ using Abrams' deformation retraction of $F(\Gamma, 2)$ onto $D(\Gamma, 2)$ (see [1, Theorem 2.4]).

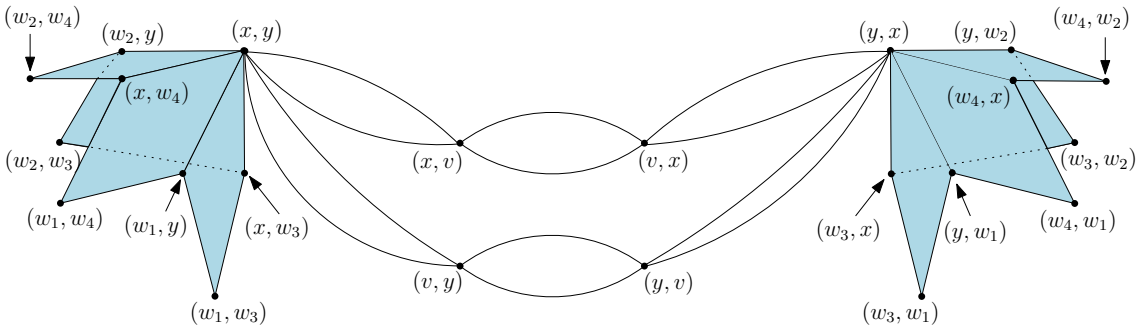

Figure 3.26: A space homotopy equivalent to $F_{1/2}(S^1 \vee S^1, 2)$

Example 3.3.4. We now generalise the results from Examples 3.3.1, 3.3.2 and 3.3.3. Let $T_{k,\ell}$ be the graph comprising k intervals and ℓ circles incident to a central vertex v, see Figure 3.27. We allow $k, \ell \geq 0$ provided $k^2 + \ell^2 \neq 0$, and we equip each edge with label 1. In this example we use PL Morse–Bott theory to compute the

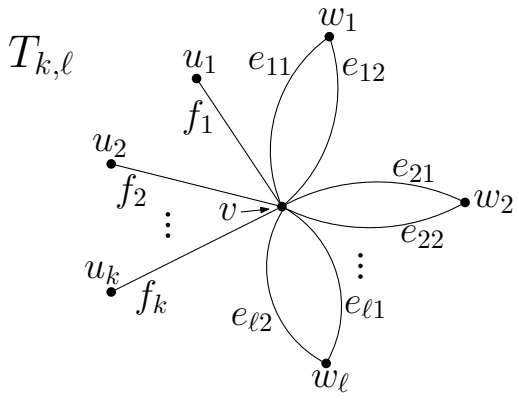

Figure 3.27: The graph structure on $T_{k,\ell}$

homotopy type and Euler characteristic of $F(T_{k,\ell}, 2)$. This calculation was first done by M. Safi–Samghabadi (a PhD student of V. Kurlin) who generalised a method due to R. Ghrist [33, Proposition 4.1] to compute the homotopy type and Euler characteristic of $F(T_{k,\ell}, N)$ for any $N \geq 2$.

Although $T_{k,\ell}$ is not simple, we observe that $\Gamma \times \Gamma$ admits a subdivision such that the metric d is piecewise affine (we are in cases 1 and 2(ii) of the proof of Proposition 2.2.1). The critical levels of d are 1 and 2, and the possible critical values are $1/2$ and 1. In particular, we have a homotopy equivalence $F_{1/2}(T_{k,\ell}, 2) \simeq F(T_{k,\ell}, 2)$. The complex $C(d, 2)$ consists of the vertex pairs

(i) (u_i, u_j) for $i, j \in \{1, \ldots, k\}$ with $i \neq j$;

(ii) (w_i, w_j) for $i, j \in \{1, \ldots, \ell\}$ with $i \neq j$;

(iii) (u_i, w_j), (w_j, u_i) for $i \in \{1, \ldots, k\}$, $j \in \{1, \ldots, \ell\}$,

giving a total of $k(k-1)+\ell(\ell-1)+2k\ell$ pairs. Moreover, $C(d, 1)$ comprises ℓ circles corresponding to antipodal configurations on the ℓ distinct cycles in Γ, together with the vertex pairs (u_i, v), (v, u_i) for $1 \leq i \leq k$. The following table shows the ascending cells incident to the cells of $C(d, 1)$.

Cell of $C(d,1)$	Ascending Cells	Ascending Link
$(u_i, v),\ 1 \leq i \leq k$	$(u_i, e_{st}),\ s \in \{1, \ldots, \ell\},\ t \in \{1, 2\}$	Q_{2l+k-1}
	$(u_i, f_j),\ j \in \{1, \ldots, k\} - \{i\}$	
$(v, u_i),\ 1 \leq i \leq k$	$(e_{st}, u_i),\ s \in \{1, \ldots, \ell\},\ t \in \{1, 2\}$	Q_{2l+k-1}
	$(f_j, u_i),\ j \in \{1, \ldots, k\} - \{i\}$	
$(w_j, v),\ 1 \leq j \leq \ell$	$(w_j, e_{st}),\ s \in \{1, \ldots, \ell\} - \{j\},\ t \in \{1, 2\}$	$Q_{2\ell-2+k}$
	$(w_j, f_i),\ 1 \leq i \leq k$	
$(v, w_j),\ 1 \leq j \leq \ell$	$(e_{st}, w_j),\ s \in \{1, \ldots, \ell\} - \{j\},\ t \in \{1, 2\}$	$Q_{2\ell-2+k}$
	$(w_j, f_i),\ 1 \leq i \leq k$	

We know from §5.1 that $F(T_{k,\ell}, 2)$ is path-connected unless $T_{k,\ell}$ is an interval (which occurs if and only if $(k, \ell) \in \{(1, 0), (2, 0)\}$). In the case $(k, \ell) = (1, 0)$ there are no ascending cells and we obtain $F(T_{1,0}, 2) \simeq S^0$ and $\chi(F(T_{1,0}, 2)) = 2$. In the case $(k, \ell) = (2, 0)$ we obtain $F(T_{2,0}, 2) \simeq [0, 1] \sqcup [0, 1] \simeq S^0$ and $\chi(F(T_{2,0}, 2)) = 2$. If $(k, \ell) \notin \{(1, 0), (2, 0)\}$ then $T_{k,\ell} \ncong [0, 1]$ and so $F(T_{k,\ell}, 2)$ is path-connected. Proposition 2.1.23 and the data from the table yield a graph G homotopy equivalent to $F_{1/2}(T_{k,\ell}, 2) \simeq F(T_{k,\ell}, 2)$; in particular, G is connected. Hence $F(T_{k,\ell}, 2)$ is homotopy equivalent to the wedge sum of $1 - \chi(G)$ circles and $\chi(F(T_{k,\ell}, 2)) = \chi(G)$. We

compute

$$\begin{aligned}\chi(G) &= \underbrace{k(k-1)+\ell(\ell-1)+2k\ell}_{\text{0–cells of } C(d,2)} + \underbrace{2k+2\ell}_{\text{0–cells of } C(d,1)} - \underbrace{2\ell}_{\text{1–cells of } C(d,1)} \\ &\quad - \underbrace{(2k(2\ell+k-1)+2\ell(2\ell-2+k))}_{\text{ascending 1–cells}} \\ &= -k^2+3k-3\ell^2+3\ell-4k\ell.\end{aligned}$$

The first three rows of the following table confirm Examples 3.3.1, 3.3.2 and 3.3.3.

(k,ℓ)	$\chi(F(T_{k,\ell},2))$	$F(T_{k,\ell},2)\simeq$
$(3,0)$	0	S^1
$(1,1)$	-2	$S^1\vee S^1\vee S^1$
$(0,2)$	-6	$\bigvee_{i=1}^{7} S^1$
$(k,0)$	$-k^2+3k$	$\bigvee_{k^2-3k+1} S^1$
$(0,\ell)$	$-3\ell^2+3\ell$	$\bigvee_{3\ell^2-3\ell+1} S^1$

The penultimate row agrees with M. Farber's work on $F(T,2)$ for a tree T: in paper [19, Theorem 12] it is proved that $F(T,2)\simeq\bigvee_{n_T} S^1$, where $n_T=\sum_{v\in V(T)}(\mu(v)-1)(\mu(v)-2)-1$. When $T=T_{k,0}$ we have $n_T=(k-1)(k-2)-1=k^2-3k+1$. This formula also agrees with the result of [33, Proposition 4.1] (in the case $N=2$) where R. Ghrist computes $\chi(F(T_{k,0},2))$ using a different method. Additionally, row 2 agrees with [33, Example 4] (see Examples 3.1.8) where R. Ghrist constructs the configuration space $F(T_{1,1},2)\simeq S^1\vee S^1\vee S^1$.

3.4 Open thick particle configuration spaces

In this section we briefly discuss another family of thick particle configuration spaces, which we refer to as the *open* thick particle configuration spaces. We find it more convenient to work with this family for the majority of Chapter 4. As the following remarks show, the two families have the same critical values and assume the same set of homotopy types.

Remarks 3.4.1. Consider the family of spaces $\{F_r^{\mathcal{O}}(\Gamma,2)\}_{r\geq 0}$, where we define

$$F_r^{\mathcal{O}}(\Gamma,2) := d^{-1}((2r,\infty)) = \{(x,y)\in\Gamma\times\Gamma : d(x,y)>2r\} \text{ for } r\geq 0.$$

(Note that $F_0^{\mathcal{O}}(\Gamma,2) = F(\Gamma,2)$). The space $F_r^{\mathcal{O}}(\Gamma,2)$ models the collision-free motion of two objects (robots) of radius r moving on Γ, where tangencies between the objects are *not* permitted.

We now refer to the proof of Proposition 2.1.21. The deformation retraction defined there restricts to a deformation retraction of $f^{-1}((-\infty,S))$ onto $X_R = f^{-1}((-\infty,R])$ for any $S \in [R,R')$, so in particular we have $f^{-1}((-\infty,S)) \simeq X_R$.

Now let $0 < r_1 < r_2 < \cdots < r_k = \frac{1}{2}\operatorname{diam}\Gamma$ be the critical values of the family $\{F_r(\Gamma,2)\}_{r>0}$. The previous fact immediately implies that $F_s^{\mathcal{O}}(\Gamma,2) \simeq F_{r_1}(\Gamma,2)$ for all $s \in (0,r_1)$ and

$$F_s^{\mathcal{O}}(\Gamma,2) \simeq F_{r_i}(\Gamma,2), \quad \forall s \in [r_{i-1},r_i), \quad \forall i \in \{2,3,\ldots,k\}.$$

We therefore obtain the following properties:

(i) if r is a regular value of the family $\{F_r(\Gamma,2)\}_{r>0}$, then $F_r(\Gamma,2) \simeq F_r^{\mathcal{O}}(\Gamma,2)$;

(ii) if r is a critical value of the family $\{F_r(\Gamma,2)\}_{r>0}$, then $\exists \varepsilon > 0$ such that $F_s^{\mathcal{O}}(\Gamma,2) \simeq F_r(\Gamma,2)$ for all $s \in [r-\varepsilon, r)$.

(iii) the two families $\{F_r(\Gamma,2)\}_{r>0}$ and $\{F_r^{\mathcal{O}}(\Gamma,2)\}_{r>0}$ have the same critical values and assume the same set of homotopy types as r varies over $\left(0, \frac{1}{2}\operatorname{diam}\Gamma\right]$.

Chapter 4

Discrete models for the configuration spaces $\{F_r(\Gamma, 2)\}_{r>0}$

In this chapter we continue our study of the homotopy type of $F_r(\Gamma, 2)$ for variable r. A *discrete model* for a space W is a finite CW complex homotopy equivalent to W, and here we study the existence and structure of discrete models for the thick particle configuration spaces $\{F_r(\Gamma, 2)\}_{r>0}$. Firstly, Theorem 3.2.3 implies that there is a space X and $\lambda > 0$ such that $F_r(\Gamma, 2) \simeq X$ for all $0 < r \leq \lambda$. Not surprisingly, in §4.1 we show that X is the familiar configuration space $F(\Gamma, 2)$ of two zero-size points moving on Γ. We also provide a lower bound for λ valid for all sufficiently subdivided graphs, see Theorem 4.1.6. We generalise these ideas in §4.2 to show that $F_r(\Gamma, 2)$ admits a discrete model for each $r > 0$.

4.1 Thick particles of small radius

Throughout this chapter we assume that (Γ, ℓ) is simple and satisfies the cycle inequality. These conditions hold provided that Γ is sufficiently subdivided, see Lemmas 1.5.5 and 1.5.10. Following the notation from [6, Definition 2.2.2] and [7, §1], we begin with the definition of $D(\Gamma, 2)$. This is a finite CW complex proved by A. Abrams [1, Theorem 2.4] to be a deformation retract of $F(\Gamma, 2)$. It is useful to have a discrete model such as $D(\Gamma, 2)$, because $F(\Gamma, 2)$ cannot be given the structure of a finite CW complex. Indeed, $F(\Gamma, 2)$ is not closed in $\Gamma \times \Gamma$ (its closure is $\Gamma \times \Gamma$),

so it is not compact.

Definition 4.1.1. We define

$$D(\Gamma, 2) := \{(x, y) \in \Gamma \times \Gamma : \operatorname{supp}(x) \cap \operatorname{supp}(y) = \emptyset\}.$$

(The *support* of w is the smallest subgraph of Γ containing w, see Definition 1.1.6).

Remark 4.1.2. The natural CW structure on $D(\Gamma, 2)$ as a subcomplex of $\Gamma \times \Gamma$ is as follows. The 0–cells are ordered pairs (v, w) of distinct vertices of Γ. The 1–cells are pairs (v, e), (e, v) comprising an edge e and a vertex v such that $v \notin \partial e$. A 1–cell (v, e) is attached to $(v, \partial_0 e)$ and $(v, \partial_1 e)$, and similarly for (e, v). The 2–cells are ordered pairs of edges (e, f) such that $\partial e \cap \partial f = \emptyset$. A 2–cell (e, f) is attached to the 1–skeleton of $D(\Gamma, 2)$ along the four 1–cells $(\partial_0 e, f)$, $(\partial_1 e, f)$, $(e, \partial_0 f)$ and $(e, \partial_1 f)$. There are no cells in higher dimensions, so $\dim D(\Gamma, 2) \leq 2$.

Example 4.1.3. Let $\Gamma = [0, 1]$ be the labelled graph from Example 3.1.5. In this case $D(\Gamma, 2)$ comprises the two points $(0, 1)$ and $(1, 0)$ and is an obvious deformation retract of $F(\Gamma, 2) = [0, 1] \times [0, 1] \setminus \Delta$.

Example 4.1.4. Let $\Gamma = S^1$ have the graph structure with three vertices u, v, w and three edges e, f, g as shown in Figure 4.1. In this case $D(\Gamma, 2)$ is also a circle, subdivided with six vertices and six edges. It has no 2–cells because no two edges have non-intersecting boundaries.

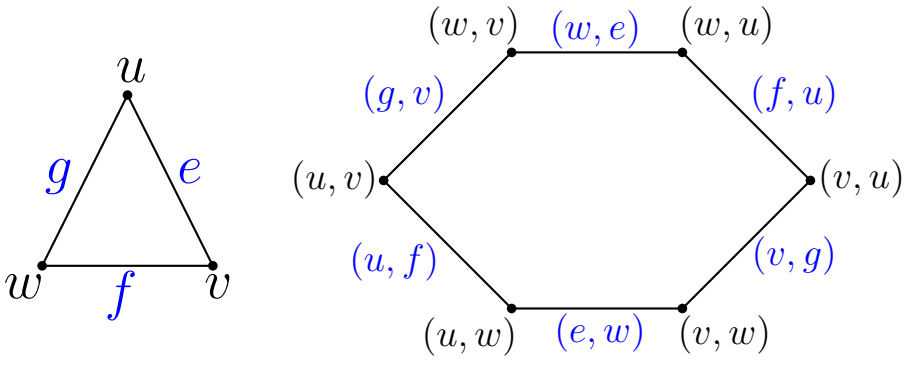

Figure 4.1: The minimal simple graph structure on Γ, and $D(\Gamma, 2)$ on the right

Example 4.1.5. Let Γ be the Y–graph from Example 3.1.7. In this case $D(\Gamma, 2)$ has twelve 0–cells comprising the pairs of distinct vertices of Γ, and twelve 1–cells

comprising the edge-vertex pairs (f, w), (w, f) such that $w \notin \partial f$. The configuration space $F(\Gamma, 2)$ is shown on the left of Figure 4.2 and $D(\Gamma, 2)$ is shown on the right.

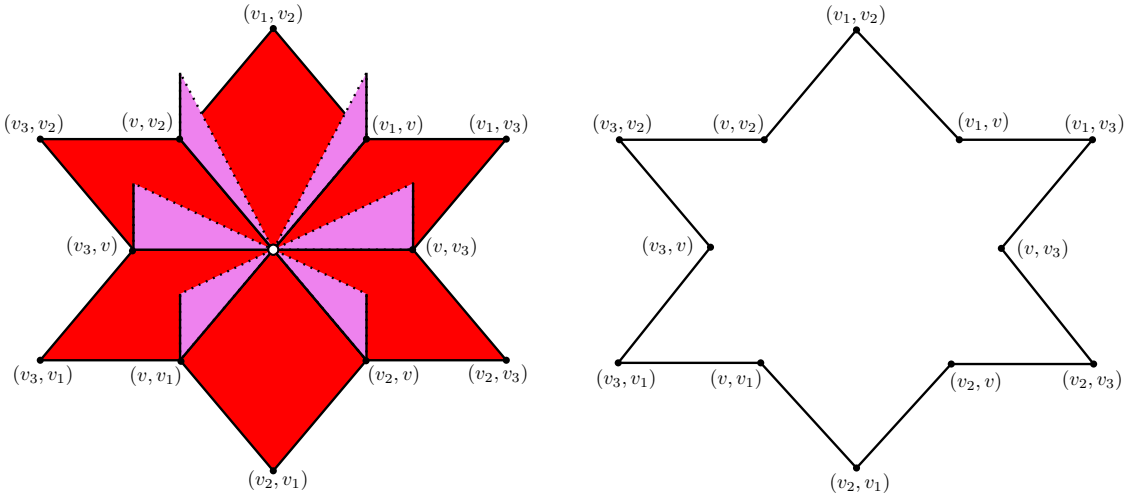

Figure 4.2: $D(\Gamma, 2)$ is a deformation retract of $F(\Gamma, 2)$

Some further examples of $D(\Gamma, 2)$ are as follows (see [1, Examples 5.1,5.2]): if K_5 denotes the complete graph on 5 vertices, then $D(K_5, 2)$ is the closed orientable surface of genus 6. If $K_{3,3}$ denotes the complete bipartite graph on two sets of three vertices, then $D(K_{3,3}, 2)$ is the closed orientable surface of genus 4. A fascinating theorem due to A. Abrams (see [1, Theorem 5.1]) shows that if Γ is connected and has no loops, then $D(\Gamma, 2)$ is a closed 2–manifold only when $\Gamma = K_5$ or $\Gamma = K_{3,3}$.

The following theorem is the main result of this section.

Theorem 4.1.6. *There is a homotopy equivalence $F_r(\Gamma, 2) \simeq F(\Gamma, 2)$ for each $r \in (0, r_0]$, where $r_0 := \frac{1}{2} \min_{e \in E(\Gamma)} \{\ell(e)\}$.*

Proof. If $\mathrm{supp}(x) \cap \mathrm{supp}(y) \neq \emptyset$, then $d(x, y) \geq 2r_0$, so $D(\Gamma, 2) \subset F_r(\Gamma, 2)$. We show that the deformation retraction of $F(\Gamma, 2)$ onto $D(\Gamma, 2)$ given in [1, Theorem 2.4] restricts to a deformation retraction of $F_r(\Gamma, 2)$ onto $D(\Gamma, 2)$. We first deformation retract $F_r(\Gamma, 2)$ onto its subspace

$$Y := F_r(\Gamma, 2) - \bigcup_{e \in E(\Gamma)} e \times e.$$

If $(x, y) \in F_r(\Gamma, 2) - Y$, then x, y are distinct points lying on an edge e. Push x and y apart at constant speed until at least one of the points reaches a vertex,

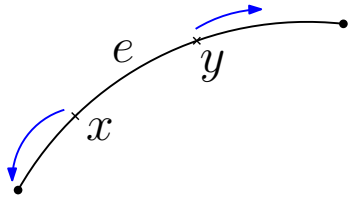

Figure 4.3: Deformation retraction of $F_r(\Gamma, 2)$ onto Y

see Figure 4.3. Since (Γ, ℓ) is simple and satisfies the cycle inequality, the distance between the points under this motion increases with time $t \in [0, 1]$. Therefore, this procedure defines a continuous map $F_r(\Gamma, 2) \times [0, 1] \to F_r(\Gamma, 2)$ starting with the identity, finishing with a retraction $F_r(\Gamma, 2) \to Y$ and leaving each point of Y fixed.

The second step is to deformation retract Y onto its subspace $D(\Gamma, 2)$. If $(x, y) \in Y - D(\Gamma, 2)$, then one of the following conditions holds.

(i) One of x, y is a vertex v and the other lies in an edge e incident to v.

(ii) The points x and y lie in distinct edges incident to v, see Figure 4.4.

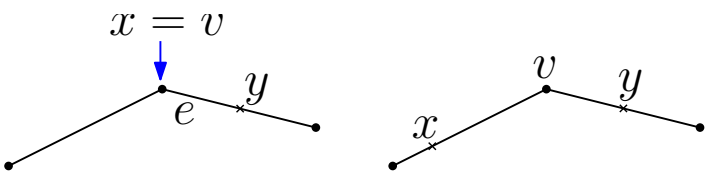

Figure 4.4: A pair $(x, y) \in Y - D(\Gamma, 2)$

Now move the points x and y away from v at speeds proportional to their distance from v. (This distance is zero for one of the points in case (i)). In case (i), proceed until the point which is not v reaches the other vertex of e. In case (ii), proceed until at least one point reaches a vertex, see Figure 4.5. In case (i), the distance

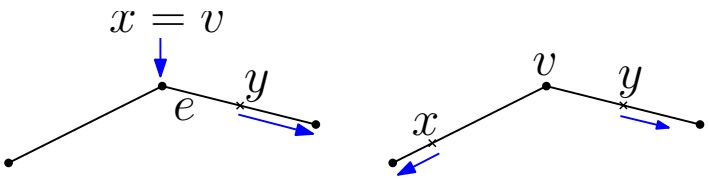

Figure 4.5: Deformation retraction of Y onto $D(\Gamma, 2)$

between the points under this motion increases with time $t \in [0, 1]$, because they lie

in the same closed edge and the cycle inequality is satisfied. In case (ii), the pairs (x^t, y^t), $t \in [0,1]$, joining $(x^0, y^0) = (x, y)$ to $(x^1, y^1) \in D(\Gamma, 2)$ under this motion satisfy $d(x^t, y^t) \geq 2r$ for all $t \in [0,1]$. Indeed, if $d(x^t, y^t) < 2r$ for some $t \in [0,1]$, then we have either

$$d(x, y) \leq d(x^t, v) + d(v, y^t) \leq d(x^t, y^t) < 2r,$$

or the existence of an edge with label strictly less than $2r$, both of which are impossible. Therefore, this procedure defines a continuous map $Y \times [0,1] \to Y$ starting with the identity, finishing with a retraction $Y \to D(\Gamma, 2)$ and leaving each point of $D(\Gamma, 2)$ fixed. □

Remark 4.1.7. If Γ is the Y–graph from Example 3.1.7, then $r_0 = 1/2$ and $F_r(\Gamma, 2) \simeq F(\Gamma, 2) \simeq S^1$ for all $r \in (0, r_0]$ and $F_r(\Gamma, 2) \not\simeq S^1$ if $r > r_0$. Hence r_0 is sharp, meaning that if we increase it above $\frac{1}{2} \min_{e \in E(\Gamma)} \{\ell(e)\}$ then Theorem 4.1.6 is false for some labelled graphs.

4.1.1 Corollaries of Theorem 4.1.6

We now discuss some corollaries of Theorem 4.1.6, applying known results on the topology of $F(\Gamma, 2)$ from the literature. This material is not needed elsewhere in this thesis and is included purely for interest. In view of Theorem 4.1.6 and [1, Theorem 2.4], we have $\chi(F_r(\Gamma, 2)) = \chi(D(\Gamma, 2))$ for all $r \in (0, r_0]$. The computation of $\chi(D(\Gamma, 2))$ is given in [7, Corollary 1.2]. It is also a consequence of a theorem of S. Gal [30, Theorem 2] determining $\chi(F(X, n))$ for any finite polyhedron X and any $n \geq 1$ (see also [20, Corollary 2.7]).

Corollary 4.1.8. *For $r \in (0, r_0]$ we have*

$$\chi(F_r(\Gamma, 2)) = \chi(\Gamma)^2 + \chi(\Gamma) - \sum_{v \in V(\Gamma)} (\mu(v) - 1)(\mu(v) - 2).$$

Proof (after [7], Corollary 1.2). Write $V := |V(\Gamma)|$ and $E := |E(\Gamma)|$. There are $V^2 - V$ 0–cells of $D(\Gamma, 2)$, since each 0–cell is a pair of distinct vertices of Γ. Each edge e of Γ contributes the 1–cells (e, v) and (v, e) to $D(\Gamma, 2)$ for $v \notin \partial e$. Hence $D(\Gamma, 2)$ has $2E(V - 2)$ 1–cells. The product $\Gamma \times \Gamma$ has E^2 2–cells, and E of these

are the diagonal cells (e, e) for $e \in E(\Gamma)$. The number of 2–cells (e, f) of $\Gamma \times \Gamma$ such that $e \neq f$ and $\partial e \cap \partial f \neq \emptyset$ is $\sum_{v \in V(\Gamma)} \mu(v)(\mu(v) - 1)$. Hence the number of 2–cells of $D(\Gamma, 2)$ is

$$E^2 - E - \sum_{v \in V(\Gamma)} \mu(v)(\mu(v) - 1).$$

Hence

$$\chi(D(\Gamma, 2)) = V^2 - V - 2E(V - 2) + E^2 - E - \sum_{v \in V(\Gamma)} \mu(v)(\mu(v) - 1),$$

and since $\chi(\Gamma) = V - E$ and $2E = \sum_{v \in V(\Gamma)} \mu(v)$, we obtain

$$\begin{aligned}
\chi(D(\Gamma, 2)) &= \chi(\Gamma)^2 + \chi(\Gamma) - 2V + 4E - \sum_{v \in V(\Gamma)} \mu(v)(\mu(v) - 1) \\
&= \chi(\Gamma)^2 + \chi(\Gamma) - \left(\sum_{v \in V(\Gamma)} (2 - 2\mu(v) + \mu(v)^2 - \mu(v)) \right) \\
&= \chi(\Gamma)^2 + \chi(\Gamma) - \sum_{v \in V(\Gamma)} (\mu(v) - 1)(\mu(v) - 2).
\end{aligned}$$

□

The path-connectedness of $F_r(\Gamma, 2)$ is addressed fully in Chapter 5, but Theorem 4.1.6 together with results from the literature gives the following statement.

Corollary 4.1.9. *If Γ is not homeomorphic to the interval $[0, 1]$, then $F_r(\Gamma, 2)$ is path-connected and aspherical for all $r \in (0, r_0]$.*

Proof. Provided that $\Gamma \ncong [0, 1]$, S. Eilenberg [18, Theorem III] has shown that $F(\Gamma, 2)$ is path-connected, see also [50, Theorem 2.4], [1, §2.2] and §5.1. Under the same assumption, C. W. Patty ([49, Theorem 2]) has shown that $F(\Gamma, 2)$ is aspherical, that is $\pi_k(F(\Gamma, 2)) = 0$ for all $k \geq 2$. Applying Theorem 4.1.6 gives the same conclusions for $F_r(\Gamma, 2)$ for any $r \in (0, r_0]$. □

We also mention the following useful result which follows from [7, Proposition 1.3].

Corollary 4.1.10. *Assume that Γ is not homeomorphic to $[0, 1]$ or S^1. For any $r \in (0, r_0]$, the inclusion $F_r(\Gamma, 2) \hookrightarrow \Gamma \times \Gamma$ induces an epimorphism $H_1(F_r(\Gamma, 2)) \to H_1(\Gamma \times \Gamma)$.*

Proof. Consider the sequence of inclusions

$$D(\Gamma,2) \hookrightarrow F_r(\Gamma,2) \overset{\iota}{\hookrightarrow} F(\Gamma,2) \overset{\alpha}{\hookrightarrow} \Gamma \times \Gamma.$$

The maps $D(\Gamma,2) \hookrightarrow F_r(\Gamma,2)$, $D(\Gamma,2) \hookrightarrow F(\Gamma,2)$ are homotopy equivalences by Theorem 4.1.6 and [1, Theorem 2.4], respectively. Hence $\iota : F_r(\Gamma,2) \hookrightarrow F(\Gamma,2)$ is a homotopy equivalence and ι_* is an isomorphism on H_1. Further, [7, Proposition 1.3] shows that α_* is an epimorphism on H_1. The inclusion $j = \alpha \circ \iota : F_r(\Gamma,2) \hookrightarrow \Gamma \times \Gamma$ satisfies $j_* = \alpha_* \circ \iota_*$, so j_* is an epimorphism on H_1. □

We finish this section with the following interesting statement about thick particle configuration spaces of trees. It follows directly from the corresponding result for $F(T,2)$ proved by M. Farber in [19, Theorem 12].

Corollary 4.1.11. *Let (T,ℓ) be a labelled tree containing at least one branched vertex $\mu(v) \geq 3$. Then $F_r(T,2) \simeq \bigvee_{n_T} S^1$ for any $r \in (0, r_0]$, where*

$$n_T = \sum_{v \in V(T)} (\mu(v)-1)(\mu(v)-2) - 1.$$

Proof. M. Farber's work ([19, Theorem 12]) shows that $F(T,2) \simeq \bigvee_{n_T} S^1$. Since T is a tree, it is simple and vacuously satisfies the cycle inequality, so applying Theorem 4.1.6 gives the result. □

4.2 Discrete thick particle configuration spaces

In this section we generalise the ideas from §4.1. The main result is that $F_r(\Gamma, 2)$ is homotopy equivalent to a finite CW complex of dimension at most two. In this section, it is more convenient to work with the family $\{F_r^{\mathcal{O}}(\Gamma, 2)\}_{r>0}$ (see §3.4). For a fixed r, we may replace $F_r(\Gamma, 2)$ with a homotopy equivalent space

$$F_s^{\mathcal{O}}(\Gamma, 2) = \{(x, y) \in \Gamma \times \Gamma : d(x, y) > 2s\} \text{ for some } s.$$

Namely, if r is a regular value we take $s = r$, and if r is a critical value we choose $s < r$ sufficiently close to r such that (s, r) contains no critical value, see Remarks 3.4.1. We show that for each s, Γ admits a subdivision such that there is a finite CW complex embedded in $F_s^{\mathcal{O}}(\Gamma, 2)$ as a deformation retract, see Theorem 4.2.4.

Definition 4.2.1 (Discrete thick particle configuration space)**.** For $r \geq 0$, we define

$$D_r(\Gamma, 2) := \{(x, y) \in \Gamma \times \Gamma : d(\mathrm{supp}(x), \mathrm{supp}(y)) > 2r\}.$$

Remarks 4.2.2.

1. Note that $d(x, y) \geq d(\mathrm{supp}(x), \mathrm{supp}(y))$ for all $(x, y) \in \Gamma \times \Gamma$, so $D_r(\Gamma, 2) \subset F_r^{\mathcal{O}}(\Gamma, 2)$ for all $r \geq 0$.

2. We have $D_r(\Gamma, 2) = D(\Gamma, 2)$ for all $r \in [0, r_0)$, since $d(\mathrm{supp}(x), \mathrm{supp}(y)) \geq 2r_0$ if $\mathrm{supp}(x) \cap \mathrm{supp}(y) = \emptyset$. In general, $D_r(\Gamma, 2) \subseteq D(\Gamma, 2)$.

3. Subdividing Γ does not change the induced metric space (Lemma 1.5.2) and hence does not change $F_r^{\mathcal{O}}(\Gamma, 2)$. However, we emphasise that $D_r(\Gamma, 2)$ depends on the subdivision of Γ.

4. The natural CW structure on $D_r(\Gamma, 2)$ is as follows. The 0–cells are ordered pairs (v, w) of vertices of Γ such that $d(v, w) > 2r$. The 1–cells are pairs (e, v), (v, e) comprising a vertex v and an edge e such that $d(v, \overline{e}) > 2r$. The 2–cells are ordered pairs (e, f) of edges such that $d(\overline{e}, \overline{f}) > 2r$. The 1–cells and 2–cells are attached in the same way as in $D(\Gamma, 2)$, see Remark 4.1.2. We note that $D_r(\Gamma, 2)$ is a finite CW complex of dimension at most two.

Example 4.2.3. Let $\Gamma = S^1 \vee S^1$ have the labelled graph structure as shown in Figure 4.6. It is simple and satisfies the cycle inequality. In this case, $D(\Gamma, 2)$ has twenty 0–cells, thirty-six 1–cells and ten 2–cells and is shown in Figure 4.7. Now, [1, Theorem 2.4] and Theorem 4.1.6 imply that $F(\Gamma, 2) \simeq D(\Gamma, 2) \simeq F_r(\Gamma, 2)$ for all $r \in (0, 1/2]$. Hence these spaces have the homotopy type of the wedge sum of seven circles $\bigvee_{i=1}^{7} S^1$.

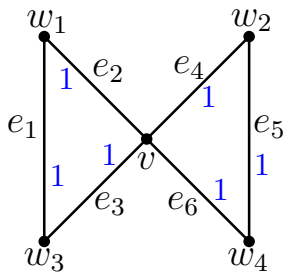

Figure 4.6: The labelled graph structure on $\Gamma = S^1 \vee S^1$

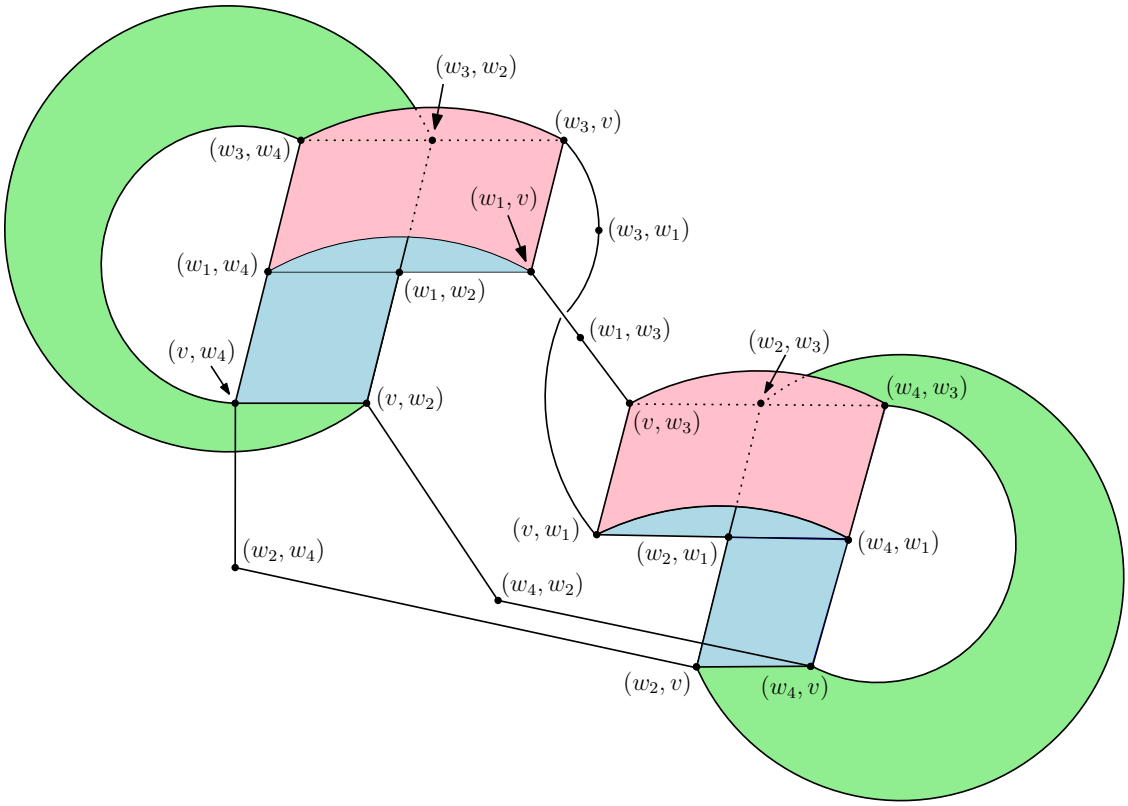

Figure 4.7: The CW complex $D(\Gamma, 2)$ when $\Gamma = S^1 \vee S^1$ has the graph structure in Figure 4.6

The non-zero distances between subgraphs of Γ are 1 and 2. We have $D_r(\Gamma, 2) = D(\Gamma, 2)$ for all $r \in [0, 1/2)$, and $D_r(\Gamma, 2)$ comprises the two squares shown in Figure 4.8 for $r \in [1/2, 1)$. If $r \geq 1$ then $D_r(\Gamma, 2) = \emptyset$.

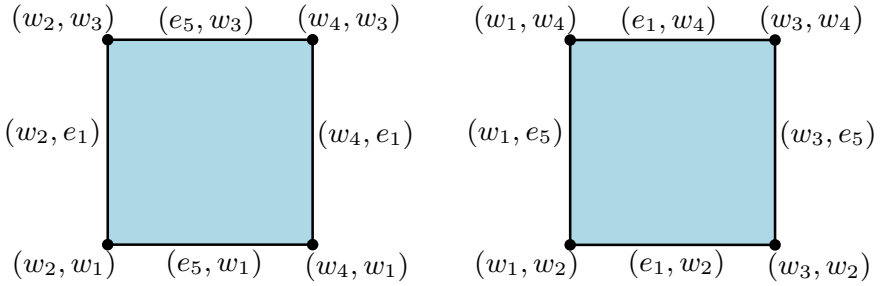

Figure 4.8: $D_r(\Gamma, 2)$ for $1/2 \leq r < 1$

In the rest of this section we prove the following main result.

Theorem 4.2.4. *For each $r \in [0, \operatorname{diam}\Gamma/2)$, there is a subdivision of Γ such that $D_r(\Gamma, 2)$ is a deformation retract of $F_r^{\mathcal{O}}(\Gamma, 2)$.*

To prove this statement, we first define two conditions (C1) and (C2) depending on r. We then show that (Γ, ℓ) admits a subdivision satisfying (C1) and (C2). Finally, we construct a deformation retraction of $F_r^{\mathcal{O}}(\Gamma, 2)$ onto $D_r(\Gamma, 2)$ for any subdivision of Γ satisfying (C1) and (C2).

Definitions 4.2.5 (Conditions (C1) and (C2))**.** For $r \in [0, \operatorname{diam}\Gamma/2)$, write

$$\Delta_r := \{(x, y) \in \Gamma \times \Gamma : d(x, y) \leq 2r\}.$$

Condition (C1) is that for any $e_1, e_2 \in E(\Gamma)$ such that

$$(\overline{e}_1 \times \overline{e}_2) \cap \Delta_r \neq \emptyset \quad \& \quad (e_1 \times e_2) \cap F_r^{\mathcal{O}}(\Gamma, 2) \neq \emptyset,$$

there exist $v_1 \in \partial e_1$, $v_2 \in \partial e_2$ such that $d(v_1, \overline{e}_2) = d(v_2, \overline{e}_1) = d(v_1, v_2) > 2r$. Condition (C2) is that for any $v \in V(\Gamma)$ and $e \in E(\Gamma)$ such that

$$d(v, \overline{e}) \leq 2r \quad \& \quad (\{v\} \times e) \cap F_r^{\mathcal{O}}(\Gamma, 2) \neq \emptyset,$$

there exists $w \in \partial e$ such that $d(v, w) > 2r$.

Lemma 4.2.6. *(Γ, ℓ) admits a subdivision satisfying conditions (C1) and (C2).*

Proof. If there are no circuits C such that $\ell(C) > 4r$, then conditions (C1) and (C2) are satisfied. Indeed, if (C1) or (C2) does not hold, then there is a circuit of length exceeding $4r$. Suppose that there is at least one circuit C such that $\ell(C) > 4r$, and define

$$\mu = \min_{\ell(C)>4r} \{\ell(C)\} - 4r.$$

Now subdivide (Γ, ℓ) so that every new edge has label in $(0, \mu/3)$. This can be done as follows. Set $\ell_{\max} := \max_{e\in E(\Gamma)}\{\ell(e)\}$, and choose $N \in \mathbb{N}$ such that $\frac{\ell_{\max}}{N} < \frac{\mu}{3}$. Now insert $N-1$ equally-spaced new vertices into each edge $e \in E(\Gamma)$, so that the N new edges obtained from e each have label $\ell(e)/N$.

We now check that (C1) and (C2) are satisfied for this subdivision.

(C1) Suppose that $e_1, e_2 \in E(\Gamma)$ are such that

$$(\overline{e}_1 \times \overline{e}_2) \cap \Delta_r \neq \emptyset \quad \& \quad (e_1 \times e_2) \cap F_r^{\mathcal{O}}(\Gamma, 2) \neq \emptyset.$$

Since $(\overline{e}_1 \times \overline{e}_2) \cap \Delta_r \neq \emptyset$, there exists $v_1' \in \partial e_1$ and $v_2' \in \partial e_2$ such that $d(v_1', v_2') \leq 2r$. Seeking a contradiction, assume that $d(v_1, v_2) \leq 2r$, where

$$\{v_1\} = \partial e_1 - \{v_1'\} \quad \text{and} \quad \{v_2\} = \partial e_2 - \{v_2'\}.$$

Let C be the circuit defined by $C = (\overline{e}_1, c_1, \overline{e}_2, c_2)$, where c_1, c_2 are minimal-length paths from v_1' to v_2' and v_2 to v_1, respectively, see Figure 4.9. We have

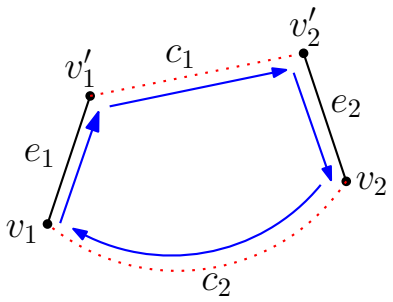

Figure 4.9: The circuit $C = (\overline{e}_1, c_1, \overline{e}_2, c_2)$

$\ell(C) > 4r$ since $(e_1 \times e_2) \cap F_r^{\mathcal{O}}(\Gamma, 2) \neq \emptyset$. On the other hand,

$$\ell(C) \leq 2r + 2r + \frac{\mu}{3} + \frac{\mu}{3} < 4r + \mu,$$

contradicting $\ell(C) \geq 4r + \mu$.

(C2) Suppose that $v \in V(\Gamma)$, $e \in E(\Gamma)$ are such that

$$d(v, \overline{e}) \leq 2r \quad \& \quad (\{v\} \times e) \cap F_r^{\mathcal{O}}(\Gamma, 2) \neq \emptyset.$$

Since $d(v, \overline{e}) \leq 2r$, there exists $v' \in \partial e$ such that $d(v, v') \leq 2r$. Seeking a contradiction, assume that $d(v, w) \leq 2r$, where $\{w\} = \partial e - \{v'\}$. Let C be the circuit defined by $C = (\overline{e}, c_1, c_2)$, where c_1, c_2 are minimal-length paths from v' to v and v to w, respectively, see Figure 4.10. We have $\ell(C) > 4r$ since

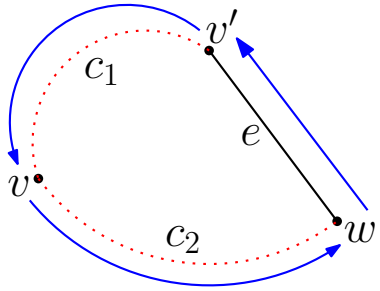

Figure 4.10: The circuit $C = (\overline{e}, c_1, c_2)$

$(\{v\} \times e) \cap F_r^{\mathcal{O}}(\Gamma, 2) \neq \emptyset$. On the other hand,

$$\ell(C) \leq 2r + 2r + \frac{\mu}{3} < 4r + \mu,$$

contradicting $\ell(C) \geq 4r + \mu$.

□

We now assume that (Γ, ℓ) is subdivided such that (C1) and (C2) hold.

Proof of Theorem 4.2.4. The argument is similar to the proof of Theorem 4.1.6. We first define a deformation retraction of $F_r^{\mathcal{O}}(\Gamma, 2)$ onto its subspace

$$Y := F_r^{\mathcal{O}}(\Gamma, 2) - \bigcup_{\substack{e,f \in E(\Gamma) \\ (e \times f) \cap \Delta_r \neq \emptyset}} e \times f.$$

If $(x, y) \in F_r^{\mathcal{O}}(\Gamma, 2) - Y$, then $(x, y) \in e \times f$ for some $e, f \in E(\Gamma)$ such that $(e \times f) \cap \Delta_r \neq \emptyset$. Choose $(x', y') \in (e \times f) \cap \Delta_r$, and let $v \in \partial e$, $w \in \partial f$ be the vertices provided by (C1). At constant speed, push x and y away from x' and y' towards the vertices v, w respectively, until at least one point reaches a vertex, see Figure 4.11. This procedure defines a continuous map $F_r^{\mathcal{O}}(\Gamma, 2) \times [0, 1] \to F_r^{\mathcal{O}}(\Gamma, 2)$

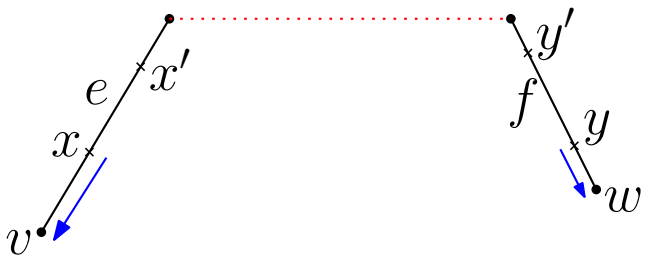

Figure 4.11: Deformation retraction of $F_r^{\mathcal{O}}(\Gamma, 2)$ onto Y

starting with the identity, finishing with a retraction $F_r^{\mathcal{O}}(\Gamma, 2) \to Y$ and fixing each point of Y.

We now define a deformation retraction of Y onto its subspace $D_r(\Gamma, 2)$. Let $(x, y) \in Y - D_r(\Gamma, 2)$. If x and y lie in edges e and f respectively, then $(e \times f) \cap \Delta_r = \emptyset$ since $(x, y) \in Y$. Thus $d(x', y') > 2r$ for all $(x', y') \in e \times f$, implying that $d(\overline{e}, \overline{f}) \geq 2r$. Since $d(\mathrm{supp}(x), \mathrm{supp}(y)) = d(\overline{e}, \overline{f}) \leq 2r$ we have $d(\overline{e}, \overline{f}) = 2r$. Let $v \in \partial e$, $w \in \partial f$ be the vertices provided by (C1). At constant speed, push x and y towards v and w, respectively, until at least one point reaches a vertex.

Next assume that at least one of x and y is a vertex. They cannot both be vertices, since otherwise

$$2r \geq d(\mathrm{supp}(x), \mathrm{supp}(y)) = d(x, y) > 2r.$$

Without loss of generality, assume that $x \in V(\Gamma)$ and $y \notin V(\Gamma)$. Let e be the edge containing y; since $\mathrm{supp}(y) = \overline{e}$ we have $d(x, \overline{e}) \leq 2r$. In particular, there exists $v \in \partial e$ such that $d(x, v) \leq 2r$. From (C2), let $w \in \partial e$ be the vertex such that $d(x, w) > 2r$. Push y at constant speed along e towards w, so that the final configuration is (x, w). □

Corollary 4.2.7. *Assuming that Γ is subdivided so that conditions (C1) and (C2) hold, the Euler characteristic $\chi(F_r^{\mathcal{O}}(\Gamma, 2))$ is given by the formula $V_r - E_r + F_r$, where*

(i) V_r is the number of ordered pairs of vertices (v, w) such that $d(v, w) > 2r$;

(ii) E_r is twice the number of pairs $(e, v) \in E(\Gamma) \times V(\Gamma)$ such that $d(\overline{e}, v) > 2r$;

(iii) F_r is the number of ordered pairs of edges (e, f) such that $d(\overline{e}, \overline{f}) > 2r$.

Chapter 5

Path-components of the configuration spaces $\{F_r(\Gamma, 2)\}_{r>0}$

In this chapter we study the path-connectivity of the spaces $\{F_r(\Gamma, 2)\}_{r>0}$. We begin in §5.1 by giving Abrams' proof (see [1, §2.2]) that the classical two-point configuration space $F(\Gamma, 2)$ is path-connected unless Γ is an interval. However, given (Γ, ℓ) and $r > 0$, $F_r(\Gamma, 2)$ is generally not path-connected (for example, see Example 3.1.7). In §5.3 we design an algorithm for computing the number of path-components of $F_r(\Gamma, 2)$ given (Γ, ℓ) and r. This algorithm constructs a finite graph G_r which embeds in $F_r(\Gamma, 2)$ such that $b_0(G_r) = b_0(F_r(\Gamma, 2))$. In §5.2 we introduce *critical* and *index zero* configurations. These are special classes of configurations that play a crucial theoretical role in our algorithm from §5.3.

5.1 Path-connectivity of $F(\Gamma, 2)$

In this section we provide Abrams' argument (see [1, §2.2]) showing that $F(\Gamma, 2)$ is path-connected unless $\Gamma \cong [0, 1]$.

Proposition 5.1.1. *$F(\Gamma, 2)$ is path-connected if and only if Γ is not homeomorphic to the interval $[0, 1]$.*

As a first step towards proving Proposition 5.1.1, we will write down the proof of [1, Theorem 2.5] for the case $n = 2$. This result is as follows.

Lemma 5.1.2. *The orbit space $B(\Gamma, 2) := F(\Gamma, 2)/S_2$ is path-connected, where S_2 acts freely on $F(\Gamma, 2)$ by permuting the factors: $(1\ \ 2) \cdot (x, y) = (y, x)$.*

Proof (after [1], Theorem 2.5). Let $\mathbf{x} = (x_1, x_2)$, $\mathbf{y} = (y_1, y_2) \in F(\Gamma, 2)$. We wish to construct a path in $B(\Gamma, 2)$ from $\{x_1, x_2\}$ to $\{y_1, y_2\}$. Define $r(\mathbf{x}, \mathbf{y}) = |\{x_1, x_2\} - \{y_1, y_2\}|$. If $r(\mathbf{x}, \mathbf{y}) = 0$, then $\{x_1, x_2\} = \{y_1, y_2\}$ and there is nothing to prove. The remaining cases are when $r(\mathbf{x}, \mathbf{y}) \in \{1, 2\}$. Assume $r(\mathbf{x}, \mathbf{y}) = 2$, and let $\gamma : I \to \Gamma$ be a minimal-length edgepath from x_1 to y_1. There is at most one time $t \in (0, 1)$ such that $\gamma(t) = x_2$, see Figure 5.1. Suppose that $x_2 \in \operatorname{Im} \gamma$. Define a path in $F(\Gamma, 2)$

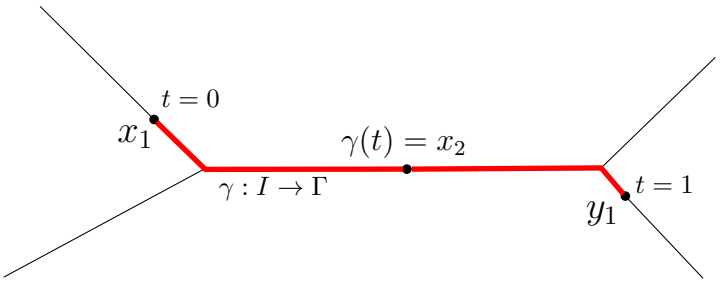

Figure 5.1: An edgepath γ from x_1 to y_1

from $\mathbf{x}$ to (x_2, y_1) as follows. Start at $\mathbf{x}$ and move x_2 to y_1 along $\gamma|_{[t,1]}$, keeping x_1 fixed throughout. Now keep y_1 fixed and move x_1 to x_2 along $\gamma|_{[0,t]}$. If $x_2 \notin \operatorname{Im} \gamma$, define a path in $F(\Gamma, 2)$ from $\mathbf{x}$ to (y_1, x_2) by $t \mapsto (\gamma(t), x_2)$. In either case, we compose with the projection map $F(\Gamma, 2) \to B(\Gamma, 2)$ and obtain a path in $B(\Gamma, 2)$ from $\{x_1, x_2\}$ to $\{x_2, y_1\}$. Hence, we may assume that $r(\mathbf{x}, \mathbf{y}) = 1$ and that we need a path from $\{x_2, y_1\}$ to $\{y_1, y_2\}$ with $x_2 \neq y_2$. Let $\delta : I \to \Gamma$ be a minimal-length edgepath from x_2 to y_2. There is at most one point $t \in (0, 1)$ with $\gamma(t) = y_1$. If $y_1 \in \operatorname{Im} \delta$, define a path in $F(\Gamma, 2)$ from (x_2, y_1) to (y_1, y_2) as follows. Hold x_2 fixed and move y_1 to y_2 along $\delta|_{[t,1]}$, and then hold y_2 fixed and move x_2 to y_1 along $\delta|_{[0,t]}$. If $y_1 \notin \operatorname{Im} \delta$, define a path in $F(\Gamma, 2)$ from (x_2, y_1) to (y_2, y_1) by $t \mapsto (\delta(t), y_1)$. In either case, composing with the projection $F(\Gamma, 2) \to B(\Gamma, 2)$ gives a path from $\{x_2, y_1\}$ to $\{y_1, y_2\}$. □

We can now prove Proposition 5.1.1.

Proof of Proposition 5.1.1. If Γ is homeomorphic to $[0, 1]$, then $F(\Gamma, 2) \cong [0, 1] \times [0, 1] \setminus \Delta$, where $\Delta = \{(x, x) \in \mathbb{R}^2 : x \in [0, 1]\}$, so $F(\Gamma, 2)$ has two contractible

path-components. If $\Gamma \ncong [0,1]$, then either Γ is a circle or Γ contains a vertex v with $\mu(v) \geq 3$. Given $(x,y) \in F(\Gamma,2)$, it suffices to show that there is a path in $F(\Gamma,2)$ from (x,y) to (y,x). Indeed, Lemma 5.1.2 shows that $B(\Gamma,2)$ is path-connected, and we can lift paths in $B(\Gamma,2)$ to $F(\Gamma,2)$ by the path-lifting property of covering spaces.[1] If Γ is a circle, we may use the path shown in Figure 5.2 to connect (x,y) to (y,x) in $F(\Gamma,2)$. If Γ contains a vertex v with $\mu(v) \geq 3$, then we may assume

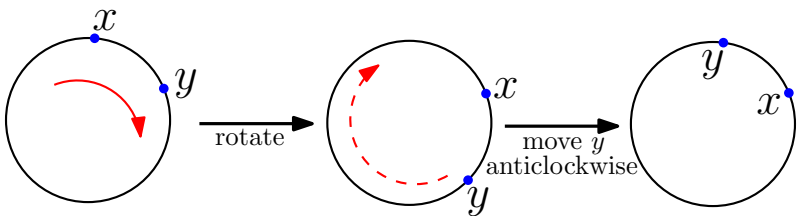

Figure 5.2: A path in $F(S^1,2)$ from (x,y) to (y,x)

(by Lemma 5.1.2) that x and y lie on distinct edges incident to v. We may use the path shown in Figure 5.3 to connect (x,y) to (y,x) in $F(\Gamma,2)$. □

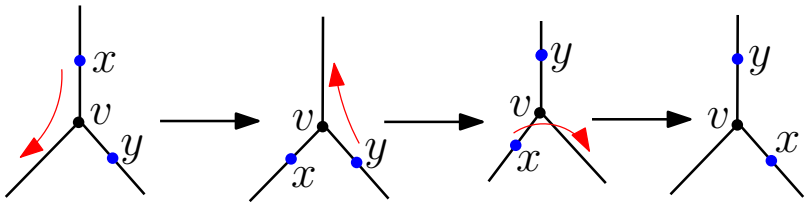

Figure 5.3: A path in $F(\Gamma,2)$ from (x,y) to (y,x)

The path shown in Figure 5.3 is represented by the animation in Figure 5.4.

5.2 Critical and index zero configurations

We now study the path-connectivity of the spaces $\{F_r(\Gamma,2)\}_{r>0}$. In contrast to the classical configuration space $F(\Gamma,2)$, the thick particle configuration space $F_r(\Gamma,2)$ is often disconnected. However, by combining Theorem 4.1.6 with Proposition 5.1.1, we deduce that $F_r(\Gamma,2)$ is path-connected for sufficiently small r, provided that

[1] The projection $F(\Gamma,2) \to B(\Gamma,2)$ is a covering map since S_2 is a finite group acting freely on the Hausdorff space $F(\Gamma,2)$.

Figure 5.4: Interchanging two thick particles on the Y–graph

$\Gamma \ncong [0,1]$. Moreover, Theorem 3.2.3 implies that as we vary r over $\left(0, \frac{1}{2}\operatorname{diam}\Gamma\right]$, the number of path-components of $F_r(\Gamma, 2)$ can only change finitely many times (since a change in $b_0(F_r(\Gamma,2))$ implies a change in homotopy type). In this section we define critical and index zero configurations and show that every path-component of $F_r(\Gamma, 2)$ contains an index zero configuration (Proposition 5.2.15). This result plays a major theoretical role in our algorithm in §5.3 for determining $b_0(F_r(\Gamma,2))$ given (Γ, ℓ) and r.

5.2.1 Critical configurations

Definition 5.2.1. Given distinct points $x, y \in \Gamma$, the *positive index* of (x, y), written $\operatorname{ind}_+(x, y)$, is the number of branches in a star neighbourhood around x on which $w \mapsto d(w, y)$ increases as we move away from x. We define the *negative index* $\operatorname{ind}_-(x, y)$ analogously, with "increases" replaced with "decreases".

Remark 5.2.2. For distinct points $x, y \in \Gamma$, we have $\mu(x) = \operatorname{ind}_+(x, y) + \operatorname{ind}_-(x, y)$.

Example 5.2.3. In the graph in Figure 5.5, $\operatorname{ind}_+(x, y) = 2$ and $\operatorname{ind}_-(x, y) = 1$, whereas $\operatorname{ind}_+(y, x) = 3$ and $\operatorname{ind}_-(y, x) = 1$.

Definition 5.2.4. A configuration $(x, y) \in F(\Gamma, 2)$ is *critical* if $\operatorname{ind}_+(x, y) \neq 1$ and $\operatorname{ind}_+(y, x) \neq 1$.

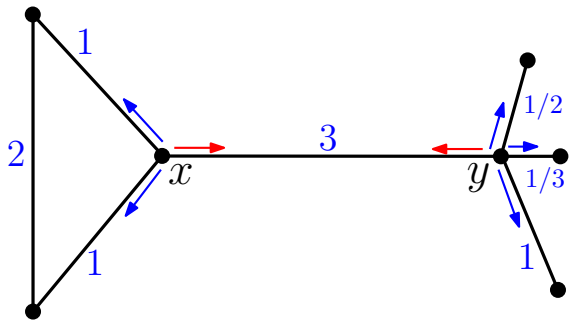

Figure 5.5: Calculating the positive and negative indices

Definition 5.2.5. A number $R > 0$ is a *critical radius* of (Γ, ℓ) if there exists a critical configuration (x, y) such that $R = \frac{1}{2}d(x, y)$.

Example 5.2.6. Let (T, ℓ) be the following labelled tree.

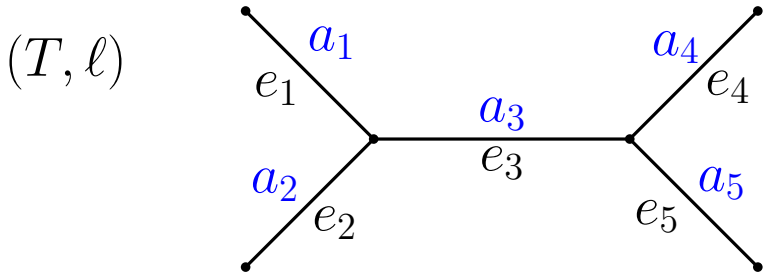

The critical configurations are precisely the pairs of distinct vertices in T, independently of the edge labels $a_1, \ldots, a_5 > 0$. Indeed, each pair of distinct vertices (v, w) satisfies $\mathrm{ind}_+(v, w), \mathrm{ind}_+(w, v) \neq 1$, and if x is not a vertex of T then $\mathrm{ind}_+(x, y) = 1$ for any $y \neq x$. The critical radii are $a_i/2$ for $1 \leq i \leq 5$, $(a_i + a_j)/2$ for incident edges e_i, e_j, and $(a_3 + a_i + a_j)/2$ for $i \in \{1, 2\}$, $j \in \{4, 5\}$.

Example 5.2.7. Consider the circle $\Gamma = S^1$ from Example 3.1.6. The set of all critical configurations is

$$\{(z, -z) \in S^1 \times S^1 : z \in S^1\},$$

comprising all pairs of antipodal points ($d(x, y) = 1/2$). There is exactly one critical radius $R = 1/4$. In particular, there are infinitely many critical configurations, but only one critical radius.

Example 5.2.8. Let $\Gamma = S^1 \vee [0, 1]$ have the labelled graph structure shown in Figure 5.6. Here, x is the point on the loop antipodal to the vertex y. The critical

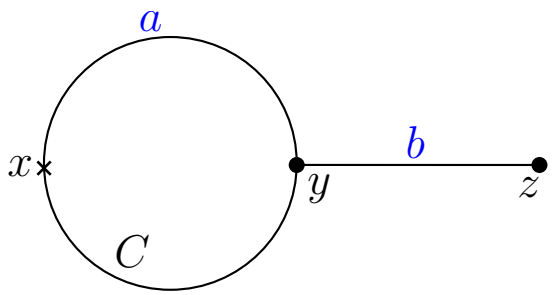

Figure 5.6: The labelled graph structure on $\Gamma = S^1 \vee [0,1]$

configurations are (y,z), (z,y), (x,z), (z,x) together with all antipodal pairs on the cycle C except (x,y) and (y,x) (since $\mathrm{ind}_+(y,x) = 1$). The critical radii are $a/4$, $b/2$ and $(b + a/2)/2$.

Remarks 5.2.9. From the definition of a critical configuration and the proof of Proposition 2.2.1, we may describe the critical configurations in $F(\Gamma, 2)$ as follows. Any minimal-length edgepath c such that $(c(0), c(1))$ is a critical configuration has the following form: a half-cycle concatenated with finitely many edges, followed by another half-cycle, see Figure 5.7. [For completeness, we allow a half-cycle to be a single point.] In particular, from the proof of Theorem 3.2.3, any critical radius

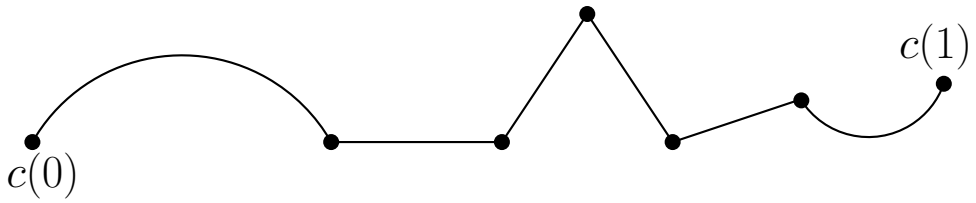

Figure 5.7: A critical configuration and a minimal-length path

$R > 0$ has the form

$$R = \frac{1}{2}\left(\frac{1}{2}\sum_{C \in Z(\Gamma)} \varepsilon_C \ell(C) + \sum_{e \in E(\Gamma)} \varepsilon_e \ell(e)\right),$$

where $\varepsilon_C, \varepsilon_e \in \{0,1\}$ for all cycles C and edges e, and at most two of $\{\varepsilon_C\}_{C \in Z(\Gamma)}$ are non-zero.

Remark 5.2.10. There may be infinitely many critical configurations $(x,y) \in F(\Gamma, 2)$ (see Example 5.2.7), but Remarks 5.2.9 show that only finitely many critical radii arise from these configurations.

5.2.2 Index zero configurations

Definition 5.2.11. A configuration $(x, y) \in F(\Gamma, 2)$ has *index zero* if $\mathrm{ind}_+(x, y) = \mathrm{ind}_+(y, x) = 0$.

Remark 5.2.12. An index zero configuration (x, y) is critical.

Example 5.2.13. Let (Γ, ℓ) be the labelled graph as shown in Figure 5.8. All pairs of antipodal points (w_1, w_2) on the cycle C are index zero configurations, except (x, y) and (y, x) (since $\mathrm{ind}_+(y, x) = 1 \neq 0$). These index zero configurations are not isolated[2] in $F(\Gamma, 2)$. The remaining index zero configurations are (x, z) and (z, x), which are both isolated.

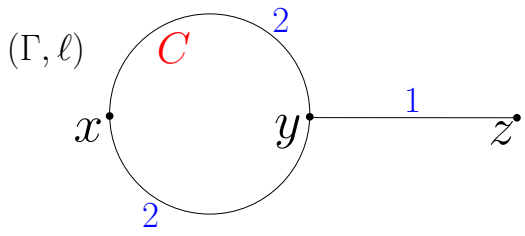

Figure 5.8: Isolated and non-isolated index zero configurations

We now characterise index zero configurations in terms of the metric d. This result is not needed in subsequent material, but we include it for completeness.

Lemma 5.2.14. *A configuration (x, y) has index zero if and only if it is a local maximum of d.*

Proof. See Appendix A, Lemma A.3.1. □

The next statement is the main result of this section; it provides an upper bound on $b_0(F_r(\Gamma, 2))$.

Proposition 5.2.15. *For any $r \in \left(0, \frac{1}{2}\operatorname{diam}\Gamma\right]$, $b_0(F_r(\Gamma, 2))$ is bounded above by $b_0(Z_r)$, where Z_r is the set of index zero configurations (x_0, y_0) with $d(x_0, y_0) \geq 2r$.*

[2] A point $a \in A \subset Y$ is *isolated* if it has a neighbourhood $U \subset Y$ such that $U \cap A = \{a\}$.

Proof. Let P be any path-component of $F_r(\Gamma, 2)$, and fix $(x, y) \in P$. Suppose that (x, y) is not an index zero configuration, and let γ be a minimal-length edgepath from x to y.

(a) If $\mathrm{ind}_+(x, y) > 0$, choose a branch incident to x on which $w \mapsto d(w, y)$ increases as we move away from x. Now push x along this branch, stopping if we reach a point x_0 with $\mathrm{ind}_+(x_0, y) = 0$. By continuing to choose branches in this way if necessary, this procedure terminates with a point x_0 such that $\mathrm{ind}_+(x_0, y) = 0$, see Figure 5.9. Let γ_1 be an edgepath from x_0 to x obtained from this procedure. By construction, the concatenation $\gamma_1 \cdot \gamma$ is a minimal-length edgepath from x_0 to y.

(b) If $\mathrm{ind}_+(x, y) = 0$, then we have $\mathrm{ind}_+(y, x) > 0$, so apply the above procedure to obtain a point y_0 such that $\mathrm{ind}_+(y_0, x) = 0$.

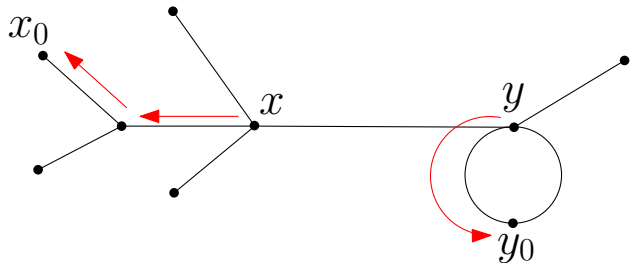

Figure 5.9: Finding an index zero configuration (x_0, y_0)

If case (a) applies and if $\mathrm{ind}_+(y, x_0) > 0$, use the same procedure to push y away from x_0 until we reach a point y_0 with $\mathrm{ind}_+(y_0, x_0) = 0$. Let γ_2 be an edgepath from y to y_0 obtained from this procedure. Then by construction, $(\gamma_1 \cdot \gamma) \cdot \gamma_2$ is a minimal-length edgepath from x_0 to y_0. Seeking a contradiction, assume that $\mathrm{ind}_+(x_0, y_0) > 0$. Then there exists a branch of a star neighbourhood U_{x_0} on which $w \mapsto d(w, y_0)$ increases as we move away from x_0. Choose a point x_0' on this branch with $d(x_0', y_0) > d(x_0, y_0)$. There exists an edgepath p connecting x_0 with y and passing through x_0' which does not pass through x_0, see Figure 5.10. Indeed, if such an edgepath does not exist then we have $\mathrm{ind}_+(x_0, y) > 0$, a contradiction. We can also assume that p has minimal-length. Indeed, we do not have $L_p < L_{\gamma_1 \cdot \gamma}$, since $\gamma_1 \cdot \gamma$ is a minimal-length edgepath from x_0 to y. If no minimal-length edgepath with the properties of p exists,

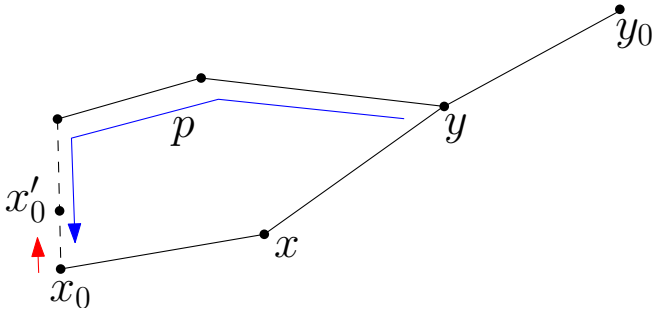

Figure 5.10: The point x'_0 and the edgepath p

then $L_p > L_{\gamma_1 \cdot \gamma}$ and we can move x_0 away from y along p in the direction of x'_0, contradicting $\mathrm{ind}_+(x_0, y) = 0$. Hence $L_p = L_{\gamma_1 \cdot \gamma}$. In particular, $d(x'_0, y_0)$ is equal to $L_{\gamma_2} + L_{p|_{[\varepsilon,1]}}$ for some $\varepsilon \in (0, 1)$. Thus $d(x'_0, y_0) < d(x_0, y_0) = L_{\gamma_2} + L_p$, a contradiction. Therefore $\mathrm{ind}_+(x_0, y_0) = 0$ and so (x_0, y_0) is an index zero configuration. If case (b) applies and if $\mathrm{ind}_+(x, y_0) > 0$, push x away from y_0 as above to obtain a point x_0 with $\mathrm{ind}_+(x_0, y_0) = \mathrm{ind}_+(y_0, x_0) = 0$. This defines a continuous path in $F_r(\Gamma, 2)$ from (x, y) to an index zero configuration (x_0, y_0). Hence, P contains at least one configuration $(x_0, y_0) \in Z_r$, and so contains at least one path-component of Z_r. □

Example 5.2.16. Let T be the labelled tree shown in Figure 5.11. The index zero

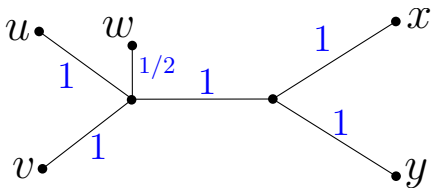

Figure 5.11: The labelling on T

configurations are (x, y), (x, u), (x, v), (x, w), (y, w), (y, u), (y, v), (w, u), (w, v) and (u, v), together with their images under the involution $\tau : T^2 \to T^2$, $(x_1, x_2) \mapsto (x_2, x_1)$. Applying Proposition 5.2.15 gives the following table.

Interval	Upper bound on $b_0(F_r(\Gamma, 2))$
$0 < r \leq 3/4$	20
$3/4 < r \leq 1$	16
$1 < r \leq 5/4$	12
$5/4 < r \leq 3/2$	8

5.3 An algorithm for computing $b_0(F_r(\Gamma, 2))$

In this section we provide an algorithm for computing $b_0(F_r(\Gamma, 2))$ given (Γ, ℓ) and $r \in \left(0, \frac{1}{2} \operatorname{diam} \Gamma\right]$. Our method is to construct algorithmically a graph $G_r = G_r(\Gamma)$ embedding in $F_r(\Gamma, 2)$ such that there is a bijection between the path-components of G_r and the path-components of $F_r(\Gamma, 2)$.

5.3.1 Constructing the graph G_r

We view G_r as a one-dimensional CW complex, so that G_r is permitted to contain loops and multiple edges.

Definition 5.3.1. We write $\mathrm{Crit}(r)$ for the set of all critical configurations (x, y) such that $d(x, y) \geq 2r$.

The construction of G_r is as follows.

1. Find $\mathrm{Crit}(r)$. For each isolated configuration $(x, y) \in \mathrm{Crit}(r)$, construct a corresponding vertex $(x, y) \in G_r$.

2. For each cycle C which contains non-isolated configurations in $\mathrm{Crit}(r)$ (namely, antipodal points on C) construct a copy of $C = S^1$ in G_r, realised as the pairs (x, y) of antipodal points on C. If there are common pairs of antipodal points between cycles, then identify these in the copies of the cycles in G_r.

3. To construct the remaining edges of G_r, let $(x, y) \in \mathrm{Crit}(r)$ be an isolated configuration which does not have index zero. There is a path in $F_r(\Gamma, 2)$ from (x, y) to an index zero configuration, which need not be unique, see Proposition 5.2.15. For each point $V = (x, s)$ or $V = (t, y)$ of G_r which is joined to (x, y) via such a path, construct edges in G_r from (x, y) to V, one for each distinct path and making the appropriate identifications if the paths overlap. If V is not index zero, repeat this procedure for V.

4. Apply step 3 to any pair (x, y) not of index zero lying on a cycle C from step 2. If $(x, y) \in C$ is not critical, it may be necessary to move both x and y to reach a configuration V in G_r. In this case, insert edges in G_r from (x, y)

to V as in step 3. Also apply step 3, if no corresponding edge has already been constructed, to any isolated index zero configuration joined by a path in $F_r(\Gamma, 2)$ to elements of G_r from steps 1 and 2.

5. If any circle from step 2 is left isolated after these steps, then designate one of its points to be a vertex of G_r. This is simply to ensure that G_r is a graph.

Remarks 5.3.2. We emphasise that G_r is dependent on r. If $r, s \in \left(0, \frac{1}{2}\operatorname{diam}\Gamma\right]$ and $r < s$, then G_s is a subgraph of G_r, possibly equal to G_r. By construction, a change in G_r may occur only as we pass a critical radius (Definition 5.2.5).

We now present several examples of constructing the graphs $\{G_r\}_{r>0}$ for specific labelled graphs (Γ, ℓ).

Example 5.3.3. Let Γ be the Y–graph as shown.

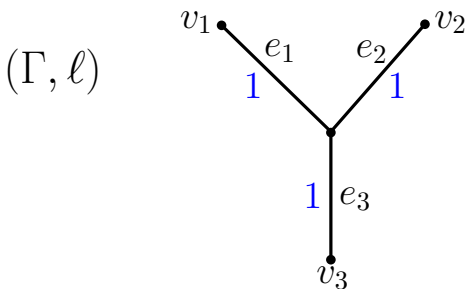

The critical configurations are precisely the pairs of distinct vertices, so the critical radii are $1/2$ and 1. For $0 < r \leq 1/2$, $\mathrm{Crit}(r)$ comprises the 12 pairs of distinct vertices (all critical configurations), so G_r has 12 vertices, see Figure 5.12. For each $i \in \{1, 2, 3\}$, v can be pushed away from v_i in two distinct directions, so G_r has 12 edges. If $1/2 < r \leq 1$, then G_r comprises the six vertices (v_i, v_j), for $i \neq j$, shown in Figure 5.12.

Example 5.3.4. Let $\Gamma = S^1$ be equipped with the graph structure comprising one vertex v and one edge e with label 1, see Figure 5.13. The only critical radius is $1/4$. For any $0 < r \leq 1/4$, G_r is a copy of S^1 consisting of the antipodal pairs (x, y) on Γ.

Example 5.3.5. Let $\Gamma = S^1 \vee [0, 1]$ have the labelled graph structure shown in Figure 5.14. The critical radii are $1/4$, $1/2$ and $3/4$. The graph G_r for $r \in (0, 1/4]$

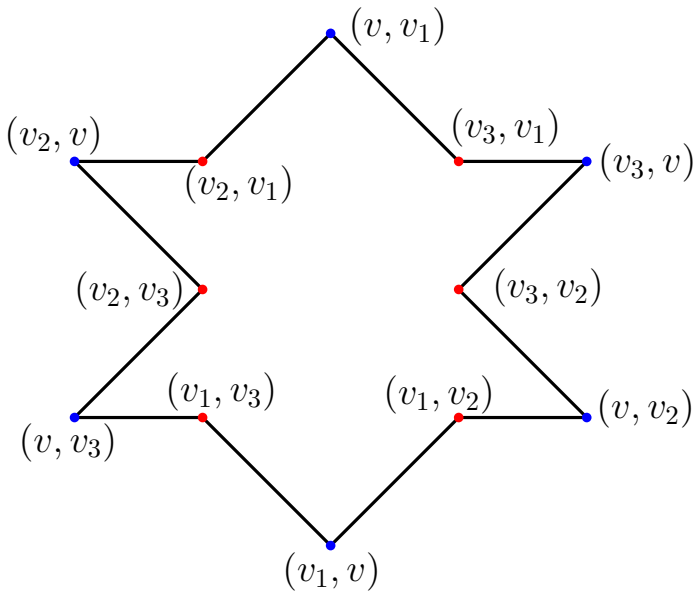

Figure 5.12: G_r for $0 < r \leq 1/2$

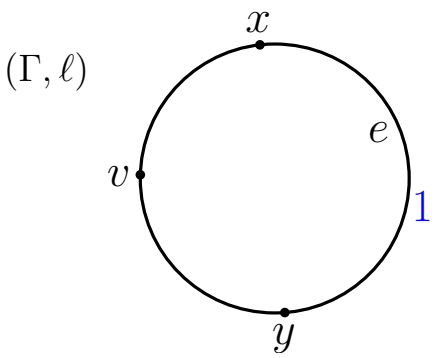

Figure 5.13: Antipodal points $x, y \in \Gamma$

is shown at the left of Figure 5.15. As we pass the critical radius $1/4$, G_r loses the circle corresponding to the antipodal configurations on the cycle in Γ, as well as its incident edges. These edges correspond to extending (x, y) or (y, x) to the index zero configurations (x, z) and (z, x), respectively. We obtain that G_r is the disjoint union of two circles shown in the middle of Figure 5.15. As we pass the critical radius $1/2$, G_r loses the configurations (y, z) and (z, y) as well as their incident edges. These edges correspond to the possible ways of extending (y, z) and (z, y) to the index zero configurations (x, z) and (z, x), respectively (there are two such possibilities for each of (y, z) and (z, y)). It follows that for $r \in (1/2, 3/4]$, G_r comprises the two points (x, z) and (z, x) as shown at the right of Figure 5.15.

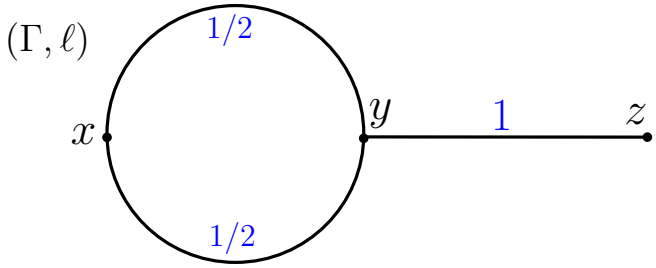

Figure 5.14: The graph structure on $\Gamma = S^1 \vee [0, 1]$

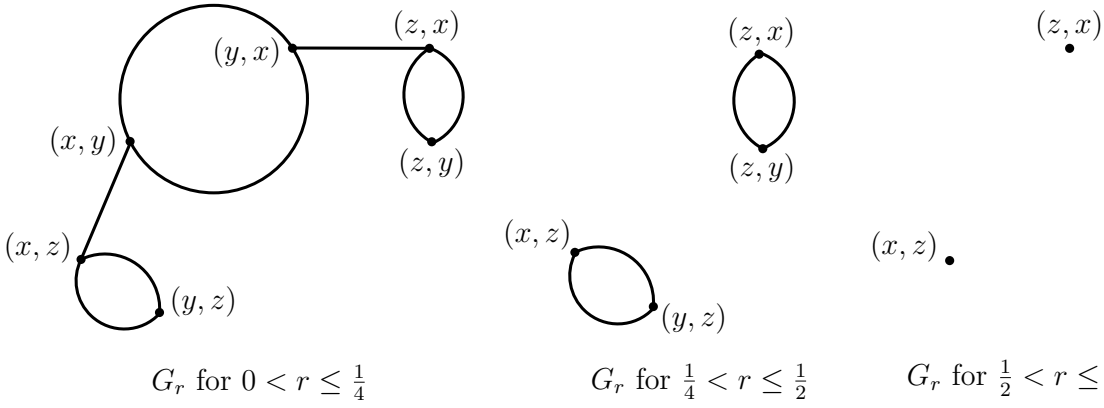

Figure 5.15: Evolution of G_r with r

Example 5.3.6. Let $\Gamma = S^1 \vee S^1$ have the graph structure shown in Figure 5.16. The critical configurations are the pairs of antipodal points on either of the two

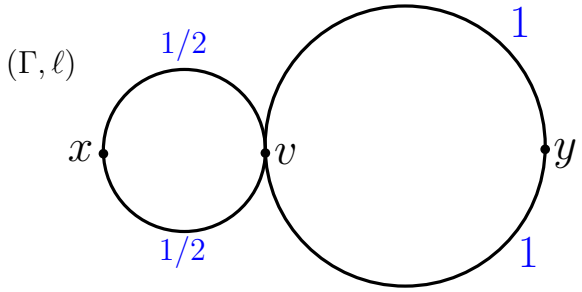

Figure 5.16: The graph structure on $\Gamma = S^1 \vee S^1$

cycles, together with the configurations (x, y) and (y, x). Hence the critical radii are 1/4, 1/2 and 3/4. Figure 5.17 shows the three possibilities for G_r. On the left, we have all critical configurations together with edges connecting (x, v) and (v, y) to (x, y) and (v, x) and (y, v) to (y, x). There are two edges in each case since there are two ways of extending to the index zero configurations (x, y) and (y, x). As we pass the critical radius 1/4, G_r loses the circle corresponding to the antipodal pairs

on the shorter cycle in Γ, together with its incident edges. This gives the graph G_r shown in the middle of Figure 5.17. As we pass the critical radius $1/2$, G_r loses the circle corresponding to the antipodal pairs on the larger cycle in Γ, together with its incident edges. This leaves us with the two configurations (x, y) and (y, x), shown on the right of Figure 5.17.

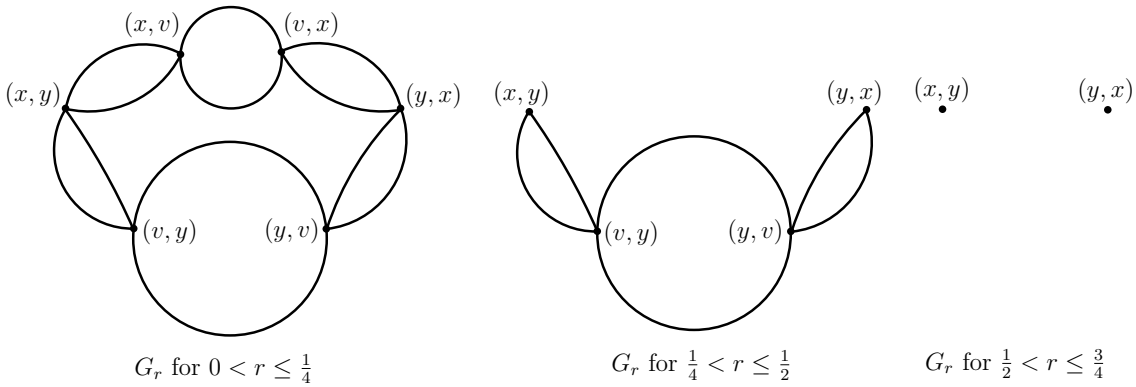

Figure 5.17: Evolution of G_r with r

Example 5.3.7. Let (T, ℓ) be the labelled Y–graph shown in Figure 5.18. The

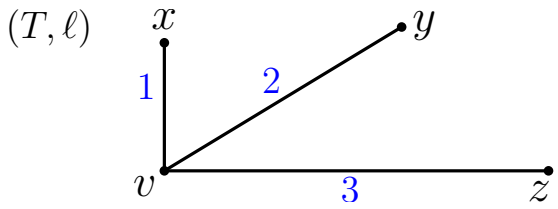

Figure 5.18: The labelled graph (T, ℓ)

critical radii are $1/2$, 1, $3/2$, 2 and $5/2$. The following table describes G_r for $r \in (0, 5/2]$. We use the notation Q_k for a discrete set of k points.

Interval	G_r	$b_0(G_r)$
$0 < r \leq 1/2$	S^1	1
$1/2 < r \leq 1$	$[0,1] \amalg [0,1]$	2
$1 < r \leq 3/2$	$[0,1] \amalg [0,1] \amalg Q_2$	4
$3/2 < r \leq 2$	Q_4	4
$2 < r \leq 5/2$	Q_2	2

For $0 < r \leq \frac{1}{2}$, $G_r = S^1$ is subdivided with 12 vertices and 12 edges. For $\frac{1}{2} < r \leq 1$, both intervals in $G_r = [0,1] \amalg [0,1]$ are subdivided with 5 vertices and 4 edges. For

$1 < r \leq \frac{3}{2}$, both of the intervals in $G_r = [0,1] \amalg [0,1] \amalg Q_2$ are subdivided with 3 vertices and 2 edges. For $\frac{3}{2} < r \leq 2$, $G_r = Q_4$ comprises the four configurations (x,z), (y,z), (z,x) and (z,y). Finally, for $2 < r \leq \frac{5}{2}$, $G_r = Q_2$ comprises the two configurations (y,z) and (z,y).

Example 5.3.8. Let Γ be the θ–graph shown in Figure 5.19. It has two vertices v and w and three edges, each with label 1. The only critical radius is $1/2$. For $0 < r \leq 1/2$, there are three distinct cycles contributing non-isolated critical configurations to $\mathrm{Crit}(r)$. The graph G_r is shown in Figure 5.20.

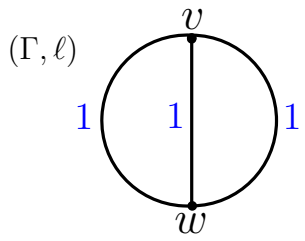

Figure 5.19: The labelled θ–graph Γ

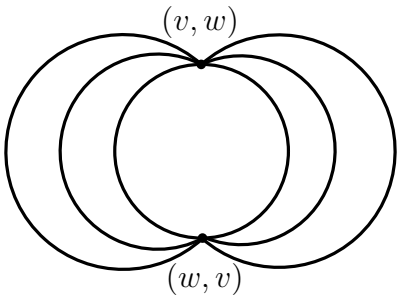

Figure 5.20: G_r for $0 < r \leq 1/2$

5.3.2 The main result and algorithm

We now prove the main result of this chapter, establishing a bijection between the path-components of $F_r(\Gamma, 2)$ and the components of the graph G_r from subsection 5.3.1, see Theorem 5.3.10. We first make the following simple observation.

Lemma 5.3.9. *There is an embedding $G_r \hookrightarrow F_r(\Gamma, 2)$.*

Proof. From the construction of G_r, the isolated configurations from step 1 and the circles from step 2 are included in $F_r(\Gamma, 2)$. Suppose that E is an edge from step

3 or step 4, joining two configurations (x, y) and (x', y'). Let $\gamma : [0, 1] \to F_r(\Gamma, 2)$ be the constant-speed path from (x, y) to (x', y') corresponding to E. Identifying $(E, \partial_0 E)$ with $([0, 1], 0)$ gives an embedding $E \to F_r(\Gamma, 2)$. Patching together these embeddings over all edges of G_r gives an embedding $G_r \hookrightarrow F_r(\Gamma, 2)$. □

Theorem 5.3.10. *We have $b_0(F_r(\Gamma, 2)) = b_0(G_r)$.*

Proof. We show that the inclusion map $\iota : G_r \hookrightarrow F_r(\Gamma, 2)$ induces a bijection

$$\iota_* : \pi_0(G_r) \to \pi_0(F_r(\Gamma, 2)).$$

By Proposition 5.2.15, each path-component of $F_r(\Gamma, 2)$ contains an index zero configuration (x_0, y_0) with $d(x_0, y_0) \geq 2r$. Since $(x_0, y_0) \in G_r$, ι_* is surjective. Now suppose that $\iota_*([x, y]) = \iota_*([x', y'])$, so that there is a path in $F_r(\Gamma, 2)$ from (x, y) to (x', y'). By Proposition 5.2.15, we may assume that (x, y) and (x', y') are index zero configurations. By the construction of G_r, any pair of index zero configurations joined by a path in $F_r(\Gamma, 2)$ are joined by a path in G_r, so $[(x, y)] = [(x', y')]$ in G_r. Hence, ι_* is injective. □

Corollary 5.3.11. *An algorithm for computing $b_0(F_r(\Gamma, 2))$ given Γ and r is as follows. We construct G_r using the algorithm described in subsection 5.3.1 and compute the Betti number $b_0(G_r)$.*

Example 5.3.12. Let T be the labelled tree from Example 5.2.16, see Figure 5.11. Constructing the graphs $\{G_r\}_{r>0}$ and applying Theorem 5.3.10 gives the following table (compare with the table from Example 5.2.16).

Interval	$b_0(F_r(T, 2))$
$0 < r \leq 1/2$	1
$1/2 < r \leq 3/4$	10
$3/4 < r \leq 1$	6
$1 < r \leq 5/4$	12
$5/4 < r \leq 3/2$	8

5.4 Further examples of computing $b_0(F_r(\Gamma, 2))$

In this section, we give further examples of computing $b_0(F_r(\Gamma, 2))$ for specific labelled graphs (Γ, ℓ).

Example 5.4.1. Let $\Gamma = S^1 \vee S^1$ be equipped with the labelled graph structure shown in Figure 5.21. (It is useful to compare this example with Example 5.3.6). The critical radii are $1/4$ and $1/2$. For $0 < r \leq 1/4$, G_r is shown in Figure 5.22.

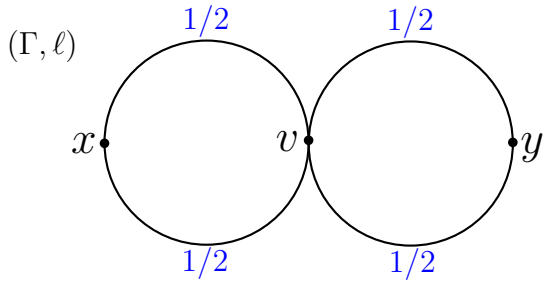

Figure 5.21: The labelled graph structure on $\Gamma = S^1 \vee S^1$

The two circles in G_r correspond to the pairs of antipodal points on the two cycles

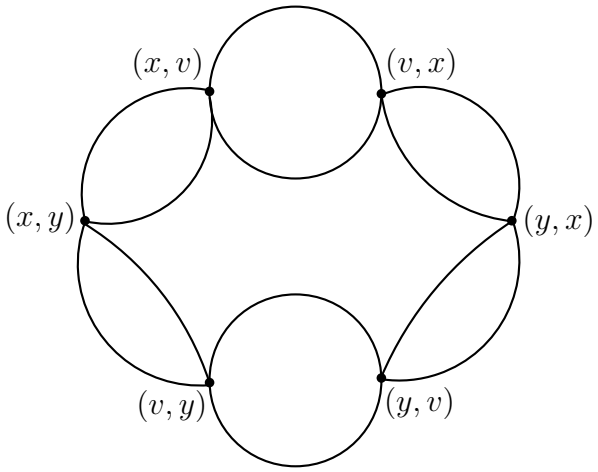

Figure 5.22: G_r for $0 < r \leq 1/4$

in Γ. We have two edges from each of (x, v) and (v, y) to (x, y), since we can extend (x, v) and (v, y) to (x, y) using two distinct paths. Similarly, we have two edges from each of (v, x) and (y, v) to the index zero configuration (y, x). To obtain G_r for $1/4 < r \leq 1/2$, we remove everything from $G_{1/4}$ apart from the two index zero configurations (x, y) and (y, x). Thus $G_r = \{(x, y), (y, x)\}$ for $1/4 < r \leq 1/2$.

Applying Theorem 5.3.10 gives the following table.

Interval	$b_0(F_r(\Gamma, 2))$
$0 < r \leq 1/4$	1
$1/4 < r \leq 1/2$	2

Example 5.4.2. Consider the labelled graph shown in Figure 5.23. The critical

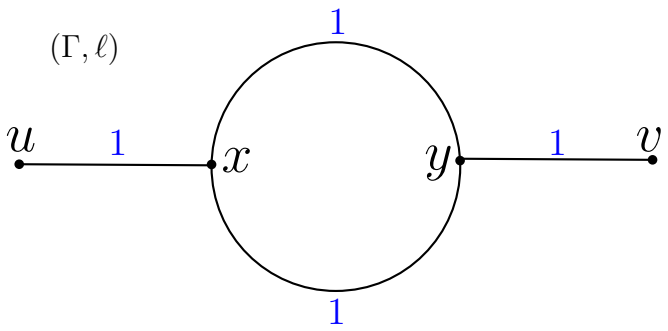

Figure 5.23: The labelled graph (Γ, ℓ)

configurations are the pairs of antipodal points on the cycle in Γ, apart from (x, y) and (y, x), together with (u, x), (u, v), (y, v), (x, u), (v, u) and (v, y). Hence, the critical radii are $1/2$ and $3/2$. For $0 < r \leq 1/2$, G_r is shown in Figure 5.24. For

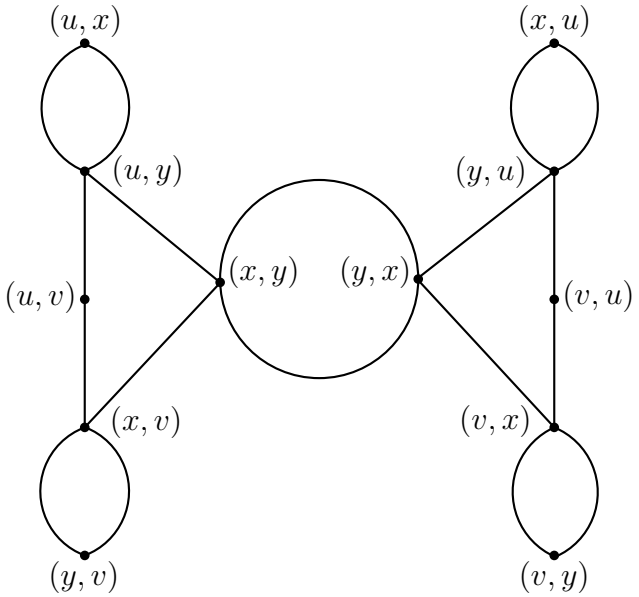

Figure 5.24: G_r for $0 < r \leq 1/2$

$1/2 < r \leq 3/2$, $G_r = \{(u, v), (v, u)\}$. Theorem 5.3.10 gives the following table.

Interval	$b_0(F_r(\Gamma, 2))$
$0 < r \leq 1/2$	1
$1/2 < r \leq 3/2$	2

Example 5.4.3. Let Γ be the labelled graph shown in Figure 5.25. The critical

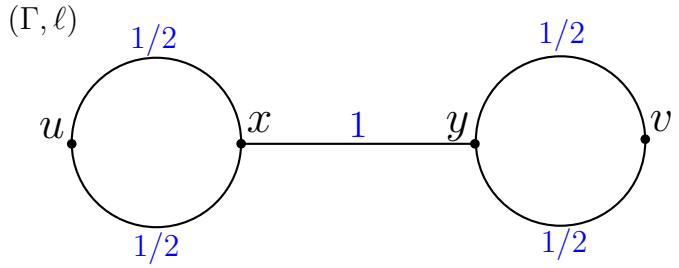

Figure 5.25: The labelled graph (Γ, ℓ)

radii are $1/4$, $1/2$, $3/4$ and 1. For $0 < r \leq 1/4$, G_r is shown in Figure 5.26. To

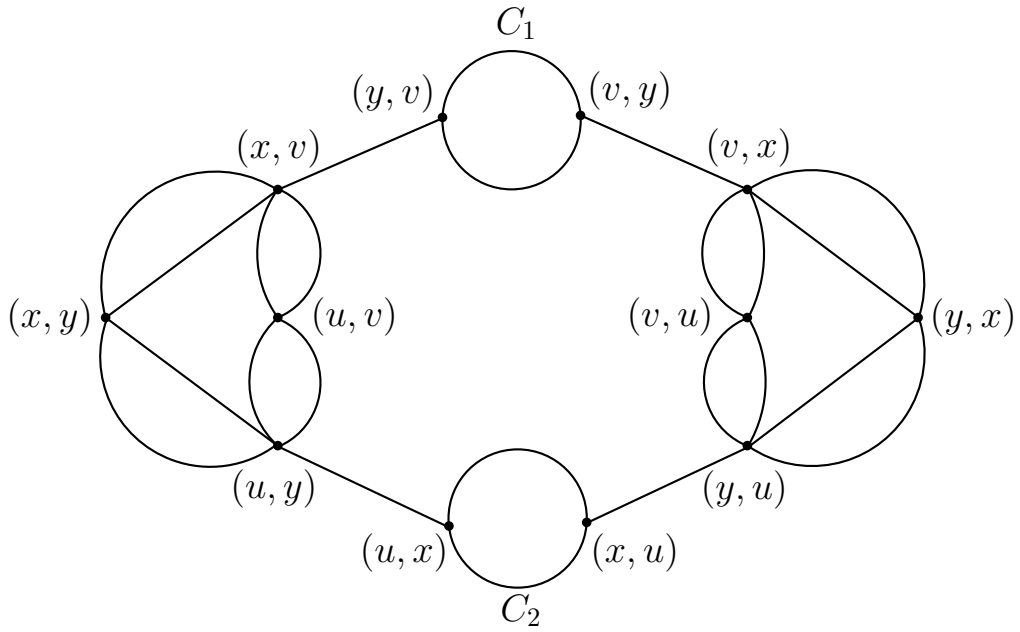

Figure 5.26: G_r for $0 < r \leq 1/4$

obtain G_r for $1/4 < r \leq 1/2$, we remove the cycles marked C_1 and C_2 from Figure 5.26. These correspond to antipodal pairs of points on the two distinct cycles in Γ. We also remove the edges incident to C_1 and C_2. The result is shown in Figure 5.27. To obtain G_r for $1/2 < r \leq 3/4$, we remove the critical configurations at

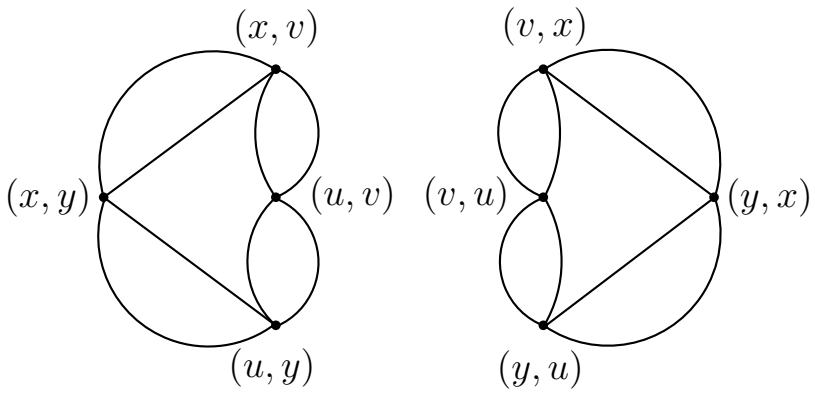

Figure 5.27: G_r for $1/4 < r \leq 1/2$

level 1, namely (x, y) and (y, x), together with their incident edges. This gives the graph shown in Figure 5.28. To determine G_r for $3/4 < r \leq 1$, we remove the

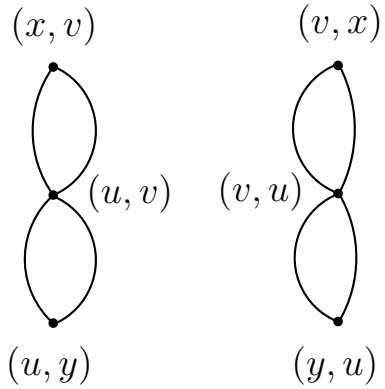

Figure 5.28: G_r for $1/2 < r \leq 3/4$

critical configurations at level $3/2$, namely (x, v), (v, x), (u, y) and (y, u), together with their incident edges. We obtain $G_r = \{(u, v), (v, u)\}$ for $3/4 < r \leq 1$. Applying Theorem 5.3.10 gives the following table.

Interval	$b_0(F_r(\Gamma, 2))$
$0 < r \leq 1/4$	1
$1/4 < r \leq 1/2$	2
$1/2 < r \leq 3/4$	2
$3/4 < r \leq 1$	2

Example 5.4.4. Let Γ be labelled graph shown in Figure 5.29. Here, w is the point on the cycle C antipodal to y, and z is the point antipodal to x. The cycle C has

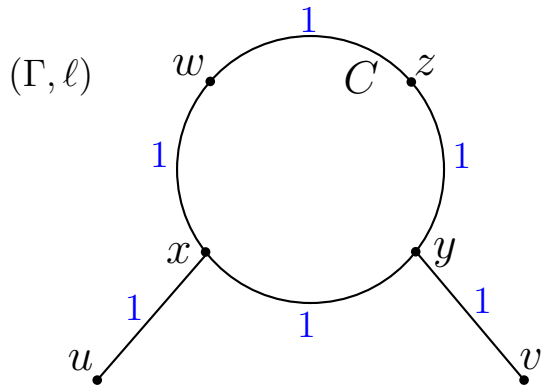

Figure 5.29: The labelled graph (Γ, ℓ)

length 4 and Γ has 6 vertices and 6 edges. The critical radii are $1/2$, 1 and $3/2$. For $0 < r \leq 1/2$, G_r is shown in Figure 5.30. To obtain G_r for $1/2 < r \leq 1$, we

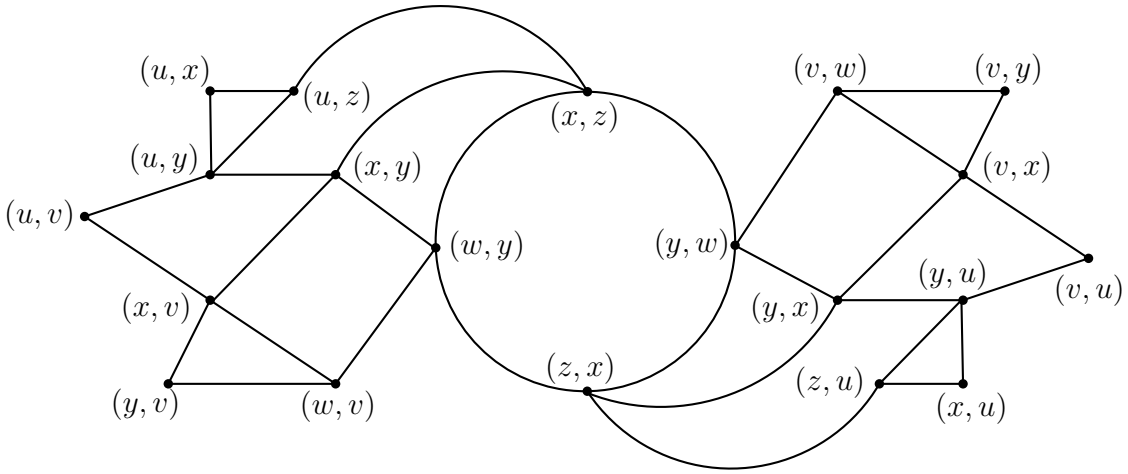

Figure 5.30: G_r for $0 < r \leq 1/2$

remove the critical configurations (x, y), (y, v), (u, x), (x, u), (v, y) and (y, x) at level 1, together with their incident edges. The resulting graph is shown in Figure 5.31. To obtain G_r for $1 < r \leq 3/2$, we now remove the central circle corresponding to the antipodal pairs on C in Γ, the configurations (u, y), (x, v), (v, x) and (y, u) and all their incident edges. This leaves six isolated points, see Figure 5.32.

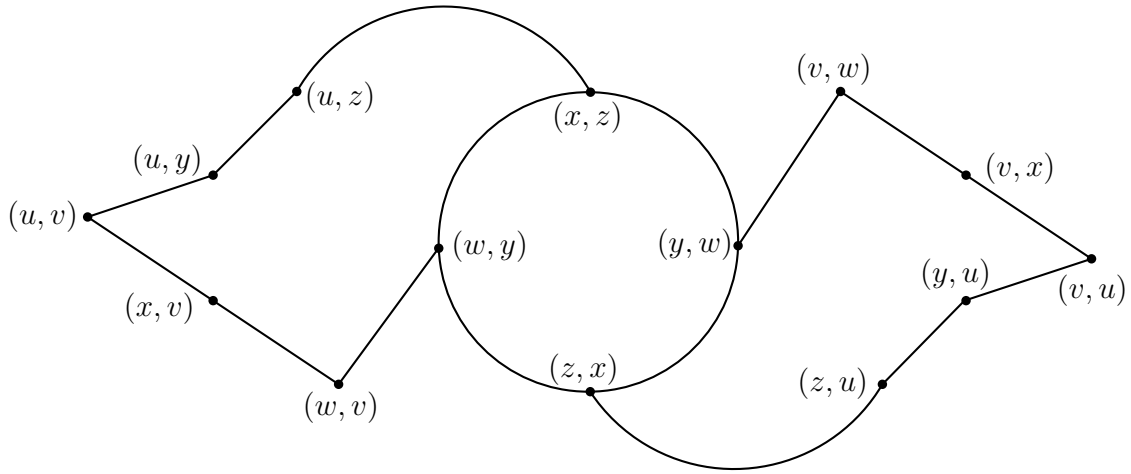

Figure 5.31: G_r for $1/2 < r \leq 1$

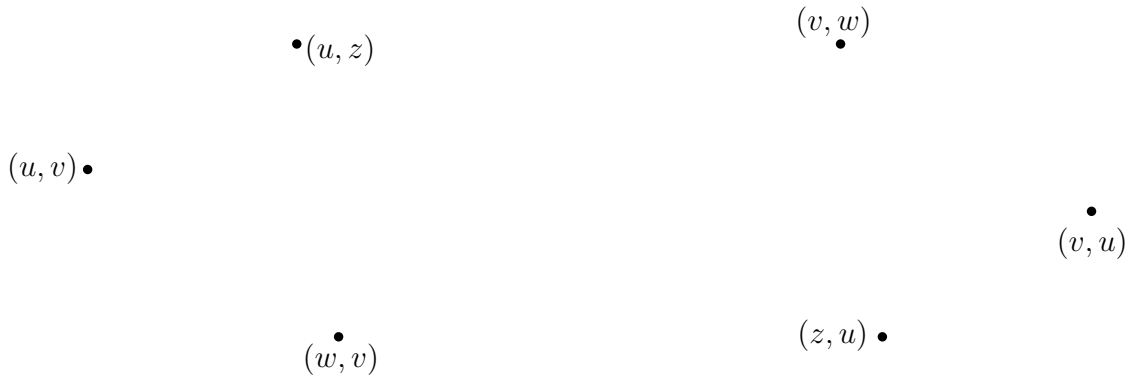

Figure 5.32: G_r for $1 < r \leq 3/2$

Applying Theorem 5.3.10 yields the following table.

Interval	$b_0(F_r(\Gamma, 2))$
$0 < r \leq 1/2$	1
$1/2 < r \leq 1$	1
$1 < r \leq 3/2$	6

Example 5.4.5. Let Γ_μ be the tree comprising $\mu \geq 3$ edges incident to a central vertex v, see Figure 5.33. The free vertices are $v_1, \ldots, v_\mu$ and all μ edges have label 1. The critical configurations are precisely the pairs of distinct vertices, so there are $\mu(\mu + 1)$ vertices in G_r for $0 < r \leq \frac{1}{2}$. Each pair (v, v_i) (respectively, (v_i, v)) extends to a pair (v_j, v_i) with $j \neq i$ (respectively, (v_i, v_j)) in $(\mu - 1)$ possible ways, so G_r has $2\mu(\mu - 1)$ edges for $0 < r \leq \frac{1}{2}$. There is one edge from (v, v_i) to (v_j, v_i)

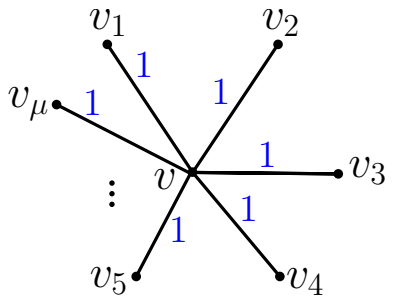

Figure 5.33: The graph Γ_μ

for each $j \neq i$, and similarly for (v_i, v) to (v_i, v_j). For $\frac{1}{2} < r \leq 1$, G_r comprises the $\mu(\mu-1)$ isolated vertices (v_i, v_j) for $i \neq j$. Applying Theorem 5.3.10 gives the following table.

Interval	$b_0(F_r(\Gamma_\mu, 2))$
$0 < r \leq 1/2$	1
$1/2 < r \leq 1$	$\mu(\mu-1)$

Remark 5.4.6 (Evolution of G_r with r). Suppose that R is the only critical radius in the interval $(a, b) \subset \left(0, \frac{1}{2} \operatorname{diam} \Gamma\right]$. We describe how to obtain G_b from G_a (recall that $G_b \subset G_a$). Firstly, remove all vertices (x, y) of G_a comprising a critical configuration with $d(x, y) = 2R$. Next, remove all circles in G_a arising from cycles containing antipodal pairs (x, y) with $d(x, y) = 2R$. Let $S \subset G_a$ be the points of G_a removed in these two steps. Finally, remove any edge E such that $\overline{E} \cap S \neq \emptyset$. We obtain the graph G_b. These remarks follow directly from the construction of the graphs $\{G_r\}_{r>0}$ in §5.3.1.

Chapter 6

Configuration spaces $\{F_r(\Gamma, n)\}_{r>0}$ for $n \geq 3$

In this chapter we study configuration spaces of three or more thick particles on a graph. In §6.1 we begin with the definitions and then apply PL Morse–Bott theory to derive statements about the family $\{F_r(\Gamma, n)\}_{r>0}$ analogous to Theorems 3.2.3 and 4.1.6. In §6.2 we discuss the special case when Γ is a tree. We obtain further information about the critical values of the family $\{F_r(\Gamma, n)\}_{r>0}$ in this case.

6.1 Homotopy type

Throughout this chapter, we fix $n \geq 3$ (the number of thick particles in the configuration space).

6.1.1 Definitions and basic properties

Definition 6.1.1. For $r > 0$, we define

$$F_r(\Gamma, n) := \{\mathbf{x} = (x_1, \ldots, x_n) \in \Gamma^n : f(\mathbf{x}) \geq 2r\} = f^{-1}([2r, \infty)),$$

where $f : \Gamma^n \to \mathbb{R}$ is the function

$$f(x_1, \ldots, x_n) := \min_{i<j}\{d(x_i, x_j)\}, \quad \forall (x_1, \ldots, x_n) \in \Gamma^n.$$

(Here, d is the metric on Γ as defined in §1.3).

Remarks 6.1.2. We topologise $F_r(\Gamma, n)$ as a subspace of the product Γ^n; it is a closed subspace since f is continuous. In the context of topological robotics, $F_r(\Gamma, n)$ models the collision-free motion of n robots of radius r on Γ such that tangencies between robots are permitted, see Figure 6.1.

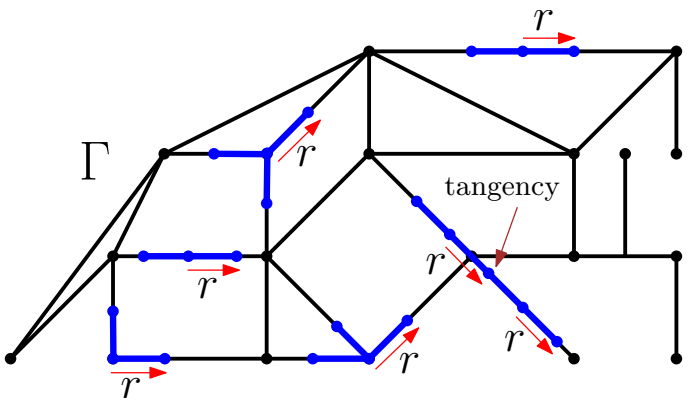

Figure 6.1: n robots of radius r moving on Γ

We begin with a simple result analogous to Lemma 3.1.4 from §3.1 which dealt with the case $n = 2$. However, I have been unable to improve the following statement (see Chapter 7, Problem 1).

Lemma 6.1.3. *$F_r(\Gamma, n) \neq \emptyset$ if $r \leq R := \frac{1}{2(n-1)} \operatorname{diam} \Gamma$.*

Proof. Choose $(x, y) \in \Gamma \times \Gamma$ such that $d(x, y) = \operatorname{diam} \Gamma$, and let $\gamma : [0, 1] \to \Gamma$ be a minimal-length edgepath from x to y. The configuration

$$(\gamma(0), \gamma(1/(n-1)), \gamma(2/(n-1)), \ldots, \gamma((n-2)/(n-1)), \gamma(1))$$

(see Figure 6.2) lies in $F_R(\Gamma, n)$ since $d(\gamma(s), \gamma(t)) = |s - t| d(x, y) = |s - t| \operatorname{diam} \Gamma$ for all $s, t \in [0, 1]$. Hence $F_r(\Gamma, n) \supseteq F_R(\Gamma, n) \neq \emptyset$ for all $r \in (0, R]$. □

Example 6.1.4. Let Γ be the Y–graph from Example 3.1.7, and let $n = 3$. The configuration (v_1, v_2, v_3) comprising the three free vertices lies in $F_1(\Gamma, 3)$, whereas $\frac{1}{2(n-1)} \operatorname{diam} \Gamma = \frac{1}{2(3-1)} \times 2 = \frac{1}{2} < 1$. Thus, the number R from Lemma 6.1.3 is not sharp for general n, as it is for the special case $n = 2$ (see Lemma 3.1.4).

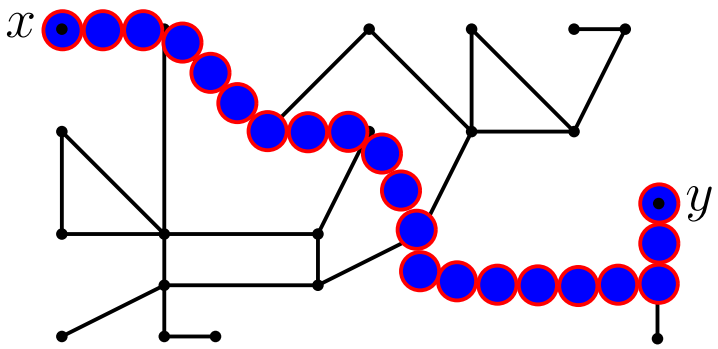

Figure 6.2: Illustration of the proof of Lemma 6.1.3

6.1.2 Examples: the interval and the circle

In this subsection we study the configuration spaces $F(\Gamma, n)$ and $F_r(\Gamma, n)$ when Γ is the interval $[0, 1]$ or the circle S^1.

The interval $[0, 1]$

Let $\Gamma = [0, 1]$ have the minimal graph structure comprising two vertices v_1, v_2 and one edge e, see Figure 6.3. Let $\mathbf{x} = (x_1, \ldots, x_n) \in F(\Gamma, n)$ be an arbitrary

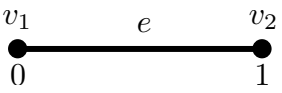

Figure 6.3: The interval $X = [0, 1]$

configuration of n distinct points in X. Write the points in order from left to right, producing a configuration $(x_{\sigma(1)}, \ldots, x_{\sigma(n)})$ for some unique permutation $\sigma \in S_n$. There is a path

$$[0, 1] \ni t \mapsto H_{\mathbf{x}}(t) \in F(\Gamma, n)$$

connecting $\mathbf{x}$ with the equally-spaced configuration

$$(0, 1/(n-1), 2/(n-1), \ldots, (n-2)/(n-1), 1) \in F(\Gamma, n),$$

moving $x_{\sigma(i)}$ to $(i-1)/(n-1)$ for each $i \in \{1, \ldots, n\}$, see Figure 6.4. Moreover, each $H_{\mathbf{x}}$ can be chosen so that the associated map $H : F(\Gamma, n) \times [0, 1] \to F(\Gamma, n)$ is continuous. Hence, each path-component of $F(\Gamma, n)$ deformation retracts onto a point space. There are $n!$ such path-components, each corresponding to a different

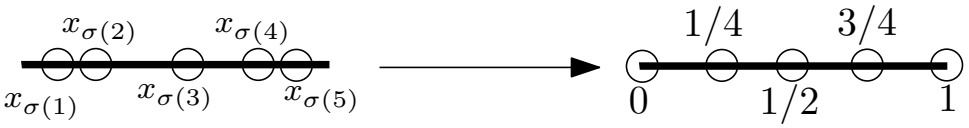

Figure 6.4: Moving $\mathbf{x}$ to an equally-spaced configuration

permutation of the points on $[0,1]$. Thus $F(\Gamma, n) \simeq Q_{n!}$, a discrete set of $n!$ points. Let $R := \frac{1}{2(n-1)}\ell(e)$, where $\ell(e)$ is the label of e. Using a similar argument, there is a deformation retraction of $F_r(\Gamma, n)$ onto the same set of $n!$ points for each $r \in (0, R]$. The case $r = R$ is the degenerate case when $F_R(\Gamma, n)$ comprises the $n!$ points

$$\{\sigma \cdot (0, 1/(n-1), \ldots, (n-2)/(n-1), 1) : \sigma \in S_n\}$$

and the deformation retraction is the identity map for all time. We have $F_r(\Gamma, n) = \emptyset$ for $r > R$.

The circle S^1

Let $\Gamma = S^1$ have the graph structure shown in Figure 6.5. We can apply a similar

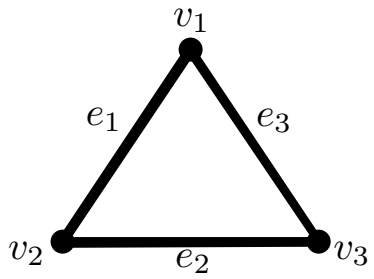

Figure 6.5: The graph structure on the circle $X = S^1$

argument as used above for the interval to compute the homotopy type of $F(\Gamma, n)$. Let $\mathbf{x} = (x_1, \ldots, x_n) \in F(\Gamma, n)$. Starting from x_1 and moving anticlockwise, write the remaining $n-1$ points in order, producing a configuration $(x_{\tau(1)}, \ldots, x_{\tau(n-1)})$ for some unique $\tau \in S_{n-1}$. There is a path

$$[0,1] \ni t \mapsto H_{\mathbf{x}}(t) \in F(\Gamma, n)$$

fixing x_1 and connecting $\mathbf{x}$ to the equally-spaced configuration

$$(x_1, x_1 e^{2\pi i/n}, x_1 e^{4\pi/n}, \ldots, x_1 e^{2\pi i(n-1)/n}),$$

such that $x_{\tau(k)}$ moves to $x_1 e^{2\pi i k/n}$ for $1 \leq k \leq n-1$, see Figure 6.6. As before, each map $H_{\mathbf{x}}$ can be chosen so that the associated map $H : F(\Gamma, n) \times [0,1] \to F(\Gamma, n)$ is continuous. Hence, each path-component of $F(\Gamma, n)$ deformation retracts onto a

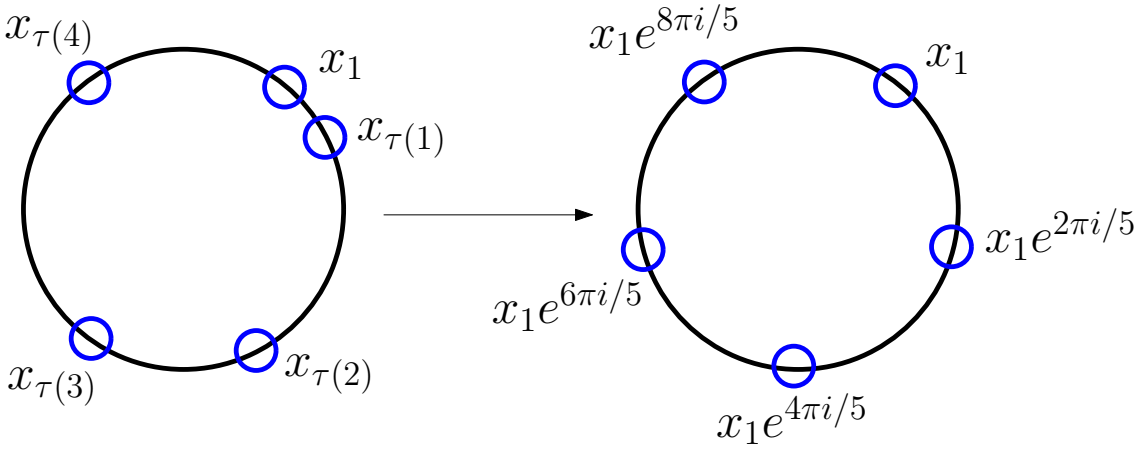

Figure 6.6: Moving $\mathbf{x}$ to an equally-spaced configuration

circle S^1. There are $(n-1)!$ such path-components, so $F(\Gamma, n) \simeq \coprod_{(n-1)!} S^1$. Let $R := \frac{1}{n} \operatorname{diam} \Gamma$. As above, we have a deformation retraction of $F_r(\Gamma, n)$ onto the disjoint union of $(n-1)!$ circles for each $r \in (0, R]$. The case $r = R$ is the degenerate case when $F_R(\Gamma, n)$ comprises the $(n-1)!$ disjoint circles and the deformation retraction is the identity map for all time. We have $F_r(\Gamma, n) = \emptyset$ for $r > R$.

6.1.3 Critical values

In this subsection we prove the main results of this chapter, which are the analogues of Theorems 3.2.3 and 4.1.6 for the general case $n \geq 3$. We assume that Γ is simple and satisfies the cycle inequality (see §1.5).

Definitions 6.1.5. A number $R > 0$ is a *regular value* of the family $\{F_r(\Gamma, n)\}_{r>0}$ if there is an open set $U_R \subset (0, \infty)$ containing R such that $F_{r_2}(\Gamma, n)$ is a deformation retract of $F_{r_1}(\Gamma, n)$ for all $r_1, r_2 \in U_R$ with $r_1 \leq r_2$. A number $R > 0$ is a *critical value* of $\{F_r(\Gamma, n)\}_{r>0}$ if it is not a regular value.

The following theorem is the analogue of Theorem 3.2.3.

Theorem 6.1.6. *For each $n \geq 3$, the family $\{F_r(\Gamma, n)\}_{r>0}$ has finitely many critical values.*

Proof. The statement follows immediately from Proposition 2.1.21 provided that $f : \Gamma^n \to \mathbb{R}$ is an affine Morse–Bott function. To justify the latter, we construct a finite subdivision S of Γ^n such that f is piecewise affine on S (that is, on each cell K of S, $f|_K$ extends to an affine function $\mathbb{R}^n \to \mathbb{R}$).

For each unordered pair $\{i, j\} \subset \{1, \dots, n\}$, $i \neq j$, let $f_{\{i,j\}} : \Gamma^n \to \mathbb{R}$ be the map $f_{\{i,j\}}(x_1, \dots, x_n) = d(x_i, x_j)$. (There are $\binom{n}{2}$ different functions $f_{\{i,j\}}$, and $f = \min_{i<j}\{f_{\{i,j\}}\}$). We note that $f_{\{i,j\}}$ is the composition of the projection

$$\Gamma^n \ni (x_1, \dots, x_n) \mapsto (x_i, x_j)$$

(a piecewise affine function with respect to the product CW decomposition of Γ^n) followed by the metric $d : \Gamma^2 \to \mathbb{R}$ (a piecewise affine function with respect to some subdivision of the product CW structure on Γ^2, see Proposition 2.2.1).

Write $\Gamma^n = \Gamma_1 \times \cdots \times \Gamma_n$, where $\Gamma_i = \Gamma$ for each $i = 1, \dots, n$.[1] We subdivide Γ^n as follows. Take the first two factors Γ_1 and Γ_2 and subdivide $\Gamma_1 \times \Gamma_2$ so that $d : \Gamma_1 \times \Gamma_2 \to \mathbb{R}$ is piecewise affine. Extend this to a subdivision S_1 of Γ^n by defining new cells $(F \times K) \times L$, where $F \times K$ is a cell of the new subdivision of $\Gamma_1 \times \Gamma_2$ and L is a cell of $\Gamma_3 \times \cdots \times \Gamma_n$. This subdivision ensures that $f_{\{1,2\}} : \Gamma^n \to \mathbb{R}$ is piecewise affine. Now repeat this process of subdivision, starting with S_1 and subdividing factors 1 and 3, resulting in a subdivision S_2 of S_1 such that $f_{\{1,2\}}$ and $f_{\{1,3\}}$ are both piecewise affine with respect to S_2. Repeating this process over the remaining pairs of factors given by the sequence

$$\begin{array}{ccccccc} (1,2) & (1,3) & (1,4) & \dots & (1,n) \\ & (2,3) & (2,4) & \dots & (2,n) \\ & & (3,4) & \dots & (3,n) \\ & & & \ddots & \vdots \\ & & & & (n-1,n) \end{array}$$

results in a subdivision $S_{\binom{n}{2}}$ of Γ such that $f_{\{i,j\}}$ is piecewise affine on $S_{\binom{n}{2}}$ for each pair $\{i, j\}$ with $i < j$.

Write $g_1 = f_{\{1,2\}}$, $g_2 = f_{\{1,3\}}, \dots g_{\binom{n}{2}} = f_{\{n-1,n\}}$. Take a cell of $S_{\binom{n}{2}}$ of dimension n, and subdivide it such that $\min\{g_1, g_2\}$ is piecewise affine on K. For each cell from

[1] Note that Γ^n is a cube complex and therefore an APC with respect to the product CW structure.

the resulting subdivision of K, do the same for $\min\{g_1, g_3\}$. Continue the process over all pairs of functions $\{g_i, g_j\}$, working with all pairs $\{i, j\} \subset \left\{1, \ldots, \binom{n}{2}\right\}$ in the order

$$\begin{array}{ccccc} (1,2) & (1,3) & (1,4) & \ldots & \left(1, \binom{n}{2}\right) \\ & (2,3) & (2,4) & \ldots & \left(2, \binom{n}{2}\right) \\ & & (3,4) & \ldots & \left(3, \binom{n}{2}\right) \\ & & & \ddots & \vdots \\ & & & & \left(\binom{n}{2} - 1, \binom{n}{2}\right). \end{array}$$

Now repeat the process on the remaining cells of $S_{\binom{n}{2}}$ of dimension n. This results in a subdivision S of Γ^n such that $\min\{g_i, g_j\}$ is piecewise affine for each pair $\{i, j\} \subset \left\{1, \ldots, \binom{n}{2}\right\}$. Hence, we have a subdivision S of Γ^n such that $f : \Gamma^n \to \mathbb{R}$ is piecewise affine. □

Remark 6.1.7. Theorem 6.1.6 implies that there is a space X and $\varepsilon > 0$ such that there are homotopy equivalences

$$X \simeq F_r(\Gamma, n), \quad \forall r \in (0, \varepsilon].$$

The next theorem is analogous to Theorem 4.1.6.

Theorem 6.1.8. *We have $F_r(\Gamma, n) \simeq F(\Gamma, n)$ for all $r \in (0, \varepsilon]$, where ε is the number from Remark 6.1.7.*

Before proving Theorem 6.1.8, we first establish the following two simple results.

Lemma 6.1.9. *Choose $M \in \mathbb{N}$ such that $\frac{1}{M} < \varepsilon$. We have*

$$F(\Gamma, n) = \bigcup_{m=M}^{\infty} F_{1/m}(\Gamma, n).$$

Proof. We have $F_r(\Gamma, n) \subset F(\Gamma, n)$ for all $r > 0$, so $\bigcup_{m=M}^{\infty} F_{1/m}(\Gamma, n) \subset F(\Gamma, n)$. On the other hand, if $(x_1, \ldots, x_n) \in F(\Gamma, n)$, then $x_i \neq x_j$ for all $i \neq j$. Hence $f(x_1, \ldots, x_n) > 0$ and so $f(x_1, \ldots, x_n) \geq 2/K$ for some $K \geq M$. Thus $(x_1, \ldots, x_n) \in F_{1/K}(\Gamma, n) \subset \bigcup_{m=M}^{\infty} F_{1/m}(\Gamma, n)$. □

Lemma 6.1.10. *Suppose that $((X_n, d_n))_{n \geq 1}$ is a sequence of metric spaces such that for all $n \geq 1$,*

(i) X_{n+1} *deformation retracts onto* X_n *and contains an open neighbourhood* U_n *of* X_n*, and*

(ii) $d_{n+1}|_{X_n \times X_n} = d_n$.

Then $X_* := \bigcup_{n=1}^{\infty} X_n$ *deformation retracts onto* X_1.

Proof. Define $F : X_* \times [0,1] \to X_*$ as follows: for each $n \geq 1$, perform a deformation retraction of X_{n+1} onto X_n in the time interval $[1/2^n, 1/2^{n-1}]$, and set $F(x,0) = x$ for all $x \in X_*$. Then $F(y,s) = y$ for all $y \in X_1$ and $s \in [0,1]$, so F is a deformation retraction of X_* onto X_1 provided that it is continuous. It is continuous on $X_* \times (0,1]$ by construction, so it suffices to show continuity on $X_* \times \{0\}$. To this end, fix $x_* \in X_*$ and choose a sequence $\{(x_k, t_k)\}_{k \geq 1}$ in $X_* \times [0,1]$ converging to $(x_*, 0)$. Choose the smallest $n \geq 1$ such that $x_* \in X_n \setminus X_{n-1}$ (setting $X_0 := \emptyset$), and let $\varepsilon > 0$ be arbitrary. Since $x_k \to x_*$ and $t_k \to 0$ as $k \to \infty$, there exists $K \in \mathbb{N}$ such that $x_k \in U_n$, $d_{n+1}(x_k, x_*) < \varepsilon$ and $t_k < 1/2^n$ for all $k \geq K$. Hence, we have $F(x_k, t_k) = x_k$ for all $k \geq K$ and so

$$d_{n+1}(F(x_k, t_k), F(x_*, 0)) = d_{n+1}(x_k, x_*) < \varepsilon, \quad \forall k \geq K,$$

showing that $F(x_k, t_k) \to F(x_*, 0)$ in X_* as $k \to \infty$. Hence F is continuous on $X_* \times \{0\}$. □

Proof of Theorem 6.1.8. Proposition 2.1.21 implies that for $a < b < \varepsilon$, there is a deformation retraction of $F_a(\Gamma, n)$ onto its subspace $F_b(\Gamma, n)$. In particular, $F_{1/(m+1)}(\Gamma, n)$ deformation retracts onto $F_{1/m}(\Gamma, n)$ for all $m \geq M$. Further, $F_a(\Gamma, n)$ contains the open neighbourhood

$$\left\{ (x_1, \ldots, x_n) \in \Gamma^n : \min_{i<j} \{d(x_i, x_j)\} > a + b \right\}$$

of $F_b(\Gamma, n)$. For each $m \geq M$, $F_{1/m}(\Gamma, n)$ is a metric subspace[2] of the product Γ^n, so conditions (i) and (ii) of Lemma 6.1.10 are satisfied. Applying the statement of Lemma 6.1.10 and using Lemma 6.1.9 shows that $F(\Gamma, n)$ deformation retracts onto $F_{1/M}(\Gamma, n)$. The homotopy type of $F_r(\Gamma, n)$ is constant as r varies over $(0, \varepsilon]$, so $F(\Gamma, n) \simeq F_r(\Gamma, n)$ for all $r \in (0, \varepsilon]$ since $1/M < \varepsilon$. □

[2]With respect to a metric on Γ^n such as $\rho(\mathbf{x}, \mathbf{y}) = \sum_{i=1}^{n} d(x_i, y_i)$.

6.1.4 Remarks on path-connectedness

A result contained in A. Abrams' thesis (see [1, Theorem 2.7]) shows that if Γ is not the interval or the circle, then $F(\Gamma, n)$ is path-connected for any $n \geq 3$. We deduce from Theorem 6.1.8 that $F_r(\Gamma, n)$ is path-connected for sufficiently small r, provided that $\Gamma \ncong [0,1], S^1$. However, $F_r(\Gamma, n)$ is generally disconnected (see §6.1.2) as it is for the case $n = 2$ (see Chapter 5). It would be interesting to have an algorithm for computing $b_0(F_r(\Gamma, n))$ for given Γ, $n \geq 3$ and $r > 0$ (see Chapter 7, Problem 2).

6.2 Thick particles on trees

In this section we study configuration spaces of thick particles on trees. We assume that T is a tree containing no vertices of degree 2. The main result is Theorem 6.2.11 which explicitly describes all possible critical values of the family $\{F_r(T, n)\}_{r>0}$ in terms of the metric data.

6.2.1 Definitions and terminology

The following definitions are valid for a general labelled graph (Γ, ℓ).

Definitions 6.2.1. A configuration $\mathbf{x} = (x_1, \ldots, x_n) \in F(\Gamma, n)$ is *expandable* if there exists $i \in \{1, \ldots, n\}$ and a unique branch $([0,1), 0)$ of a star neighbourhood (U_{x_i}, x_i) such that the function

$$[0,1] \ni y \mapsto \min_{j \neq i}\{d(y, x_j)\}$$

increases as we move away from x_i. (Using the notation of §5.2.1, this is equivalent to the condition that $\mathrm{ind}_+(x_i, x_j) = 1$ for at least one index $j \neq i$.) A configuration $\mathbf{x}$ is *critical* if it is not expandable.

Examples 6.2.2. The configuration (x_1, x_2, x_3) on the left of Figure 6.7 is expandable, because there is a unique branch of U_{x_3} on which $y \mapsto \min\{d(y, x_1), d(y, x_2)\}$ increases as we move away from x_3. In particular $\mathrm{ind}_+(x_3, x_1) = \mathrm{ind}_+(x_3, x_2) = 1$. However, the configuration (x_1, x_2) is critical. On the right of Figure 6.7, the con-

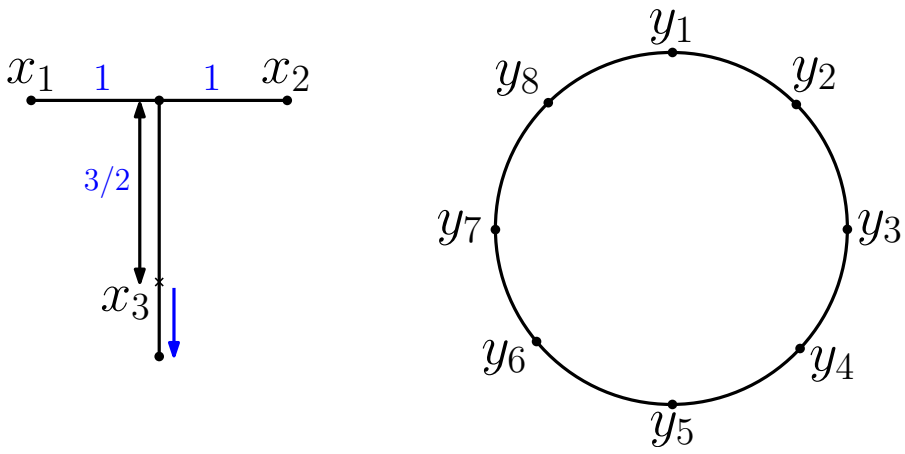

Figure 6.7: Expandable and critical configurations

figuration

$$\mathbf{y} = (y_1, \ldots, y_8)$$

is critical because $y \mapsto \min_{\substack{1 \le j \le 8 \\ j \neq i}} \{d(y, y_j)\}$ decreases as move away from y_i on both branches of U_{y_i} for each $i \in \{1, \ldots, 8\}$. On the other hand, if we remove any point of this configuration, say y_1, then the resulting configuration $(y_2, \ldots, y_8)$ is expandable. Indeed, there are now unique branches of U_{y_2} and U_{y_8} on which $y \mapsto \min_{3 \le j \le 8} \{d(y, y_j)\}$ and $y \mapsto \min_{2 \le j \le 7} \{d(y, y_j)\}$ increase as we move away from y_2 and y_8, respectively.

Definition 6.2.3. A critical configuration $\mathbf{x} = (x_1, \ldots, x_n)$ is *weakly essential* if for each $i \in \{1, \ldots, n\}$, the $(n-1)$–configuration

$$(x_1, \ldots, x_{i-1}, \widehat{x}_i, x_{i+1}, \ldots, x_n)$$

obtained from $\mathbf{x}$ by deleting the point x_i is expandable.

Definition 6.2.4. A critical configuration $\mathbf{x} = (x_1, \ldots, x_n)$ is *essential* if for each subset S of $\{x_1, \ldots, x_n\}$ with $1 \le |S| \le n-2$, the $(n - |S|)$–configuration obtained from $\mathbf{x}$ by deleting the elements of S is expandable.

Remark 6.2.5. An essential configuration is weakly essential.

Examples 6.2.6. Consider the circle from Example 3.1.6, and let $y_k = e^{2\pi i(k-1)/p}$ for $k \in \{1, \ldots, p\}$, where p is an odd prime. It follows that the configuration

$\mathbf{y} = (y_1, \ldots, y_p)$ is essential. The configuration $\mathbf{y} = (y_1, \ldots, y_8)$ on the right of Figure 6.7 is weakly essential but not essential. To see that it is not essential, note that deleting y_2, y_4, y_6 and y_8 from $\mathbf{y}$ results in the critical 4–configuration (y_1, y_3, y_5, y_7). In fact, for equally-spaced configuration points $y_1, \ldots, y_n$ on S^1, $\mathbf{y} = (y_1, \ldots, y_n)$ is essential if and only if n is prime.

For equally-spaced points

$$\left\{x_i = \tfrac{i-1}{n-1} : 1 \leq i \leq n\right\}$$

on the interval $[0, 1]$, the critical configuration $\mathbf{x} = (x_1, \ldots, x_n)$ is essential if and only if $n = 2$. Indeed, if $n \geq 3$ then deleting $S = \{x_2, \ldots, x_{n-1}\}$ from $\mathbf{x}$ leaves the critical configuration (x_1, x_n). The configuration $\mathbf{x} = (x_1, \ldots, x_n)$ is weakly essential if and only if $n \neq 3$, since if $n \geq 4$ then deleting any x_i from $\mathbf{x}$ leaves an expandable configuration.

Remarks 6.2.7. If $\mathbf{x}$ is expandable at x_i such that

$$[0, 1] \ni y \mapsto f(x_1, \ldots, x_{i-1}, y, x_{i+1}, \ldots, x_n)$$

increases as we move away from x_i, then $R := f(\mathbf{x})$ is not a critical value of the family $\{F_r(T, n)\}_{r>0}$. Indeed, since we are working with a tree T, we need only perform the second subdivision from Theorem 6.1.6 to ensure that $f : T^n \to \mathbb{R}$ is piecewise affine on T^n. The proof of Proposition 2.1.21 then shows that $F_R(T, n)$ deformation retracts onto $F_{R'}(T, n)$ for some $R' > R$ sufficiently close to R. In particular, any critical value occurs as a distance $d(x, y)$ between two points of a weakly essential configuration $\mathbf{y}$ (we emphasise that this is for the special case when T is a tree).

6.2.2 Components of configurations

We now focus on classifying weakly essential configurations in a tree T. We need the following concepts for the proof of the main result (Theorem 6.2.11).

Definitions 6.2.8. Let $\mathbf{x} = (x_1, \ldots, x_n) \in F(T, n)$, and write $[\mathbf{x}] = \{x_1, \ldots, x_n\}$. Define a relation $\sim$ on the elements of $[\mathbf{x}]$ as follows. For $x, y \in [\mathbf{x}]$, say that $x \sim y$

if and only if $x = y$ or there exists a sequence $x = w_0, w_1, \ldots, w_k = y$ in $[\mathbf{x}]$ such that $d(w_i, w_{i+1}) = f(\mathbf{x})$, for all $i = 0, 1, \ldots, k$. Then $\sim$ is an equivalence relation; call the equivalence classes of $[\mathbf{x}]$ the *components* of $\mathbf{x}$. A component is *proper* if it has size at least two. A point $x \in [\mathbf{x}]$ is *isolated* if its component is not proper.

Remark 6.2.9. Every configuration contains at least one proper component.

Lemma 6.2.10. *If $\mathbf{x} \in F(T, n)$ is critical, then the proper components of $\mathbf{x}$ are also critical configurations.*

Proof. Let $C \subseteq [\mathbf{x}]$ be a proper component and choose $x, y \in C$ such that

$$d(x, y) = \max_{w_1, w_2 \in C} \{d(w_1, w_2)\}.$$

Since T is a tree, there is a unique minimal-length edgepath γ from x to y. Since $x \sim y$, there is an equally-spaced sequence $x = w_0, w_1, \ldots, w_k = y$ of points of C lying on $\operatorname{Im}\gamma =: I_1$ from x to y, see Figure 6.8. If any elements of C do not appear in

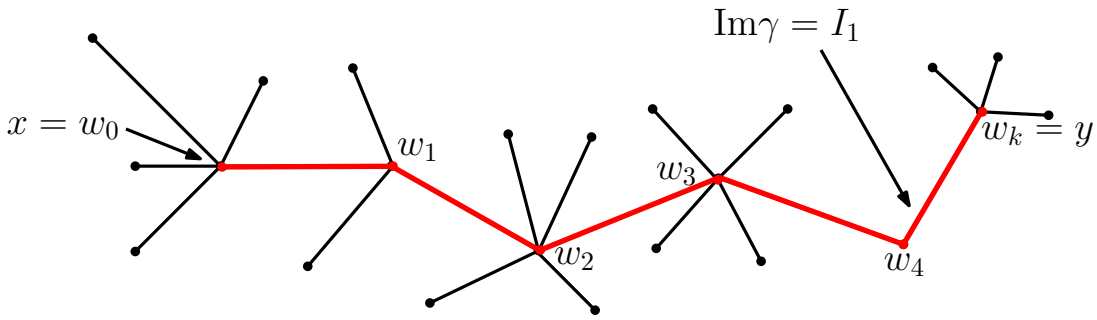

Figure 6.8: The points x, y and the path γ

this sequence, repeat the argument for $C - \{w_0, \ldots, w_k\}$. Continuing until all points of C are accounted for, we obtain unique intervals $I_1, \ldots, I_q$ such that $C \subset \bigcup_{j=1}^{q} I_j$, the points of $C \cap I_j$ are equally-spaced on I_j and $|I_j \cap I_k| \leq 1$ for all $j \neq k$, see Figure 6.9. Write $\langle C \rangle = \bigcup_{j=1}^{q} I_j$. We can give $\langle C \rangle$ a tree structure as follows. The vertex set V comprises the endpoints of I_j, $j = 1, \ldots, q$, and the points of intersection of I_j and I_k for $j \neq k$. (The edges are the components of $\langle C \rangle - V$.)

Let $x_{i_1}, \ldots, x_{i_K}$ be the points of C. We now show that the K–configuration $\mathbf{y} = (x_{i_1}, \ldots, x_{i_K})$ is critical. If x_{i_j} is not a free vertex of $\langle C \rangle$, then $y \mapsto \min_{k \neq j}\{d(y, x_{i_k})\}$ is decreasing on all branches of $U_{x_{i_j}}$ as we move away from x_{i_j}, so $\mathbf{y}$ is not expandable

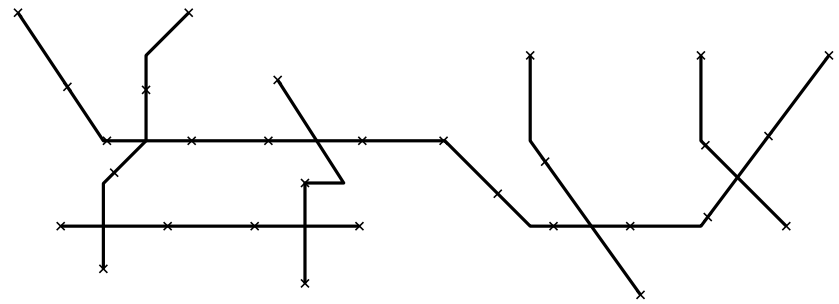

Figure 6.9: The intervals $I_1, \ldots, I_q$ in T

at such x_{i_j}. If $\mathbf{y}$ is expandable at a free vertex x_{i_j} of $\langle C \rangle$, then $\mathbf{x}$ is expandable at x_{i_j}, a contradiction. □

6.2.3 The main result

In this subsection $V(T)$ and $E(T)$ are the vertex and edge sets of T, respectively.

Theorem 6.2.11. *For a tree T, the critical values of the family $\{F_r(T,n)\}_{r>0}$ are contained in the set*

$$F := \left\{ \frac{1}{2(m-1)} d(v,w) : 2 \leq m \leq n,\ v,w \in V(T),\ v \neq w \right\}. \tag{1}$$

Remark 6.2.12. Since we can write $d(v,w) = \sum_{e \in E(T)} \varepsilon_e \ell(e)$ for some coefficients $\varepsilon_e \in \{0,1\}$, each critical value has the form $\frac{1}{2(m-1)} \sum_{e \in E(T)} \varepsilon_e \ell(e)$, for some $m \in \{2, \ldots, n\}$ and $\{\varepsilon_e\}_{e \in E(T)} \subset \{0,1\}$. In particular, given the metric data (T, ℓ), we can write down a finite set of size less than $(n-1)2^{|E(T)|}$ containing all critical values.

Proof of Theorem 6.2.11. Let $\mathbf{x}$ be a critical configuration. From Lemma 6.2.10, we may assume that $\mathbf{x}$ has one proper component, namely $C = \{x_1, \ldots, x_n\}$. Form the tree $\langle C \rangle$ as in Lemma 6.2.10. The free vertices of $\langle C \rangle$ are vertices of T, otherwise $\mathbf{x}$ is expandable. Hence $\langle C \rangle$ is a subtree of T, and points of $\mathbf{x}$ are distributed equally on each of a finite set of intervals $\{I_1, \ldots, I_q\}$ such that $\langle C \rangle = \bigcup_{j=1}^{q} I_j$ and $|I_j \cap I_k| \leq 1$, for all $j \neq k$. We now identify the weakly essential configurations from this description. If $\mathbf{x}$ is weakly essential then there is a pair $x, y \in C$ with

$$d(x,y) = \max_{w_1, w_2 \in C} \{d(w_1, w_2)\},$$

and the remaining points of C either

(i) lie (equally-spaced) on the unique interval I from x to y, or

(ii) lie on the endpoint of an edge e incident to U such that $\ell(e) = f(\mathbf{x})$.

In the latter case, $\overline{e} \cap I$ is a configuration point and a vertex of T, see Figure 6.10. Hence if $\mathbf{x}$ is a weakly essential configuration, then $f(\mathbf{x}) = \frac{1}{m-1} d(v, w)$ for some

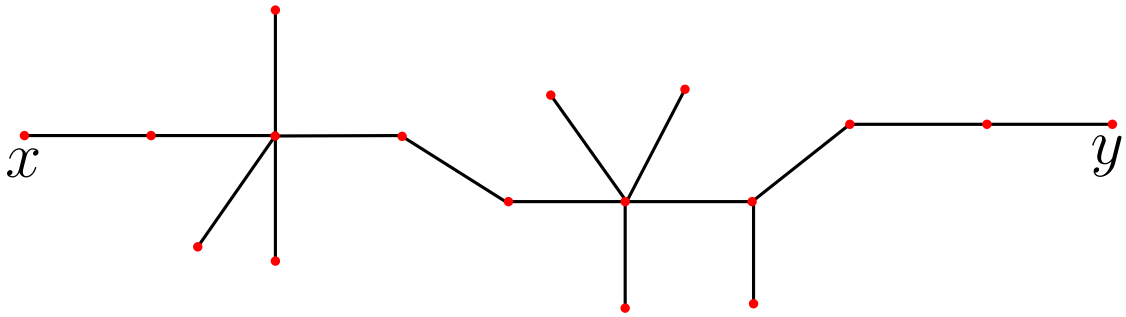

Figure 6.10: Points of a weakly essential configuration

$m \in \{2, \ldots, n\}$ and $v, w \in V(T)$ with $v \neq w$. The factor of $\frac{1}{2}$ in formula (1) comes from the definition of $F_r(T, n)$. □

Corollary 6.2.13. *We have* $F_r(T, n) \simeq F(T, n)$ *for all* $r \in \left(0, \frac{1}{2(n-1)} \min_{e \in E(T)} \{\ell(e)\}\right]$.

Proof. Combine Theorems 6.1.8 and 6.2.11. □

Corollary 6.2.14. *The essential configurations in a tree* T *are precisely the critical* 2*–configurations, and therefore comprise pairs of distinct vertices in* T*.*

Proof. The proof of Theorem 6.2.11 describes the weakly essential configurations; from this description, the essential configurations have size two. Every pair of distinct vertices in T is a critical configuration, since we have assumed that T has no vertices of degree two. □

Chapter 7

Possibilities for future work

In this final chapter, we discuss some possibilities for future work extending the results contained in this thesis. We focus mainly on unsolved problems arising from the study of the configuration spaces $\{F_r(\Gamma, n)\}_{r>0}$ for $n \geq 3$ (see Chapter 6). We also discuss some ideas for studying different configuration spaces related to those studied in this thesis. These configuration spaces may be useful for modelling other problems of practical robotics. Finally, we also mention some possibilities for extending the work of [7, 22] and Chapter 4 to obtain further homological information about the family $\{F_r(\Gamma, 2)\}_{r>0}$.

Questions arising from the family $\{F_r(\Gamma, n)\}_{r>0}$ for $n \geq 3$

PROBLEM 1. We know that $F_r(\Gamma, n) \neq \emptyset$ for $0 < r \leq \frac{1}{2(n-1)} \operatorname{diam} \Gamma$ (see Lemma 6.1.3). Find $R = R(\Gamma, n)$ such that $F_r(\Gamma, n) \neq \emptyset$ if and only if $r \in (0, R]$ (for $n = 2$ we have $R = \frac{1}{2} \operatorname{diam} \Gamma$, see Lemma 3.1.4).

PROBLEM 2. Find an upper bound on $b_0(F_r(\Gamma, n))$ as a function of (Γ, ℓ), n and r. Develop an algorithm, similar to that described in §5.3, for computing $b_0(F_r(\Gamma, n))$.

PROBLEM 3. There is a homotopy equivalence $F_r(\Gamma, n) \simeq F(\Gamma, n)$ for sufficiently small r (see Theorem 6.1.8). For trees, we have a sharp upper bound for r_n such that $F_r(\Gamma, n) \simeq F(\Gamma, n)$ for all $r \in (0, r_n]$, namely $r_n := \frac{1}{2(n-1)} \min_{e \in E(T)} \{\ell(e)\}$ (see Corollary 6.2.13). For the case $n = 2$, the same upper bound holds for a general graph Γ (see Theorem 4.1.6). For $n \geq 3$, do we have $F_r(\Gamma, n) \simeq F(\Gamma, n)$

for all $r \in (0, r_n]$ for a general graph? If so, is

$$\sup\{r > 0 : F_s(\Gamma, n) \simeq F(\Gamma, n), \ \forall s \in (0, r]\}$$

equal to r_n?

PROBLEM 4. Find the essential critical configurations in a general graph, generalising the result for trees stated in Theorem 6.2.14.

Different configuration spaces

In practical situations involving AGV motion (see §0.1.2), there will be restrictions on the guidepath network Γ. For example, Γ will be planar if the robots are constrained to move on one level of a factory. It may be useful to study a thick particle configuration space modelling the collision-free motion of n AGVs such that at most k vehicles are permitted in a subgraph $K \subset \Gamma$. For example, K may simply be a closed edge in the graph, or a cycle.

PROBLEM 5. Investigate the topology of the configuration spaces $\{F_r(\Gamma, n, K, k)\}_{r>0}$, where $F_r(\Gamma, n, K, k)$ is the space

$$\left\{(x_1, \ldots, x_n) \in \Gamma^n : \min_{i<j}\{d(x_i, x_j)\} \geq 2r, |K \cap \{x_1, \ldots, x_n\}| \leq k\right\}.$$

Questions arising from [7, 22] and Chapter 4

In paper [7], K. Barnett and M. Farber compute explicit generators for $H_2(F(\Gamma, 2))$ (for a planar graph Γ) in terms of disjoint cycles in Γ. The main tool of paper [7] is an intersection theory for cycles in graphs.

PROBLEM 6. Generalise the theory from paper [7] to compute explicit generators for the second homology group of $F_r(\Gamma, 2)$ (for planar graphs Γ), working with the discrete model $D_r(\Gamma, 2)$ for $F_r(\Gamma, 2)$. Can $H_2(F_r(\Gamma, 2))$ be expressed in terms of pairs of cycles (C_1, C_2) in Γ such that $d(C_1, C_2) \geq 2r$?

Moreover, E. Hanbury and M. Farber [22] compute the Betti numbers of $F(\Gamma, 2)$ for a large class of graphs (known as "mature" graphs – see [22]).

PROBLEM 7. Generalise the results from paper [22] and compute the Betti numbers of $F_r(\Gamma, 2)$ for mature graphs.

Appendix A

Alternative proof of Theorem 3.2.3

In this appendix we show how the main result of Chapter 3 (Theorem 3.2.3) may be proved without PL Morse–Bott theory. This is achieved by constructing an explicit deformation retraction. We also include the proof of the characterisation of index zero configurations (see §5.2.2) in terms of the metric d (see Lemma A.3.1).

A.1 Critical radii revisited

We begin by showing that a finite labelled graph has finitely many critical radii (see Definition 5.2.5) without using PL Morse–Bott theory.

Proposition A.1.1. *The set of critical radii is finite.*

Proof. It suffices to show that any minimal-length edgepath c such that $(c(0), c(1))$ is a critical configuration has the following form: a half-cycle concatenated with finitely many edges, followed by another half-cycle, see Figure 5.7. [For completeness, we allow a half-cycle to be a single point.] This suffices because in a finite graph there are finitely many distances $d(c(0), c(1))$ arising from such paths. Let c be such a path and write $(x, y) = (c(0), c(1))$. If $\mu(x), \mu(y) \neq 2$ then both x and y are vertices and c has the above form with both half-cycles trivial. Suppose $\mu(x) = 2$, so that x lies in an edge e. Since (x, y) is a critical configuration, $w \mapsto d(w, y)$ decreases on both branches of a star neighbourhood U_x as we move away from x. Hence, there is a point $x' \in \operatorname{Im} c$ and a cycle $K \subset \Gamma$ such that x, x' are antipodal on K, see Figure A.1. The same argument applies if $\mu(y) = 2$. □

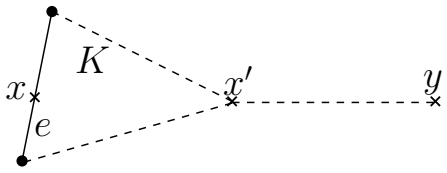

Figure A.1: The point x' and the cycle K

Corollary A.1.2. *Let $E(\Gamma), Z(\Gamma)$ denote the sets of edges and cycles in Γ, respectively, and let $\ell(C) := \ell(e_1)+\cdots+\ell(e_K)$ denote the length of a cycle $C = (e_1, \ldots, e_K)$. Any critical radius R has the form*

$$R = \frac{1}{2}\left(\frac{1}{2}\sum_{C\in Z(\Gamma)} \varepsilon_C \ell(C) + \sum_{e\in E(\Gamma)} \varepsilon_e \ell(e)\right),$$

where $\varepsilon_C, \varepsilon_e \in \{0, 1\}$ for all cycles C and edges e, and at most two of $\{\varepsilon_C\}_{C\in Z(\Gamma)}$ are non-zero.

Next, we show that every path-component of $F_r(\Gamma, 2)$ contains a critical configuration. The proof is very similar to that of Proposition 5.2.15 and, in view of Remark 5.2.12, the result is actually implied by Proposition 5.2.15.

Proposition A.1.3. *For any $r \in (0, \operatorname{diam}\Gamma/2]$, every path-component of $F_r(\Gamma, 2)$ contains a critical configuration.*

Proof. Let P be any path-component of $F_r(\Gamma, 2)$, and fix $(x, y) \in P$. Suppose that (x, y) is not a critical configuration, and let γ be a minimal-length edgepath from x to y.

(a) If $\operatorname{ind}_+(x, y) = 1$, move x along the unique branch incident to x on which $w \mapsto d(w, y)$ increases as we move away from x. Stop when we reach the unique point x_0 obtained in this way such that $\operatorname{ind}_+(x_0, y) \neq 1$, see Figure A.2. Let γ_1 be an edgepath from x_0 to x obtained from this procedure. By construction, the concatenation $\gamma_1 \cdot \gamma$ is a minimal-length edgepath from x_0 to y.

(b) If $\operatorname{ind}_+(x, y) \neq 1$, then $\operatorname{ind}_+(y, x) = 1$, so apply the procedure from (a) to obtain a point y_0 such that $\operatorname{ind}_+(y_0, x) \neq 1$.

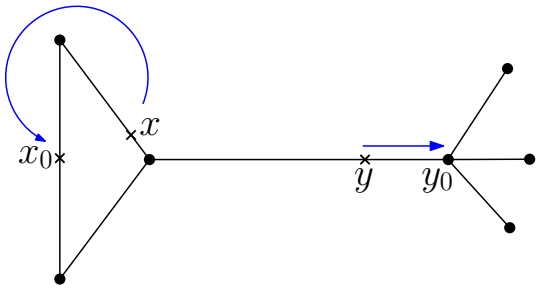

Figure A.2: Extending to a critical configuration (x_0, y_0)

If case (a) applies and if $\mathrm{ind}_+(y, x_0) = 1$, use the same procedure to push y away from x_0 until we reach a point y_0 with $\mathrm{ind}_+(y_0, x_0) \neq 1$. Let γ_2 be an edgepath from y to x_0 obtained from this procedure. Then, by construction, $(\gamma_1 \cdot \gamma) \cdot \gamma_2$ is a minimal-length edgepath from x_0 to y_0. Seeking a contradiction, assume that $\mathrm{ind}_+(x_0, y_0) = 1$. Then there is a unique branch of a star neighbourhood U_{x_0} on which $w \mapsto d(w, y_0)$ increases as we move away from x_0. Choose a point x_0' on this branch with $d(x_0', y_0) > d(x_0, y_0)$. There exists an edgepath p connecting x_0 with y and passing through x_0' which does not pass through x_0, see Figure A.3. Indeed, if such an edgepath does not exist then we have $\mathrm{ind}_+(x_0, y) = 1$, a contradiction. We

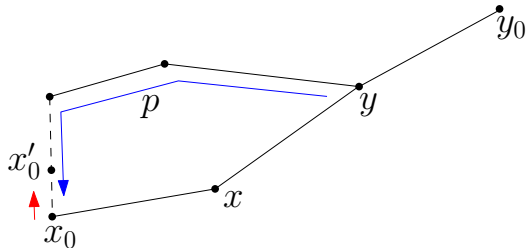

Figure A.3: The point x_0' and the path p

can also assume that p has minimal-length. Indeed, we do not have $L_p < L_{\gamma_1 \cdot \gamma}$, since $\gamma_1 \cdot \gamma$ is a minimal-length edgepath from x_0 to y. If no minimal-length edgepath with the properties of p exists, then $L_p > L_{\gamma_1 \cdot \gamma}$ and we can move x_0 away from y along p in the direction of x_0', contradicting $\mathrm{ind}_+(x_0, y) \neq 1$. Hence $L_p = L_{\gamma_1 \cdot \gamma}$. In particular, $d(x_0', y_0)$ is equal to $L_{\gamma_2} + L_{p|_{[\varepsilon,1]}}$ for some $\varepsilon \in (0, 1)$. Thus $d(x_0', y_0) < d(x_0, y_0) = L_{\gamma_2} + L_p$, a contradiction. Therefore $\mathrm{ind}_+(x_0, y_0) \neq 1$ and so (x_0, y_0) is a critical configuration.

If case (b) applies and if $\mathrm{ind}_+(x, y_0) = 1$, push x from y_0 as above to obtain a

point x_0 with $\mathrm{ind}_+(x_0, y_0), \mathrm{ind}_+(y_0, x_0) \neq 1$. This procedure defines a continuous path in $F_r(\Gamma, 2)$ from (x, y) to a critical configuration $(x_0, y_0) \in P$. □

We now introduce some notation which is useful for the proof of the main theorem in §A.2.

Definitions A.1.4. The proof of Proposition A.1.3 defines a map $\Theta : F(\Gamma, 2) \to C$, where $C \subset F(\Gamma, 2)$ is the set of critical configurations. Let $X_1, X_2 : F(\Gamma, 2) \to \Gamma$ be the components of this map, so that

$$\Theta(x, y) = (X_1(x, y), X_2(x, y)), \quad \forall (x, y) \in F(\Gamma, 2),$$

see Figure A.4. Furthermore, for each $(x, y) \in F(\Gamma, 2)$ there is a unique constant-

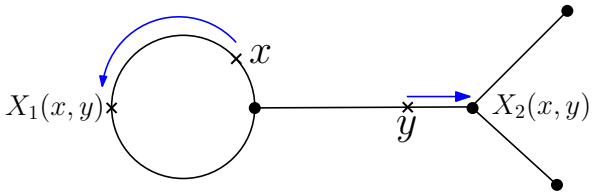

Figure A.4: The components of the map Θ

speed path $c_{(x,y)} : [0, 1] \to F(\Gamma, 2)$ defined by the proof of Proposition A.1.3 such that $c_{(x,y)}(0) = (x, y)$ and

$$c_{(x,y)}(1) = \Theta(x, y) = (X_1(x, y), X_2(x, y)).$$

It has the property that $d(c_{(x,y)}(t_1)) \leq d(c_{(x,y)}(t_2))$ for all $t_1, t_2 \in [0, 1]$ with $t_1 \leq t_2$.

Example A.1.5. Let (T, ℓ) be the labelled Y–graph from Example 3.1.7, and let x, y be the midpoints of e_1, e_2 respectively. In this case, $X_1(x, y) = v_1$ and $X_2(x, y) = v_2$.

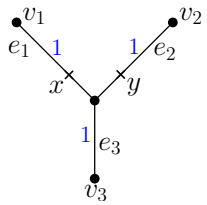

Figure A.5: The labelling on the Y–graph T

Regard $(\overline{e}_1, v_1) = ([0,1], 0)$, $(\overline{e}_2, v) = ([0,1], 0)$ as copies of $[0,1]$. The map $c_{(x,y)}$ is given by

$$c_{(x,y)}(t) = \begin{cases} ((1-2t)/2, y), & t \in [0, 1/2] \\ (v_1, t), & t \in [1/2, 1]. \end{cases}$$

Example A.1.6. Let $\Gamma = S^1$ be the circle from Example 3.1.6, and let $x = i$, $y = 1$. Then $X_1(x,y) = -1$, $X_2(x,y) = y = 1$ and $c_{(x,y)} : [0,1] \to \Gamma$ is given by

$$c_{(x,y)}(t) = \left(ie^{i\pi t/2}, 1\right), \quad \forall t \in [0,1],$$

see Figure A.6. We have $d(x,y) = 1/4$ and $d(\Theta(x,y)) = 1/2$. For each $r \in (1/4, 1/2)$,

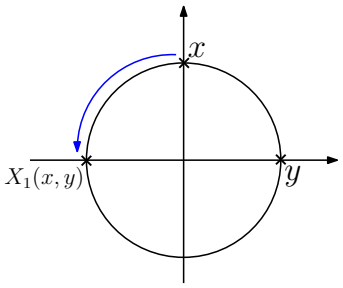

Figure A.6: The map $c_{(x,y)}$

there is a unique $t_0 \in (0,1)$ such that $d(c_{(x,y)}(t_0)) = r$.

Remark A.1.7. In general, for each $r \in (d(x,y), d(\Theta(x,y)))$, there exists a unique $t_0 \in (0,1)$ such that $d(c_{(x,y)}(t_0)) = r$.

Remark A.1.8. We observe that $\Theta : F(\Gamma, 2) \to C$ is not continuous in general. For example, in Figure A.7, choose sequences $(x_n), (y_n) \subset e_1$ and $(y'_n) \subset e_2$ such that $x_n \to x$ and $y_n, y'_n \to y$. Then $(x_n, y_n), (x_n, y'_n) \to (x,y)$, but $\Theta(x_n, y_n) = (x,y)$ and $\Theta(x_n, y'_n) = (x, y')$ for all $n \in \mathbb{N}$.

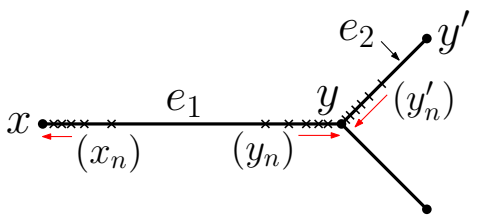

Figure A.7: The map Θ is discontinuous in general

A.2 Critical values of the family $\{F_r(\Gamma,2)\}_{r>0}$

We are now in a position to derive Theorem 3.2.3 by constructing an explicit deformation retraction.

Theorem A.2.1. *The set of critical values of the family $\{F_r(\Gamma,2)\}_{r>0}$ is finite.*

Proof. We show that the set of critical values is contained in the set of critical radii. The result then follows from Proposition A.1.1. Suppose that $r > 0$ is not a critical radius, and let $U_r \subset (0,\infty)$ be a connected open neighbourhood of r in the complement of the set of critical radii. Let $r_1 < r_2$ be any two elements of U_r. We define a deformation retraction H of $F_{r_1}(\Gamma,2)$ onto $F_{r_2}(\Gamma,2)$ as follows. If $(x,y) \in F_{r_1}(\Gamma,2) \setminus F_{r_2}(\Gamma,2)$, that is, $2r_1 \leq d(x,y) < 2r_2$, then there is a unique $t_0 \in [0,1]$ such that $d(c_{(x,y)}(t_0)) = 2r_2$, see Definitions A.1.4 and Remark A.1.7. Define $H((x,y),s) = c_{(x,y)}(st_0)$, for all $s \in [0,1]$. In other words, we push x and y away from each other until the distance between them reaches $2r_2$, subject to the following rules: one point moves at a time and x moves first if possible, and the motion takes place at constant-speed in unit time. If $(x,y) \in F_{r_2}(\Gamma,2)$ then we set $H((x,y),s) = (x,y)$ for all $s \in [0,1]$.

The map H is continuous because there is no critical radius between r_1 and r_2. Moreover, $H((x,y),0) = c_{(x,y)}(0) = (x,y)$ and $H((x,y),1) \in F_{r_2}(\Gamma,2)$ for all $(x,y) \in F_{r_1}(\Gamma,2)$. Hence, H is a deformation retraction. In particular, $F_{r_1}(\Gamma,2) \simeq F_{r_2}(\Gamma,2)$ and so r is a regular value of the family $\{F_r(\Gamma,2)\}_{r>0}$. □

Corollary A.2.2. *Each critical value R of the family $\{F_r(\Gamma,2)\}_{r>0}$ has the form*

$$R = \frac{1}{2}\left(\frac{1}{2}\sum_{C\in Z(\Gamma)} \varepsilon_C \ell(C) + \sum_{e\in E(\Gamma)} \varepsilon_e \ell(e)\right),$$

where $\varepsilon_C, \varepsilon_e \in \{0,1\}$ for all $C \in Z(\Gamma)$, $e \in E(\Gamma)$ and at most two of $\{\varepsilon_C\}_{C\in Z(\Gamma)}$ are non-zero.

Proof. Theorem A.2.1 shows that each critical value is a critical radius, so Corollary A.1.2 gives the result. □

A.3 Characterisation of index zero configurations

We characterise index zero configurations in terms of the metric d.

Lemma A.3.1. *A configuration (x, y) has index zero if and only if it is a local maximum of d.*

Proof. If (x, y) is a local maximum of d then there are star neighbourhoods U_x, U_y of x and y, respectively, such that

$$d(x', y') \leq d(x, y), \quad \forall (x', y') \in U_x \times U_y.$$

If (x, y) does not have index zero, say WLOG that $\mathrm{ind}_+(x, y) > 0$, then there is a branch of U_x on which $w \mapsto d(w, y)$ is increasing as we move away from x. In particular, there exists $x' \in U_x$ such that $d(x', y) > d(x, y)$, a contradiction.

If (x, y) has index zero, then it is critical (Remark 5.2.12) so by Proposition A.1.1 any minimal-length edgepath from x to y has the following form: a half-cycle concatenated with finitely many edges, followed by another half-cycle, see Figure 5.7. We consider two cases. Firstly, if x, y are antipodal points on a cycle, then (x, y) is a local maximum of d. If we are not in this case, choose star neighbourhoods U_x, U_y such that $w \mapsto d(w, y)$ decreases on each branch of U_x as we move away from x, and similarly for U_y. Let $x' \in U_x$, $y' \in U_y$ and choose a minimal-length edgepath c from x to y passing along the branches of U_x and U_y containing x' and y', respectively, see Figure A.8. Such a path exists since we have a complete description of minimal-

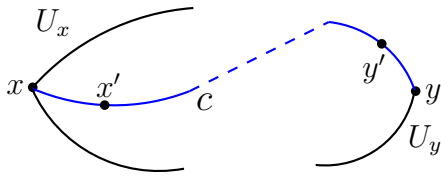

Figure A.8: A minimal-length edgepath c of the required form

length edgepaths from x to y from above and x,y are not antipodal points on a cycle. There exist unique $s, t \in [0, 1]$ such that $c(s) = x'$ and $c(t) = y'$. Since c has constant speed (Lemma 1.4.8) we obtain

$$d(x', y') = d(c(s), c(t)) = |s - t| d(x, y) \leq d(x, y).$$

□

Appendix B

Computing path-components in Octave

B.1 Introduction

In this appendix we describe an implementation of the algorithm from §5.3 for computing the number of path-components $b_0(F_r(\Gamma, 2))$ of $F_r(\Gamma, 2)$, given Γ and r. I give special thanks to A. Hayden [40] for his invaluable help with this programming project; he was also the first to implement the algorithm, using Python.

We assume that $\Gamma = T$ is a labelled tree, to be entered by the user in the form of a *distance matrix* $D = [d_{ij}]$. This is defined as follows: we assign labels $1, \ldots, V$ to the V vertices of T. If there is an edge e from vertex i to vertex j, then $d_{ij} = \ell(e)$; otherwise $d_{ij} = \infty$.

Example B.1.1. Suppose that T is the Y–graph from Example 5.3.7 as shown below.

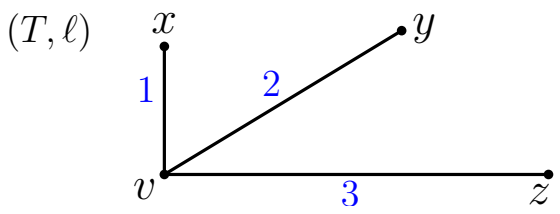

The distance matrix of (T, ℓ) is

$$D = \begin{bmatrix} \infty & \infty & \infty & 1 \\ \infty & \infty & \infty & 2 \\ \infty & \infty & \infty & 3 \\ 1 & 2 & 3 & \infty \end{bmatrix}.$$

The output of the program is a list of the critical radii of (T, ℓ), together with a list of the number of path-components of $F_r(T, 2)$ for each critical radius r.

B.2 Implementation and listing

Throughout, our programs are written in GNU Octave. We begin by writing a function `Dijkstra` to implement Dijkstra's algorithm. This is an algorithm for finding a shortest path between two vertices in a labelled graph. Further details can be found, for example, in [43, §22.3] and [56]. We then have a function `critical_radii` which computes the critical radii of a given labelled tree. Provided that there are no vertices of degree two, such critical radii are precisely the distances between distinct vertices, divided by two (see Corollary A.1.2). Next, we implement the algorithm for constructing the graph G_r from §5.3 in the function `construct_Gr`. This function actually constructs the adjacency matrix of the graph G_r. Finally, the script `PathComps` prompts the user for the distance matrix of a labelled tree (T, ℓ), then calls `critical_radii` to compute the critical radii of (T, ℓ). Next, it uses the Octave built-in function `dmperm` to calculate $b_0(G_r) = b_0(F_r(\Gamma, 2))$ from the adjacency matrix of G_r (which is computed by `construct_Gr`). Finally, it displays the results to the user.

We now provide our programming code.

B.2.1 Function `Dijkstra` implementing Dijkstra's algorithm

```
# Function implementing Dijkstra's algorithm. Inputs are the initial
# vertex, final vertex and distance matrix and the outputs
# are a shortest path from the initial vertex to the final vertex
```

```
# (given by a sequence of vertices) and the length of this path.

function [edgepath,minimum_distance]
  = Dijkstra(Initial_Vertex,Final_Vertex,Distance_Matrix)

[V,W]=size(Distance_Matrix);

# The number of vertices of the graph is V (the number of rows
# of the distance matrix).

# Initialise two vectors "parent" and "distance". "Parent"
# will list the previous vertex in the sequence, and
# "distance" will contain the distance from each vertex
# to the Initial_Vertex.

for i=1:V
parent(i)=0;
  distance(i)=Inf;
 end

queue=[];

# Initialise "queue". This vector holds the list
# of children vertices.

for i=1:V

if Distance_Matrix(Initial_Vertex,i)~=Inf

# Finds all vertices incident to Initial_Vertex.
```

```
distance(i)=Distance_Matrix(Initial_Vertex,i);

# Update "distance".

parent(i)=Initial_Vertex; #Update "parent",
queue=[queue i]; #Update "queue".
end
end

while length(queue)~=0

# (As long as there is a child vertex to check).

hop_start = queue(1); #Try the first child vertex.
  queue = queue(2:end); #Update "queue".

for hop_end=1:V

# Try all vertices for "hop_end" and implement Dijkstra's algorithm.

if distance(hop_end)>distance(hop_start)
    +Distance_Matrix(hop_start,hop_end)

distance(hop_end)=distance(hop_start)
  +Distance_Matrix(hop_start,hop_end);

parent(hop_end)=hop_start;

queue=[queue hop_end];

end # if
```

```
end # for
end # while

# Now we construct the sequence of vertices giving a shortest path.

edgepath=[Final_Vertex];
i=parent(Final_Vertex);

 while (i~=Initial_Vertex && i~=0)
  edgepath=[i edgepath];
  i=parent(i);
 end

 if (i==Initial_Vertex)
  edgepath=[i edgepath];
  else
  edgepath=[];
 end

 minimum_distance=distance(Final_Vertex);
```

B.2.2 Function `critical_radii` computing critical radii

```
function critical_radii = critical_radii(A)

[Number_of_vertices,b] = size(A);

# Finds the number of vertices of the tree
# (equal to the number of rows of the adjacency matrix)

critical_radii=[]; #Initialises the vector critical_radii
```

```
# Now calculate the critical radii of the
# tree from the adjacency matrix A.

for i=1:Number_of_vertices

for j=1:Number_of_vertices #Loop over all entries of A

if i<j
  [b,distance]=Dijkstra(i,j,A);

# Calculates the distance between vertex i and vertex j

critical_radii=[critical_radii,distance/2];

# Updates the list of critical radii

end # if
end # for
end # for

critical_radii=unique(critical_radii);

# Removes the repeated critical radii and sorts them into order
```

B.2.3 Function `construct_Gr` constructing the adjacency matrix

```
function [Gr_Adjacency_Matrix]=construct_Gr(A,r)

[V,W]=size(A);
```

```
# We need V, the number of vertices of the tree
# (equal to the number of rows of A).

Matrix_of_pairs=zeros(V); #Constructs VxV matrix of zeros

#Now construct Matrix_of_pairs, the matrix with (i,j)th
# entry equal to the distance between vertex v_i and
# vertex v_j for i~=j, and zeros on the diagonal.

for i=1:V

for j=1:V

if i~=j
[edgepath,minimum_distance]=Dijkstra(i,j,A);

# Calculate the distance between vertex i and vertex j

Matrix_of_pairs(i,j)=minimum_distance;

end # if
end # for
end # for

Gr_Vertices=[]; #Initialise vector of vertices of G_r

# Now construct the vertices of G_r. A pair of
# distinct vertices (v,w) of the tree T is included
# in G_r if and only if d(v,w)>=2*r.

for i=1:V
```

```
for j=1:V

if (Matrix_of_pairs(i,j)>2*r || Matrix_of_pairs(i,j)==2*r)
Gr_Vertices=[Gr_Vertices,[i,j]'];

end # if
end # for
end # for

[C,v]=size(Gr_Vertices);

# We need v, the number of vertices of G_r
# (equal to the number of columns of Gr_Vertices).

Gr_Adjacency_Matrix=zeros(v);

# Initialise the adjacency matrix of Gr.

# Construct the adjacency matrix of G_r. A pair ((v,w),(v',w'))
# of vertices of G_r is connected by an edge in G_r if and
# only if (v=v' or w=w') and there is an edge
# between the other two coordinates in T.

for i=1:v

for j=1:v

if ((Gr_Vertices(1,i)==Gr_Vertices(1,j)
&& A(Gr_Vertices(2,i),Gr_Vertices(2,j))~=Inf)
|| (Gr_Vertices(2,i)==Gr_Vertices(2,j)
```

```
&& A(Gr_Vertices(1,i),Gr_Vertices(1,j))~=Inf))


Gr_Adjacency_Matrix(i,j)=1;


end # if
end # for
end # for
```

B.2.4 Script PathComps implementing the algorithm from §5.3

```
disp("\n")
disp("Welcome! This program computes the number of
path-components")
disp("of the thick particle configuration spaces
F_r(T,2) for a given")
disp("labelled tree T and all values of r>0.\n")
disp("The program takes as input the distance matrix of T")
disp("and outputs a list of all critical radii together")
disp("with the corresponding numbers of path-components
of F_r(T,2).\n")
disp("Please press enter to continue.")
pause
disp( "The distance matrix D is a symmetric matrix
defined as follows:")
disp("if there is an edge from vertex i to vertex j
with label d>0, ")
disp("then D_{i,j}=d. If there is no edge from vertex i
to vertex j, ")
disp("then D_{i,j}=Inf (logical infinity).\n")
disp("Example: if T is the Y-graph with edge labels
1,2 and 3, then")
```

```
disp("D=[[Inf,Inf,Inf,1];[Inf,Inf,Inf,2];
[Inf,Inf,Inf,3];[1,2,3,Inf]].\n")
disp("Please press enter to continue.
You will be prompted")
disp("for the distance matrix of your labelled tree.
Please ensure that")
disp("your tree has no vertices of degree 2 and at
least one edge.")
pause

A=input("Please enter the distance matrix of the tree T: \n");

#Error checking.

[m,n]=size(A);

if (m~=n || m==1  || m==0)

error("It appears that you have not entered
a valid distance matrix.\n");

end

for i=1:m
for j=1:n

if (abs(A(i,j))~=A(i,j) || A(i,j)==0)
error("It appears that one of your matrix entries
is neither Inf nor a positive number.\n");
end
```

```
if (A(i,j)~=A(j,i))
error("It appears that your matrix is not symmetric.");
end

end
end

counter=zeros(1,n);

for i=1:m
for j=1:n

if A(i,j)~=Inf
counter(i)=counter(i)+1;
end

if (i==j && A(i,j)~=Inf)
error("It appears that one of your diagonal elements
 is not Inf. \n");
end

end
end

E=sum(counter)/2;
Euler=m-E;

if Euler~=1
error("It appears that you have not entered the distance
matrix of a tree (the Euler characteristic is not 1).\n");
end
```

```
chck=counter-2*ones(1,n);

if all(chck)==0
error("It appears that your tree contains a vertex of degree 2. \n");
end

tic; # Start timer.

criticalradii=critical_radii(A);

# Calculates the critical radii of T by invoking
# the function "critical_radii".

L=size(criticalradii,2);

# The number of critical radii (equal to the number
# of columns of criticalradii).

components=zeros(1,L); #Initialise vector "components".

#Now we construct the graphs G_r and compute their
# zero-dimensional Betti numbers.
# We invoke the function "construct_Gr" to construct the
# adjacency matrix of Gr and the built-in function "dmperm"
# to compute b_0(G_r) from this adjacency matrix.

for i=1:L
Gr=construct_Gr(A,criticalradii(i));
[a,b]=size(Gr);
B=Gr+eye(a);
```

```
[p,q,r,s]=dmperm(B);
components(i)=length(r)-1;
end


elapsed_time=toc; #Stop timer.


#Now display the results.


disp("\n")
disp("Finished! It took me")
disp(elapsed_time)
disp("seconds. Please press enter to display the critical radii. \n")
pause
disp("The critical radii of your labelled tree are: \n")
disp(criticalradii)
disp("\n")
disp("Please press enter to continue.")
pause
disp("The corresponding numbers of path-components are:\n")
disp(components)
M=criticalradii(L);
disp("\n")
disp("Also, F_r(T,2) is empty for r>")
disp(M)
disp(". Thank you!")
```

B.3 Sample program output

In this section we run our program on two specific labelled trees and display the program output.

Example B.3.1. We first consider the labelled tree (T, ℓ) from Example 5.3.7,

namely, the Y–graph with edge labels 1, 2 and 3. A distance matrix for (T, ℓ) is

$$D = \begin{bmatrix} \infty & 1 & 2 & 3 \\ 1 & \infty & \infty & \infty \\ 2 & \infty & \infty & \infty \\ 3 & \infty & \infty & \infty \end{bmatrix}.$$

We display the program output below.

```
Welcome! This program computes the number of path-components
of the thick particle configuration spaces F_r(T,2) for a given
labelled tree T and all values of r>0.

The program takes as input the distance matrix of T
and outputs a list of all critical radii together
with the corresponding numbers of path-components of F_r(T,2).

Please press enter to continue.

The distance matrix D is a symmetric matrix defined as follows:
if there is an edge from vertex i to vertex j with label d>0,
then D_{i,j}=d. If there is no edge from vertex i to vertex j,
then D_{i,j}=Inf (logical infinity).

Example: if T is the Y-graph with edge labels 1,2 and 3, then
D=[[Inf,Inf,Inf,1];[Inf,Inf,Inf,2];[Inf,Inf,Inf,3];[1,2,3,Inf]].

Please press enter to continue. You will be prompted
for the distance matrix of your labelled tree. Please ensure that
your tree has no vertices of degree 2 and at least one edge.

Please enter the distance matrix of the tree T:
 [[Inf,1,2,3];[1,Inf,Inf,Inf];[2,Inf,Inf,Inf];[3,Inf,Inf,Inf]]
```

```
Finished! It took me
 0.13341
seconds. Please press enter to display the critical radii.


The critical radii of your labelled tree are:

   0.50000    1.00000    1.50000    2.00000    2.50000


Please press enter to continue.

The corresponding numbers of path-components are:

   1    2    4    4    2


Also, F_r(T,2) is empty for r > 2.5000. Thank you!
```

Example B.3.2. Let (T, ℓ) be the labelled H–tree shown in Figure B.1. A distance

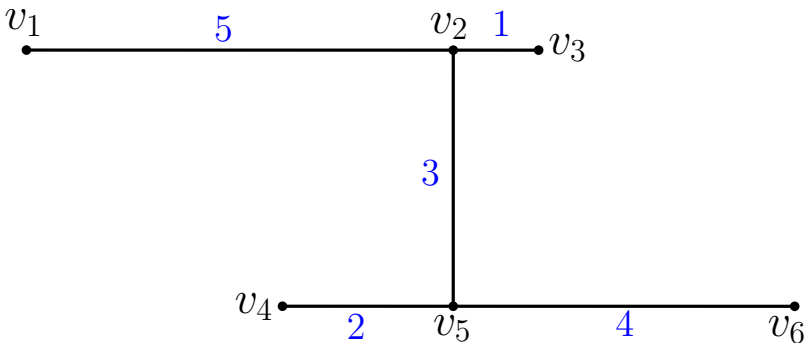

Figure B.1: The labelled H–tree (T, ℓ)

matrix for (T, ℓ) is

$$D = \begin{bmatrix} \infty & 5 & \infty & \infty & \infty & \infty \\ 5 & \infty & 1 & \infty & 3 & \infty \\ \infty & 1 & \infty & \infty & \infty & \infty \\ \infty & \infty & \infty & \infty & 2 & \infty \\ \infty & 3 & \infty & 2 & \infty & 4 \\ \infty & \infty & \infty & \infty & 4 & \infty \end{bmatrix}.$$

We display the program output below.

```
Welcome! This program computes the number of path-components
of the thick particle configuration spaces F_r(T,2) for a given
labelled tree T and all values of r>0.

The program takes as input the distance matrix of T
and outputs a list of all critical radii together
with the corresponding numbers of path-components of F_r(T,2).

Please press enter to continue.

The distance matrix D is a symmetric matrix defined as follows:
if there is an edge from vertex i to vertex j with label d>0,
then D_{i,j}=d. If there is no edge from vertex i to vertex j,
then D_{i,j}=Inf (logical infinity).

Example: if T is the Y-graph with edge labels 1,2 and 3, then
D=[[Inf,Inf,Inf,1];[Inf,Inf,Inf,2];[Inf,Inf,Inf,3];[1,2,3,Inf]].

Please press enter to continue. You will be prompted
for the distance matrix of your labelled tree. Please ensure that
your tree has no vertices of degree 2 and at least one edge.

Please enter the distance matrix of the tree T:
```

```
[[Inf,5,Inf,Inf,Inf,Inf];[5,Inf,1,Inf,3,Inf];[Inf,1,Inf,Inf,Inf,Inf];
[Inf,Inf,Inf,Inf,2,Inf];[Inf,3,Inf,2,Inf,4];[Inf,Inf,Inf,Inf,4,Inf]]


Finished! It took me
 0.71290
seconds. Please press enter to display the critical radii.


The critical radii of your labelled tree are:

 Columns 1 through 8:

   0.50000   1.00000   1.50000   2.00000

   2.50000   3.00000   3.50000   4.00000

 Columns 9 and 10:

   5.00000   6.00000


Please press enter to continue.

The corresponding numbers of path-components are:

   1   1   2   2   4   8   2   4   4   2


Also, F_r(T,2) is empty for r > 6. Thank you!
```

References

[1] A. Abrams (2000), *Configuration spaces and braid groups of graphs*, PhD thesis, University of California at Berkeley. Available at: `http://www.mathcs.emory.edu/~abrams/research/Papers/index.html`.

[2] A. Abrams (2002), *Configuration spaces of colored graphs*, Geometriae Dedicata, Volume 92, 185–194. Available at: `http://www.mathcs.emory.edu/~abrams/research/Papers/index.html`.

[3] A. Abrams, D. Gay and V. Hower (2010), *Discretized configurations and partial partitions*, `arXiv:1009.2935v1`.

[4] A. Abrams and R. Ghrist (2002), *Finding topology in a factory: configuration spaces*, American Mathematics Monthly, 109, 140-150. Available at: `arXiv:math/0009118v1`.

[5] M. Baker and X. Faber (2005), *Metrized graphs, electrical networks, and Fourier analysis*, `arXiv:math/0407428v2`.

[6] K. Barnett (2009), *The configuration space of two particles moving on a graph*, PhD thesis, Durham University. Available at: `http://etheses.dur.ac.uk/view/departments/DDD21.html`.

[7] K. Barnett and M. Farber (2009), *Topology of configuration space of two particles on a graph, I*, Algebraic and Geometric Topology, Volume 9, Issue 1, 593–624. Available at: `arXiv:0903.2180v1`.

[8] M. Bestvina and N. Brady (1997), *Morse theory and finiteness properties of groups*, Invent. Math. 129, 445–470.

[9] M. Bestvina (2008), *PL Morse theory*, Mathematical Communications **13**, 149–162. Available at: `http://hrcak.srce.hr/file/48930`.

[10] D. Burago, Y. Burago and S. Ivanov (2001), *A course in metric geometry*, American Mathematical Society.

[11] F. Connolly and M. Doig (2004), *Braid groups and right angled Artin groups*, `arXiv:math/0411368v1`.

[12] A. H. Copeland (1965), *Homology of deleted products in dimension one*, Proc. AMS, **16**, 1005–1007.

[13] A. H. Copeland and C. W. Patty (1970), *Homology of deleted products of one-dimensional spaces*, TAMS, **151**, 499–510.

[14] K. Deeley (2011), *Configuration spaces of thick particles on a metric graph*, accepted on 26/4/2011, to appear in Algebraic and Geometric Topology.

[15] B. Demir, A. Deniz, S. Koçak (2009), *Stability of graphs*, The Electronic Journal of Combinatorics **16**, # N6. Available at: `http://www.combinatorics.org/Volume_16/PDF/v16i1n6.pdf`.

[16] P. Diaconis (2009), *The Markov chain Monte Carlo revolution*, Bull. Amer. Math. Soc. 46, 179–205.

[17] M. Doig (2004), *Stellar braiding*, `arXiv:math/0412531v2`.

[18] S. Eilenberg (1941), *Ordered topological spaces*, American Journal of Mathematics, **63**, 39–45.

[19] M. Farber (2005), *Collision free motion planning on graphs*, in: "Algorithmic Foundations of Robotics IV", M. Erdmann, D. Hsu, M. Overmars, A. Frank van der Stappen editors, Springer, 123–138. Available at: `arXiv:math/0406361v1`.

[20] M. Farber (2008), **Invitation to topological robotics**, European Mathematical Society.

[21] M. Farber (2008), Private Communication.

[22] M. Farber and E. Hanbury (2010), *Topology of configuration space of two particles on a graph, II*, Algebraic and Geometric Topology, Volume 10, Issue 4, 2203–2227. Available at: `arXiv:1005.2300v1`.

[23] M. Farber, M. Grant and S. Yuzvinsky (2007), *Topological complexity of collision-free motion planning algorithms in the presence of multiple moving obstacles*, "Topology and Robotics" (M. Farber, R. Ghrist et al editors), Contemporary Mathematics AMS, Volume 438, 75–83. Available at: `arXiv:math/0609476v1`.

[24] D. Farley (2006), *Homology of tree braid groups*, in: "Topological and Asymptotic Aspects of Group Theory", Contemp. Math. **394**, 101–112.

[25] D. Farley (2007), *Presentations for the cohomology rings of tree braid groups*, in: "Topology and Robotics", Contemp. Math. **438**, 145–172.

[26] D. Farley and L. Sabalka (2005), *Discrete Morse theory and graph braid groups*, Algebraic and Geometric Topology **5**, 1075–1109. Available at: `arXiv:math/0410539v3`.

[27] D. Farley and L. Sabalka (2008), *On the cohomology rings of tree braid groups*, Journal of Pure and Applied Algebra **212**, 53-71. Available at: `arXiv:math/0602444v2`.

[28] D. Farley and L. Sabalka (2009), *Presentations of graph braid groups*, `arXiv:0907.2730v1`.

[29] R. Forman (1998), *Morse theory for cell complexes*, Adv. Math. **134**, 90–145. Available at: `http://math.ucsd.edu/~justin/formanmorsecell.pdf`.

[30] S. R. Gal (2001), *Euler characteristic of the configuration space of a complex*, Colloquium Mathematicum Volume 89, Issue 1, 61–67. Available at: `arXiv:math/0202143v1`.

[31] A. Georgakopoulos (2009), *Graph topologies induced by edge lengths*, arXiv:0903.1744v3.

[32] A. Georgakopoulos (2010), *Uniqueness of electrical currents in a network of finite total resistance*, arXiv:0906.4080v4.

[33] R. Ghrist (2001), *Configuration spaces and braid groups on graphs in robotics*, in Braids, Links, and Mapping Class Groups: the Proceedings of Joan Birman's 70th Birthday, AMS/IP Studies in Mathematics, Volume 24, 29–40. Available at: arXiv:math/9905023v1.

[34] R. Ghrist (2007), *Configuration spaces, braids and robotics*, survey for summer school on braids & applications at the National University of Singapore. Available at: http://www.math.uiuc.edu/~ghrist/preprints/singaporetutorial.pdf.

[35] R. Ghrist and D. Koditschek (1998), *Safe cooperative robotic motions via dynamics on graphs*, Eighth Intl. Symp. on Robotic Research, Y. Nakayama, ed., Springer–Verlag, 81-92. Available at: http://www.math.uiuc.edu/~ghrist/preprints/AGV.pdf.

[36] R. Ghrist and D. Koditschek (2002), *Safe, cooperative robot dynamics on graphs*, SIAM J. Control & Optimization, 40(5), 1556–1575. Available at: arXiv:cs/0002014v1.

[37] S. Gibilisco (2003), **Concise Encyclopedia of Robotics**, McGraw–Hill.

[38] A. Hatcher (2002), **Algebraic topology**, Cambridge University Press. Available at: http://www.math.cornell.edu/~hatcher/.

[39] M. Hägele, K. Nilsson, J. Norberto Pires (2008), *Industrial Robotics*, in: "Springer Handbook of Robotics" (B. Siciliano and O. Khatib editors), Springer, 963–986.

[40] A. Hayden (2010), Private Communication.

[41] M. Kahle (2010), *Sparse stable packings of hard discs in a box*, `arXiv:0908.1830v3`.

[42] Ki Hyoung Ko and Hyo Won Park (2011), *Characteristics of graph braid groups*, `arXiv:1101.2648v1`.

[43] E. Kreyszig (1988), **Advanced Engineering Mathematics**, Sixth Edition, John Wiley & Sons Inc.

[44] V. Kurlin (2009), *Computing braid groups of graphs with applications to robot motion planning*, to appear in Homology, Homotopy and Applications. Available at: `arXiv:0908.1067v1`.

[45] W. S. Massey (1967), **Algebraic topology: an introduction**, Harcourt, Brace and World, New York.

[46] O. Mermoud and M. Steiner (2002), *Configuration spaces of weighted graphs in high-dimensional Euclidean spaces*, Contributions to Algebra and Geometry, Volume 43, No. 1, 27–31. Available at: `http://www.emis.de/journals/BAG/vol.43/no.1/b43h1mst.pdf`.

[47] A. Neels and S. Privitera (2005), *Braid groups of the sun graph*, `arXiv:math/0508380v1`.

[48] U. Nehmzow (2006), **Scientific methods in mobile robotics: quantitative analysis of agent behaviour**, Springer series in advanced manufacturing, Springer–Verlag London Limited.

[49] C. W. Patty (1961), *Homotopy groups of certain deleted product spaces*, Proceedings of the American Mathematical Society, **12**, 369–373.

[50] C. W. Patty (1962), *The fundamental group of certain deleted product spaces*, TAMS **105**, 314–321.

[51] P. Prue and T. Scrimshaw (2009), *Abrams's stable equivalence for graph braid groups*, `arXiv:0909.5511v1`.

[52] R. Siegwart and I. Nourbakhsh (2004), **Introduction to autonomous mobile robots**, Massachusetts Institute of Technology.

[53] **Springer Handbook of Robotics** (2008), B. Siciliano and O. Khatib editors, Springer.

[54] J. Świątkowski (2001), *Estimates for homological dimension of configuration spaces of graphs*, Colloquium Mathematicum, 89, 69–79. Available at: `http://www.math.uni.wroc.pl/~swiatkow/Papers/graf2.ps`.

[55] **Oxford Dictionary and Thesaurus** (2007), Edited by Maurice Waite, Oxford University Press.

[56] Wikipedia – Dijkstra's algorithm (accessed September 2010): `http://en.wikipedia.org/wiki/Dijkstra's_algorithm`.

[57] Wikipedia – Robot (accessed January 2011): `http://en.wikipedia.org/wiki/Robot`.

[58] Wikipedia – Automated guided vehicle (accessed January 2011): `http://en.wikipedia.org/wiki/Automated_guided_vehicle`.